THE
PHYSICAL REVIEW
A Journal of Experimental and Theoretical Physics
VOL. 45, NO. 7 APRIL 1, 1934 SECOND SERIES

An Investigation of the Klein-Nishina Formula for X-Ray Scattering, in the Wave-Length Region 50 to 20 X-Units

JOHN READ AND CHARLES C. LAURITSEN, *Kellogg Radiation Laboratory, California Institute of Technology*
(Received December 15, 1933)

An x-ray tube and a spectrograph were used to produce monochromatic beams of wave-length from 50 to 20 x-units. The absorption coefficient per electron for each beam was measured in carbon and aluminum. Results indicate it is unlikely that the Klein-Nishina formula for the scattering coefficient per electron is in error by more than one percent in this region of wave-lengths.

INTRODUCTION

A BEAM of x-ray photons, in passing through matter, loses intensity partly as a result of Compton scattering by the extranuclear electrons. We shall call the Compton scattering per electron ${}_e\sigma$ and the total absorption per electron ${}_e\mu$.

In 1928 Klein and Nishina[1] derived an expression for the dependence of ${}_e\sigma$ on the frequency of the radiation. This was based on Dirac's relativistic interpretation of the quantum mechanics, and supplanted a formula derived by Dirac[2] from the older quantum mechanics.

The most advantageous region of wave-lengths in which to test the Klein-Nishina formula is from 12 to 50 x-units, where its predictions differ appreciably from those of the older theories, and where there is good reason to believe other modes of absorption are relatively small. For longer wave-lengths the photoelectric absorption becomes increasingly important. For shorter wave-lengths there is the possibility of additional absorption due to the production of positive and negative electron pairs, to nuclear absorption, and to nuclear scattering.

The total absorption coefficient for the filtered gamma-rays from thorium C'' (wave-length 4.7 x.u.) has been measured by several experimenters. The values for ${}_e\mu$ so obtained for elements of atomic number less than 14 are, on the average, about 1.28×10^{-25}, whereas the value of ${}_e\sigma$ calculated from the Klein-Nishina formula for this wave-length is 1.23×10^{-25}. Also Chao[3] has scattered the 4.7 x.u. radiation from aluminum at suitable angles to produce monochromatic beams of wave-length 7.0, 9.6, 15.5, 29.4, and 47 x.u., and measured the absorption coefficient per electron in aluminum. The values he obtained are plotted in Fig. 3. In general the values for ${}_e\mu$ are about four percent greater than the values for ${}_e\sigma$ to be expected from the Klein-Nishina formula, and the excess appears to exist for wave-lengths from 4.7 to 29.4 x.u. The excess at wave-lengths between 12 and 29.4 x.u., if real, can scarcely be due to nuclear absorption or scattering, while it is equally unlikely to be due to photoelectric absorption.

[1] Klein and Nishina, Zeits. f. Physik **52**, 853 (1928).
[2] Dirac, Proc. Roy. Soc. **A111**, 405 (1927).
[3] Chao, Phys. Rev. **36**, 1519 (1930).

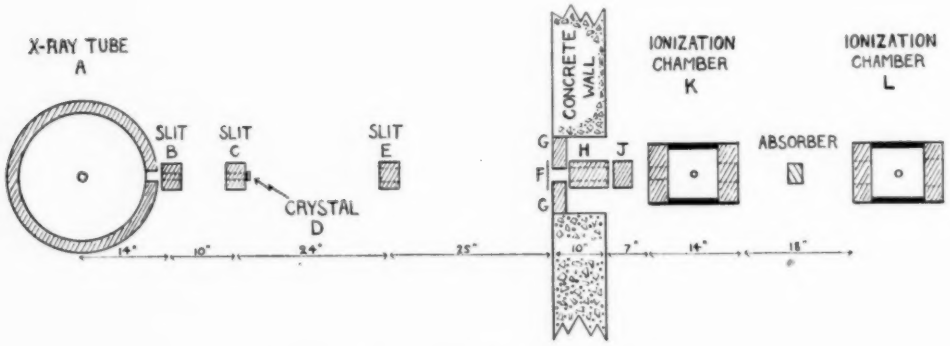

FIG. 1. Arrangement of the apparatus.

It is the purpose of this investigation to determine the absorption per electron in aluminum and carbon for monochromatic beams in the wave-length region 20 to 50 x-units, and to compare the results with the values of $_e\sigma$ calculated from the Klein-Nishina formula.

APPARATUS

The arrangement of the apparatus is given in Fig. 1. The x-ray tube *A* could be excited by voltages up to 1000 kv. Slits in the lead blocks *B* and *C* defined a plane horizontal x-ray beam, which was incident on the internal atom planes of the rocksalt crystal *D* at such an angle that radiation of the desired wave-length was reflected. A slit in the lead block *E* allowed the monochromatic beam to pass on into the ionization chambers, while the block itself absorbed the unreflected radiation. The lead filter *F* and the slit *H* reduced the intensity of stray radiation which might reach the chambers. The sliding lead block *J* acted as a shutter.

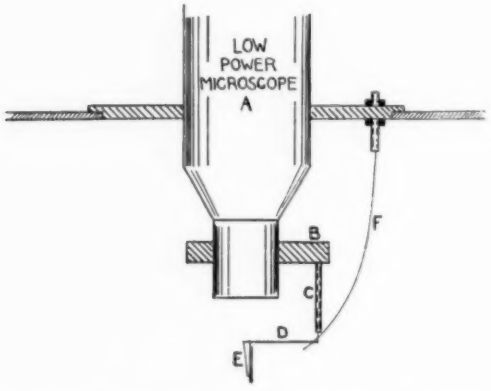

FIG. 2. Construction of the ionization chamber.

The construction of the aluminum ionization chambers is shown in Fig. 2. The low power microscope *A* had an eyepiece scale across which the foot of the L-shaped gold coated quartz fiber *E* appeared to move. Charge could be put upon the fiber system by rotating the wire *F* so as to touch the wire frame *D*, which was insulated by an amber pillar *C*.

EXPERIMENTAL PROCEDURE

A radioactive source was used to produce a constant rate of ionization in the chambers, and a discharge curve, scale reading against time, was graphed for each chamber. Since the rate of ionization was constant, a unit on the time axis could be regarded as an arbitrary unit of ionization, so that the ratios of ionizations producing discharges over different portions of the eyepiece scale could be determined. It was verified that the graphs were independent of the magnitude of the ionization currents, and that the sum of the ionizations produced by two radioactive sources acting separately equalled the ionization produced by the sources acting together.

The monochromatic x-ray beam was passed through the chambers without any absorber between them. Shutter *J* was opened for a time sufficient to permit the more rapidly moving fiber to cover almost the whole eyepiece scale. The ionization in chamber *L* was then expressed in terms of that in chamber *K*. The discharge was repeated with an absorbing screen midway between the chambers. From the ionization in chamber *K*, and the known response of *L* in terms of *K* with no absorber present, the ionization which would have occurred in *L* had

no absorber been present, was calculated. The actual ionization in L was known from the observed discharge, so that the absorption coefficient could be found. The ionizations were always corrected for stray radiation by observing the discharge of the chambers under the same conditions, except that the angle of the crystal was altered so that it no longer reflected the monochromatic beam down the slit system.

The absorption coefficient was measured for several thicknesses of the absorber, and it was found that there was no hardening of the beam with increasing thickness. The x-ray tube was operated at a peak voltage less than twice that corresponding to the wave-length reflected by the crystal. Therefore radiation of half the desired wave-length, reflected in the second order, was not present.

The wave-length of the radiation was determined by photographing the monochromatic ray and the unreflected ray at a distance of 169 cm from the crystal, where the separation of the rays was from 1 to 2 cm. A microphotometric trace of the photographic film made it possible to determine the wave-length with an error of less than one percent.

Results

The results of the measurements are given in Table I, and are plotted in Fig. 3 together with the Klein-Nishina curve for $_e\sigma$ the Dirac curve for $_e\sigma$, and the values obtained by Chao.

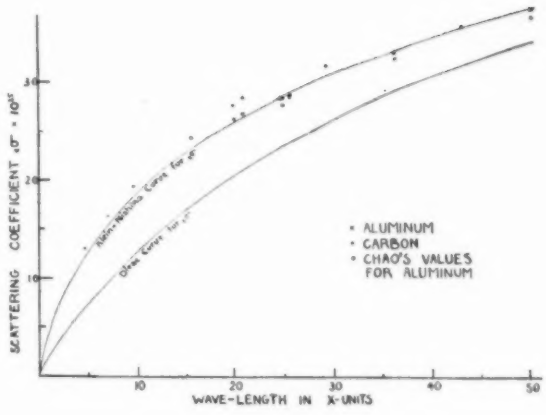

FIG. 3.

Sources of Error

Calculation shows that the x-rays scattered by the absorber, yet still able to enter chamber L, would produce an error of less than 1/10 percent in the observed absorption. The wave-length width $\Delta\lambda$ at half maximum of the monochromatic ray was from 10 to 20 percent of the wave-length λ corresponding to the peak. Since $_e\sigma$ does not vary rapidly with λ this spread would not cause the effective wave-length to differ appreciably from the peak wave-length. The error in the wave-length should be less than two percent.

Nine observations were necessary to obtain one absorption coefficient. If the maximum likely errors in these observations were cumulative,

TABLE I. *Measured values of x-ray scattering coefficient and comparison with Klein-Nishina values.*

Wave-length λ (x.u.)	$\Delta\lambda$ (x.u.)	Element	Experimental value ($\times 10^{25}$)	Probable error ($\times 10^{25}$)	No. of obs.	Weighted mean ($\times 10^{25}$)	Deviation from Klein-N. value	Klein-Nishina value ($\times 10^{25}$)
50.4	4.1	Aluminum	3.75	0.02	4	3.73	−0.5%	3.755
		Carbon	3.64	0.04	3			
36.3		Aluminum	3.24*	0.07	5	3.31	−1.2	3.350
		Carbon	3.31	0.01	3			
25.6	5.0	Aluminum	2.86	0.01	2	2.87	−1.0	2.902
		Carbon	2.88	0.01	2			
24.8	3.7	Aluminum	2.85	0.02	4	2.84	−0.7	2.864
		Carbon	2.77*	0.05	3			
20.8	3.3	Aluminum	2.68	0.03	3	2.69	+1.1	2.657
		Carbon	2.85*	0.10	3			
19.9	3.7	Aluminum	2.63	0.01	4	2.64	+1.1	2.606
		Carbon	2.76*	0.03	4			

they would lead to an error of three percent in the coefficient.

The target of the x-ray tube was carried by a steel column about 15 feet long, and was cooled by water circulated by thermo-syphon action. A small change of temperature would cause the target to move with respect to the slit system, which would alter the ratio of response of the chambers and the amount of background radiation. This was the most troublesome source of error as it could be detected only by a diminution of x-ray intensity, and by the lack of agreement between values of the absorption coefficient obtained under otherwise identical conditions. It is probable that the values in Table I marked by asterisks were affected by such an occurrence.

Discussion of the Results

The probable errors listed in Table I have not much significance, since the number of observations is small. They are added to give an idea of the agreement between the different observations.

Mention has been made of a possible cause of the larger probable errors of the four values in Table I marked by asterisks. If a smooth curve were drawn among all the points these four would deviate most from it. In each case the value obtained with the same wave-length, but with the other element, has a much smaller probable error, and would fall much closer to the curve. It would therefore seem that little weight should be attached to the four values marked by asterisks, as compared with the corresponding values for the other element.

It is to be expected that ${}_e\tau$, the photoelectric coefficient of absorption, should be less than the experimental error in this region. Otherwise the total absorption coefficient should be greater for aluminum than for carbon, and the difference should diminish regularly with increasing frequency. Furthermore, if we assume Gray's empirical law for the photoelectric absorption of lead, and also that the law ${}_e\tau \propto Z^3$ which holds for longer wave-lengths holds in this region also, then for aluminum for a wave-length of 50 x.u. ${}_e\tau$ is 0.008×10^{-25}. For all other wave-lengths used, and for carbon, ${}_e\tau$ calculated in this manner is much less than the experimental error.

The weighted means given in Table I are obtained by compounding the values for aluminum with those for carbon, giving each a weight inversely proportional to the square of its probable error. If these weighted means were plotted, and a smooth curve were drawn among them, it would not deviate from the Klein-Nishina curve by more than one percent at any point between 50 and 20 x.u.

This work was made possible by a grant from the Seeley W. Mudd fund. The authors express their gratitude for this assistance.

The Yield of Fluorescence X-Rays from the *K*-Shells of Thirteen Elements*

DONALD K. BERKEY,† *University of Cincinnati*

(Received August 28, 1933)

The fluorescence yield w_K has been measured by the ionization method as developed by A. H. Compton for thirteen elements. The following results have been obtained:

Element	w_K	Element	w_K	Element	w_K
27 Co	0.38	33 As	0.53	47 Ag	0.72
28 Ni	.39	34 Se	.55	48 Cd	.70
29 Cu	.43	38 Sr	.72	50 Sn	.66
30 Zn	.45	42 Mo	.79	51 Sb	.64
				52 Te	.59

These results show that w_K reaches a maximum value of 0.79 for molybdenum. It then rapidly drops to lower values for the heavier elements.

INTRODUCTION

THE fluorescence yield w_K from the K-shells of an assemblage of atoms has been defined by Auger[1] as the ratio of the number of fluorescence K-quanta that leave the atoms in the group to the number of quanta that are photoelectrically absorbed in the K-shells of those atoms. The same definition can be applied *mutatis mutandis* to the yield from the L-shell. Auger[1,2] and Locher[3] have measured the yield by counting the electron-tracks in cloud chambers. Values of the fluorescence yield based on ionization-chamber measurements have been reported by several investigators.[4–13] In spite of the number of investigations bearing on this subject, the amount of data is not large, for no one investigator worked with more than six elements, and some with only one. Furthermore, there is considerable divergence among the data.

The present investigation was undertaken in order to obtain data on a large number of elements with the same apparatus, and to determine the trend of the fluorescence yield with increase of atomic number.

THEORY

The fluorescence yield w_K is determined by comparing the intensities of the primary and the fluorescence beams by means of an ionization-chamber. Compton[9] used this method in his investigations and developed the appropriate equations. He found

$$w_K = \frac{4\pi r^2}{A''(\delta-1)/\delta} = \frac{\mu'+\mu''}{\mu'} \times \frac{\lambda''}{\lambda'} \times \frac{i''}{i'} \times \frac{f'}{f''} \times \frac{S'}{S''} \times \frac{R'}{R''}, \quad (1)$$

* From a thesis presented in partial fulfillment of the requirements for the degree of Doctor of Philosophy.

† Laws Fellow in Physics. At present in the Research Laboratory, The Beech-Nut Packing Company, Canajoharie, N. Y.

[1] P. Auger, Ann. d. Physik **6**, 183 (1926).
[2] P. Auger, Comptes Rendus **180**, 65 (1925).
P. Auger, J. de Phys. et le Rad. **6**, 205 (1925).
[3] Gordon L. Locher, Phys. Rev. **40**, 484 (1932).
[4] W. Kossel, Zeits. f. Physik **19**, 333 (1923).
[5] W. Bothe, Phys. Zeits. **26**, 410 (1925).
[6] G. E. M. Jauncey and O. K. De Foe, Proc. Nat. Acad. Sci. **11**, 520 (1925).
[7] L. Balderston, Phys. Rev. **27**, 695 (1926).
[8] M. I. Harms, Ann. d. Physik **82**, 87 (1926).
[9] A. H. Compton, Phil. Mag. **8**, 961 (1929).
[10] L. H. Martin, Proc. Roy. Soc. **A115**, 420 (1927).
[11] R. J. Stephenson, Phys. Rev. **43**, 527 (1933).
[12] W. Stockmeyer, Ann. d. Physik [5] **12**, 71 (1932).
[13] M. Haas, Ann. d. Physik [5] **16**, 473 (1932).

where the symbols* have the same meanings as in his paper. The primed and double-primed quantities refer to the primary and secondary radiations, respectively. Compton used the approximation 85 percent for the fraction of the primary quanta absorbed in the K-shells, instead of the more exact value $(\delta-1)/\delta$ obtained from the measurements of the K-absorption jump δ. The symbol R designates the ratio of the energy spent in producing ionization to the absorbed energy.

$$R=1-\frac{\delta-1}{\delta}\times e^{-\mu''x}\times\left(w_K\times\frac{\tau}{\mu}\times\frac{\lambda}{\lambda''}\right)_{\text{Argon}}-\frac{\sigma}{\mu}\times e^{-\mu'x}. \quad (2)$$

The second term of Eq. (2) takes account of the loss of fluorescence energy excited in the gas in the ionization-chamber, while the third term takes account of the loss by scattering. In the present work, argon at atmospheric pressure was used in the chamber. This has two advantages. In the first place, it has such a high atomic number that for the wave-lengths used here the scattering is negligible in comparison to the photoelectric absorption. Thus the third term of Eq. (2) vanishes. In the second place, the fluorescence rays of argon are so soft that they will be absorbed before reaching the walls of the ionization-chamber. There will not even *be* much fluorescence, because w_K for argon is small. Thus the second term in Eq. (2) reduces (nearly) to zero,[14] and we have[15]

$$R\doteq 1.$$

A geometrical constant of the apparatus is

$$M\equiv(4\pi r^2/A'')(S'/S''). \quad (3)$$

After f' and f'' have been determined (from the values of the absorption-coefficients of argon), there is a constant C_Z for each element under investigation:

$$C_Z\equiv\frac{M}{(\delta-1)/\delta}\times\frac{\mu'+\mu''}{\mu'}\times\frac{\lambda''}{\lambda'}\times\frac{f'}{f''}. \quad (4)$$

Then Eq. (1) reduces to

$$w_K=C_Z(i''/i'). \quad (5)$$

Apparatus and Procedure

The radiator L of barium nitrate[16] is placed at an angle of 45° directly above the tungsten-target x-ray tube (Fig. 1). Fluorescence x-rays

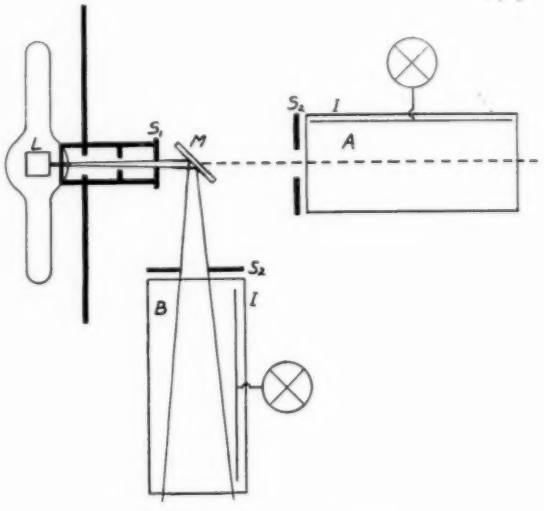

Fig. 1. Arrangement of apparatus.

* r = distance between secondary radiator M and diaphragm S_2. A'' = area of the hole in diaphragm S_2. δ = K-absorption jump. μ' = absorption coefficient of the material of the radiator M for the primary radiation falling on it from L. μ'' = absorption coefficient of the material of the radiator M for its own characteristic K-radiation. λ' and λ'' = wave-lengths of the K-radiations characteristic of the radiators L and M, respectively. i' and i'' = corrected ionization-currents obtained with the ionization-chamber in the positions A and B, respectively. S' and S'' = areas of the diaphragm S_1 when measuring the primary and secondary rays, respectively. f' and f'' = fractions of the x-ray beams absorbed in the ionization-chamber when in the positions A and B, respectively. R' and R'' = ratios of the energy spent in producing ionization to the absorbed energy, for the primary and secondary rays, respectively.

[14] S. K. Allison and V. J. Andrew, Phys. Rev. **38**, 441 (1931). These investigators have studied this phenomenon and report deviations of the order of 1–2 percent from unity. This is of the same order as the experimental error, and so is here neglected.

[15] The author is indebted to A. H. Compton for suggesting the use of argon in the chamber, as well as for several other helpful details.

[16] This is used merely as a convenient source of monochromatic x-rays.

TABLE I. *Values of* C_Z.

Element	$(\delta-1)/\delta$	μ'/ρ	μ''/ρ	$(\mu'+\mu'')/\mu'$	λ''	λ''/λ'	f''	f'/f''	C_Z
27 Co	0.886	7.0	61.	9.7	1.77	4.68	1.00	0.075	6.58
28 Ni	.884	7.7	54.	8.0	1.63	4.32	0.99	.076	5.04
29 Cu	.882	8.8	49.	6.6	1.51	4.00	.98	.077	3.88
30 Zn	.880	9.9	47.0	5.76	1.41	3.73	.96	.078	3.24
33 As	.874	12.7	37.3	3.94	1.16	3.06	.85	.088	2.07
34 Se	.872	13.9	34.0	3.45	1.09	2.87	.78	.096	1.85
38 $SrCO_3$	.865	11.3	15.6	2.38	0.859	2.27	.52	.144	1.53
42 Mo	.858	23.0	18.7	1.81	.696	1.84	.345	.217	1.43
47 Ag	.850	31.0	12.6	1.41	.549	1.45	.205	.366	1.49
48 Cd	.849	31.9	11.7	1.37	.525	1.39	.178	.406	1.54
50 Sn	.847	34.5	10.0	1.29	.482	1.28	.155	.484	1.60
51 Sb	.844	36.5	9.4	1.26	.462	1.22	.140	.536	1.66
52 Te	.843	38.2	8.4	1.22	.443	1.17	.125	.600	1.73
56 Ba	—	—	—	—	.378	—	.075	—	—

from L pass through holes in a series of baffles and finally through the diaphragm S_1, falling upon M set at 45° to the beam. The fluorescence radiation from M (the sample under investigation) is measured by the ionization-chamber I in the position B through the diaphragm S_2. The ionization-current i'' thus measured is compared with that i' caused by the direct beam with I in the position A, M being then removed and a much smaller diaphragm placed in the position S_1.

The x-ray tube was operated at 60 peak kilovolts and 34 milliamperes from a supply giving half-wave rectification by means of a kenotron. The power was supplied by a motor-generator set, with a large induction motor. This minimized fluctuations in the input voltage to the high-tension transformer, which could thus be held constant to one-tenth of a volt by means of the field rheostat. The voltage was controlled continuously during a reading. The ionization-chamber was 24 cm long, 7 cm in diameter and filled with argon at atmospheric pressure. Diaphragms were so disposed that no rays ever struck the walls. The x-rays emerged from the rear of the chamber through a cellophane window. The Compton electrometer was operated at 3000–4000 mm per volt at a scale distance of 140 cm.

AUXILIARY DATA

In order to calculate w_K, the factor C_Z (see Eq. (4)) must be calculated separately for each element used. The values of $(\delta-1)/\delta$ were obtained from a table compiled by F. Kirchner.[17] It is calculated from published data on absorption-jumps. This was plotted and a smooth curve drawn through the points. From this curve the values of $(\delta-1)/\delta$ for the elements used were read off. The values of μ' and μ'' were interpolated from tables collected by Professor S. J. M. Allen and kindly furnished to the author.

The wave-lengths λ' and λ'' were calculated from those given in the Wien-Harms *Handbuch der Experimental Physik*, Vol. 24, part 2. The values used are the weighted means wave-lengths of the α and β-lines,[18, 19] the α-line being given five times the weight of the β-line, in accordance with the work of Unnewehr and Compton.

The fractions f' and f'' of the beams absorbed in the ionization-chamber were calculated from the published absorption-coefficients of argon and nitrogen. It was necessary to take account of the nitrogen, as the argon used was the commercial grade containing 14 percent by volume of nitrogen.

Table I shows the values of C_Z for the various samples used, as well as the auxiliary data used in calculating them. Throughout the course of the investigation barium was used as the source of the primary radiation. We have

$$M=(4\pi r^2/A'')(S'/S'')=1.697,$$

[17] Wien-Harms, *Handbuch der Experimental Physik*, Vol. 24, part 1, p. 256.

[18] Unnewehr, Phys. Rev. **22**, 529 (1923).

[19] A. H. Compton, Proc. Nat. Acad. Sci. **14**, 549 (1928).

where $r=11.4$ cm, $A''=3.19$ cm^2, and $S'/S''=0.003305$.

It will be noticed that the strontium used was in the form of the carbonate. Therefore it was necessary to compute values of μ/ρ for the compound at the wave-lengths λ' and λ'' by the additive law.

Discussion of Results

The ratios of the ionization-currents caused by the primary and fluorescence beams are shown in Table II, together with the values of the fluorescence yield w_K deduced from Eq. (5).

Table II. *Ratios of currents due to primary and fluorescence radiation and values of w_K.*

Element	i''/i'	w_K	Element	i''/i'	w_K
27 Co	0.058	0.38	38 Sr	0.469	0.72
28 Ni	.077	.39	42 Mo	.549	.79
29 Cu	.111	.43	47 Ag	.480	.72
30 Zn	.140	.45	48 Cd	.452	.70
33 As	.255	.53	50 Sn	.414	.66
34 Se	.300	.55	51 Sb	.383	.64
			52 Te	.344	.59

The values given in Table II are plotted in Fig. 2. They show that there is a distinct maximum in the K-fluorescence yield at $Z=42$, molybdenum. Beyond molybdenum the yield decreases again. So far as the author is aware, this is the first investigation of the K-yields of elements of high enough atomic number to show this decrease. Heretofore many have tacitly supposed that the K-yields kept on increasing up to uranium. The work of Balderston[7] gives the only hint available that such may not be the case.

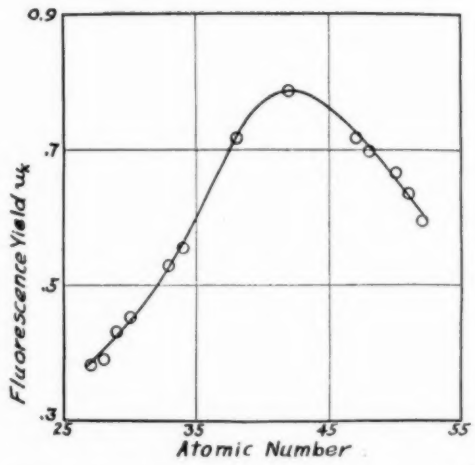

Fig. 2. Fluorescence yield as a function of atomic number.

Why does the K-fluorescence yield decrease beyond element number 42? Does it continue to decrease for the elements heavier than tellurium? These questions cannot as yet be answered, for there is at present no satisfactory theory of this effect. The wave-mechanical treatment of this subject given by Wentzel[20] contains no hint of a drop in the efficiency of production of fluorescence x-rays from the K-shells of the heavy elements.

The author is glad to acknowledge his indebtedness to Professor S. M. J. Allen for suggesting this problem, and for much helpful advice given during the course of this investigation.

[20] G. Wentzel, Zeits. f. Physik **43**, 524 (1927).

Cosmic-Ray Ionization at High Altitudes

A. H. COMPTON AND R. J. STEPHENSON, *Ryerson Physical Laboratory, University of Chicago*

(Received February 21, 1934)

A criterion for the nature of cosmic rays. Cosmic rays may be interpreted as photons only if at all altitudes $d^2(\log \psi)/dP^2>0$, where P is the barometric pressure and ψ is the intensity as a function of the pressure for rays descending vertically through the atmosphere. Gross has shown how ψ can be determined directly from the observed intensity I, due to rays from all directions. The rays may be interpreted as ionizing particles with a definite range ("r-particles") only if the relation $d^2I/dP^2>0$ is satisfied. Measurements by a recording cosmic-ray meter, with walls equivalent to 6 cm of lead to avoid transition effects, were made on the recent Settle-Fordney stratosphere balloon flight. Through the altitude range from 40 to 15 cm Hg the ionization-pressure relation satisfies the criterion for r-particles but not that for photons. This result is confirmed by comparison with other high altitude data.

Ionization of primary cosmic rays as function of altitude. The measurements when graphically analyzed show the presence of rays of two distinct range groups, A and B. Group B has ranges greater but apparently not less than the air equivalent of 27 cm Hg, with a strong maximum at 36 cm. This group is ascribed to electrically charged rays which require energies greater than that corresponding to 27 cm range in order to penetrate the earth's magnetic field. Protons and possibly positrons meet these requirements, but not α-particles nor heavier nuclei. Group A is most prominent at the shorter ranges, and shows no maximum for ranges greater than 10 cm Hg. It thus represents rays unaffected by the earth's magnetic field, and hence neutral or with a ratio of mass to charge equal to or greater than that of an alpha-particle. Apparently range group A is almost completely confined to the upper atmosphere.

Photons cannot constitute more than a negligible part of primary cosmic rays. Comparison of high altitude measurements at the equator with those at high latitudes shows that the equatorial cosmic rays are closely similar to the magnetically deviable rays both in their absorption in air and in their transition effects. This indicates that most of the cosmic rays which reach the earth are similar in character to the deviable rays, most probably protons. Any primary cosmic photons which may reach the earth apparently produce an imperceptible effect.

1. A Criterion for the Nature of Cosmic Rays

It is well known, from the studies of Kolhörster, Regener and others, that the ionization due to cosmic rays increases rapidly with increasing altitude, but that near the top of the atmosphere the rate of increase diminishes. This change in shape of the ionization curve at high altitudes is usually ascribed to a transition effect, due to the secondary rays produced as the primary cosmic rays enter the atmosphere. Only below such a depth that the secondary rays are in constant ratio to the primary rays does the observed ionization serve as a measure of the intensity of the primary cosmic rays. It is possible however to eliminate this transition effect by using an ionization chamber whose walls are so thick that all of the secondary rays from the air are absorbed, and the rays which reach the inside of the chamber are in equilibrium with the secondaries from the chamber walls. The observed ionization in such a chamber should be proportional to the intensity of the primary rays all the way to the top of the atmosphere. We have recently measured the cosmic rays up to high altitudes using a thick-walled ionization chamber in which this condition is approximately realized.

If the ionization is thus proportional to the intensity of the primary rays, the relation between the ionization and the depth below the surface of the atmosphere may be of such a form that it can be described in terms of ionizing particles but not in terms of photons. Let us determine the criterion for this distinction.

For this purpose we shall define *r-particles* as particles with a definite range, and ionizing the absorbing matter uniformly throughout that range. Alpha-rays, beta-rays, protons and positrons would fall approximately into this classifi-

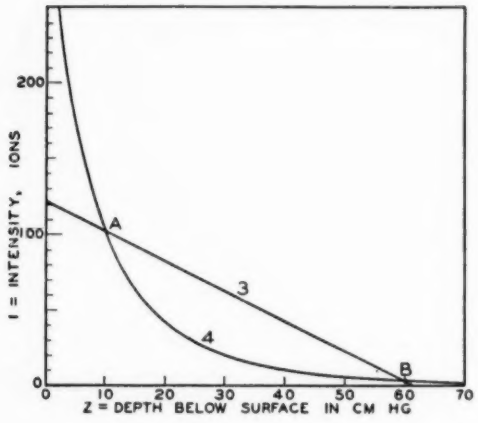

FIG. 1.

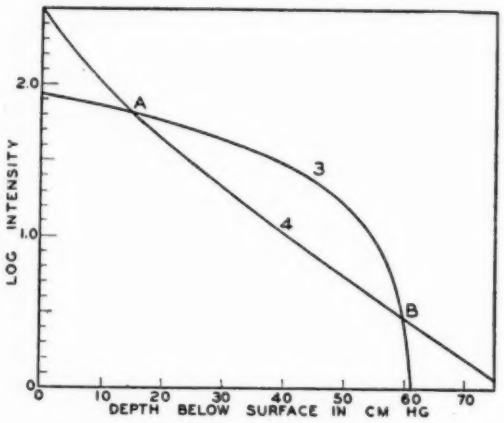

FIG. 2.

FIGS. 1 AND 2. Calculated ionization by isotropic cosmic rays, *3* by ionizing particles with a definite range, *4* by homogeneous photons.

cation. We shall assume also that a photon traverses matter without loss of energy until in one cataclysmic event it loses a large part or all of its energy. The ionization due to a homogeneous beam of *r-rays* traversing an absorbing medium parallel to the Z axis is thus,

$$\begin{aligned} I_r &= I_0 \quad [z<r] \\ &= 0, \quad [z>r], \end{aligned} \tag{1}$$

where I_0 is the ionization at the surface of the medium and r is the range of each particle. The ionization due to a homogeneous beam of photons is,

$$I_p = I_0 \exp(-\mu z), \tag{2}$$

where μ is its constant absorption coefficient.

Assuming that the cosmic rays enter the atmosphere as r-rays, uniformly from all directions, a simple integration shows that a fraction $(r-z)/r$ will penetrate to a depth z. Thus the ionization at a depth z below the surface of the atmosphere, due to homogeneous, isotropic r-rays coming from outside, should be,

$$I_r = I_0(r-z)/r. \tag{3}$$

The corresponding expression for the ionization at a depth z below the surface of the atmosphere, due to homogeneous, isotropic photons coming from outside has been shown by Millikan and Cameron[1] to be,

$$I_p = I_0 G(\mu z), \tag{4}$$

where[2]

$$G(\mu z) = 2\pi \int_0^\infty z^{-2} \exp(-\mu z x) dx. \tag{5}$$

In Figs. 1 and 2 the intensity and the logarithm of the intensity are plotted respectively against the depth z, according to expressions 3 and 4. Points A and B represent experimental values at two levels in the atmosphere. Curve 4 represents a beam of homogeneous photons. If more than one component is present, the curve becomes more strongly concave upward. Thus if an experimental ionization curve is straighter than No. 4, or is curved downward, it cannot be due to photons (except for the effect of secondary rays, as will be discussed below). The straight line of Fig. 1 represents homogeneous r-rays. If groups of r-rays of different ranges are present, it is clear that an ionization curve such as 4 might result. If we let $I = f(z)$ be the ionization depth relation, it can in fact be shown, using Eq. (3), that the number of r-particles entering the top of the atmosphere with ranges between z and $z+dr$ is[3]

$$R(r)dr = z(d^2I/dz^2)dr. \tag{6}$$

Since R must be positive to have physical significance, this means that r-rays can produce

[1] R. A. Millikan and G. H. Cameron, Phys. Rev. **28**, 860 (1926).

[2] E. Gold, Proc. Roy. Soc. **A82**, 62 (1908) gives a table of this integral for various values of (μz).

[3] This relation has been given by B. Gross, Zeits. f. Physik **83**, 217 (1933).

any curve which has at all points an upward curvature, i.e., for which

$$d^2I/dz^2>0. \qquad (7)$$

It follows that any ionization *vs.* pressure relation which can be accounted for by photons can also be accounted for in terms of ionizing particles with a definite range. On the contrary, curves lying between 3 and 4 can be represented by particles with a definite range (r-rays) but not by photons.

2. Experimental Requirements

The experimental data taken in the air at moderately high altitudes will be shown to follow curves intermediate between 3 and 4. As we have seen, this can be taken as definite evidence against their photon nature only if the ionization chamber is surrounded with a wall sufficiently thick to absorb the secondaries produced in the air, in which case the ionization by homogeneous photons should be proportional to the energy per unit area of the incident beam.

The wall thickness necessary to absorb the secondaries from air may be found from observations of transition effects. Those measured by Schindler[4] at approximately sea level are detectable through about 10 cm of lead. We have performed similar experiments[5] on Mt. Evans (4300 meters). There the "soft component," which constitutes only about 16 percent at sea level, forms about 60 percent of the cosmic rays. Fig. 3 shows the ionization as observed for lead shields of different thickness completely surrounding the chamber. The curve is similar to those given by Schindler, but shows that the transition effects are appreciable to only about 7 cm of lead.[6] This difference presumably corresponds to the higher absorption of the soft rays at this high altitude.

3. The Measurements

A cosmic-ray meter with heavy walls was accordingly carried by Commander T. G. W. Settle and Major C. L. Fordney on their stratosphere balloon flight,[7] on November 20, 1933. The ionization chamber was argon filled, and was surrounded by 9.6 cm of fine lead shot, contained in a hollow sphere of wood, equivalent to about 5.8 cm of solid lead. The 0.3 cm steel wall of the chamber, equivalent to 0.2 cm of lead, made the effective wall thickness equivalent to 6.0 cm of lead. It will be seen from Fig. 3 that this thickness is sufficient to absorb almost completely the secondary rays which are responsible for transition effects. The meter was one of those[8] used on our geographic survey of cosmic rays, fitted however with a recording camera. The argon pressure was reduced to 2.4 atmospheres, insuring saturation with 180 volts across the chamber even for the intense rays near the top of the atmosphere.

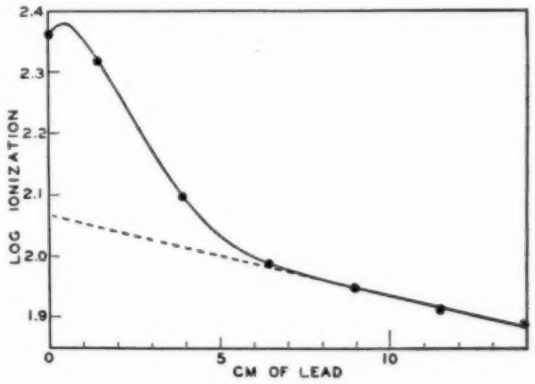

Fig. 3. Transition effect in lead at altitude of 4300 meters.

The motion of the Lindemann electrometer needle was photographed on a standard 35 mm film, moving about 2.5 mm per minute. The needle was automatically returned to a suitable

[4] H. Schindler, Zeits. f. Physik **72**, 650 (1931).

[5] These observations were made by J. C. Stearns in 1931, using the apparatus described by R. D. Bennett, J. C. Stearns and A. H. Compton, Phys. Rev. **41**, 119 (1932). The shield nearest the ionization chamber was copper.

[6] This shorter average range at high altitudes of the secondaries which produce the transition effect has previously been noted by L. M. Mott-Smith and L. G. Howell, Phys. Rev. **44**, 8 (1933), from their airplane measurements. Their data agree closely with those here given.

[7] Cf. A. H. Compton, Proc. Nat. Acad. Sci. **20**, 79 (1934), for account of the scientific observations on this flight.

[8] For description, cf. A. H. Compton and J. J. Hopfield, Rev. Sci. Inst. **4**, 491 (1933).

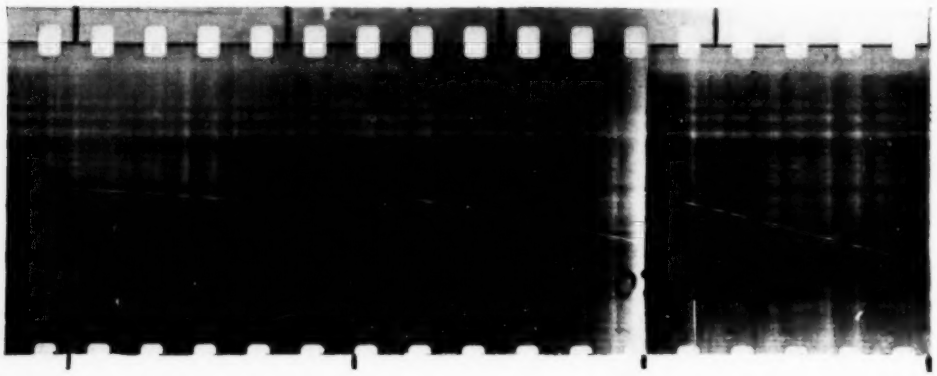

FIG. 4. Trace of shadow of electrometer needle during period of rapid ascension into stratosphere.

initial voltage at successive 10 minute intervals, and once each hour was charged to a known potential for calibration (Fig. 4).

The barometric pressure was determined (1) by direct reading of a double U-tube barometer,[9] and (2) from the record of a barograph placed outside of the gondola.[10] The times and pressures recorded by the observer in his direct reading of the barometer were used as standards, and the barograph record was used only to interpolate between the direct barometer readings. The values of the barometric pressure are probably correct to 1 mm, while the time scales of the barometer and the cosmic-ray record may differ by 1 or 2 minutes.

In Fig. 5, data thus obtained are shown both in the form of a graph of the individual determinations, and of a table showing the mean values. The small solid circles represent the values observed as the balloon ascended. These values are averages over a period of 10 minutes each, except those between 40 cm and 12 cm, which were averaged for 5 periods of one minute each because of the rapid rise of the balloon, and the point at 73.5 cm, which is the average of 2 hours of readings on the ground immediately before the flight. The small open circles show the ionization measured as the balloon descended. When the balloon had descended to a pressure of about 16 cm, the lead shot composing the shield were thrown out as ballast, and no further record was made.

For standardizing the readings, the ionization due to the cosmic rays at ground level (73.5 cm Hg) was taken as 1.81 ions per cm^3 per sec. in standard air, a mean value of many measurements made with similar meters. There was also a correction for "wall radiation" from the chamber itself of 0.85 standard ions, as shown by measurements made with the chamber in a deep mine.

4. Comparison with Other Measurements

Though we find no record of previous measurements with heavy walled chambers at heights comparable with those here attained, studies made on mountains and in airplanes give valuable comparison data. Of the mountain observations, those most directly comparable are the ones recently made by our associated expeditions using instruments essentially the same as the present one. The large open circles shown in Fig. 5 are taken from the curves[11] representing these data on mountains at about the magnetic latitude at which this balloon flight was made, corrected however for a wall radiation of 0.13 ions, which had not been applied to the published mountain data. Our method of standardization makes the balloon datum for 73.5 cm agree with

[9] This barometer was designed and built under the direction of Professor A. Piccard.

[10] We wish to thank Dr. W. G. Brombacher of the Bureau of Standards for furnishing a copy of this record and the result of his analysis for determining the official height (18,665 meters) attained by the balloon.

[11] A. H. Compton, Phys. Rev. **43**, 396 (1933) Figs. 5 and 6.

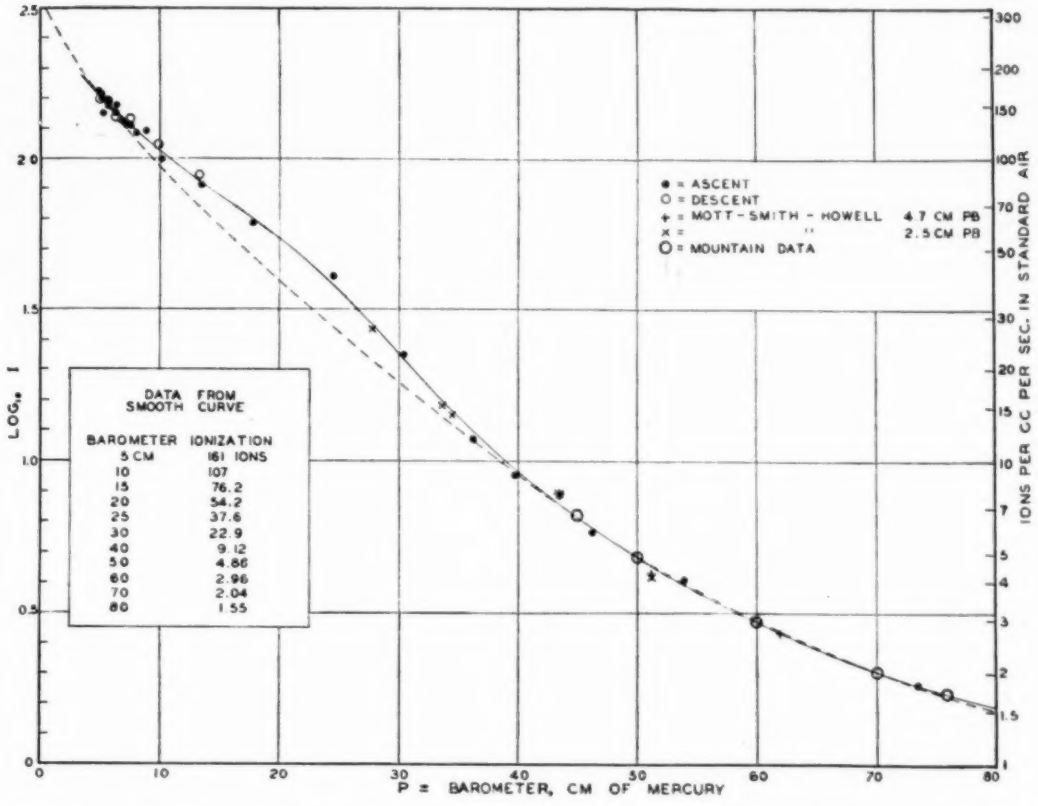

FIG. 5. Ionization as function of atmospheric pressure (altitude) in chamber with walls equivalent to 6.0 cm lead.

our value measured on the ground. The excellent agreement of the balloon data at 54 cm and 46.2 cm with the precision mountain values indicates, however, the reliability of the measurements made in the balloon.

Mott-Smith and Howell[12] have also published data taken with a heavy-walled ionization chamber carried to a high altitude in an airplane by Captain A. W. Stevens. The crosses of Fig. 5 show their data when using a chamber with 1.3 cm steel walls surrounded by 4.7 cm lead shields. Their data are multiplied by such a factor as to bring their lowest recorded datum (at 62 cm) onto our curve. At barometric pressures less than 43.5 cm, the heaviest shield used in Mott-Smith and Howell's experiments was 2.5 cm of lead. Their values thus measured for pressures below 52 cm are here represented by ×'s. These values are adjusted to fall on their datum when using the 4.7 cm shield for the 43.5 cm point. Mott-Smith and Howell's experiments thus supply an independent set of data between 62 and 28 cm that is closely comparable with our own. The agreement is highly satisfactory.

A major feature of the data shown in Fig. 5 is the marked hump in the curve at about 25 cm pressure. The only previous data taken at altitudes sufficient to show this hump clearly are those which have been obtained in balloons by using thin walled chambers. To compare our measurements with those using thin walled chambers we may apply to all the measurements Gross's transformation,[13]

$$\psi = I - PdI/dP, \tag{8}$$

where ψ is the intensity at a barometric pressure P supposing that the radiation enters normally

[12] L. M. Mott-Smith and L. G. Howell, Phys. Rev. **44**, 4 (1933).

[13] B. Gross, reference 3, p. 216. This procedure seems to be rigorous if the cosmic rays are photons, but is questionable if they are of the r-type.

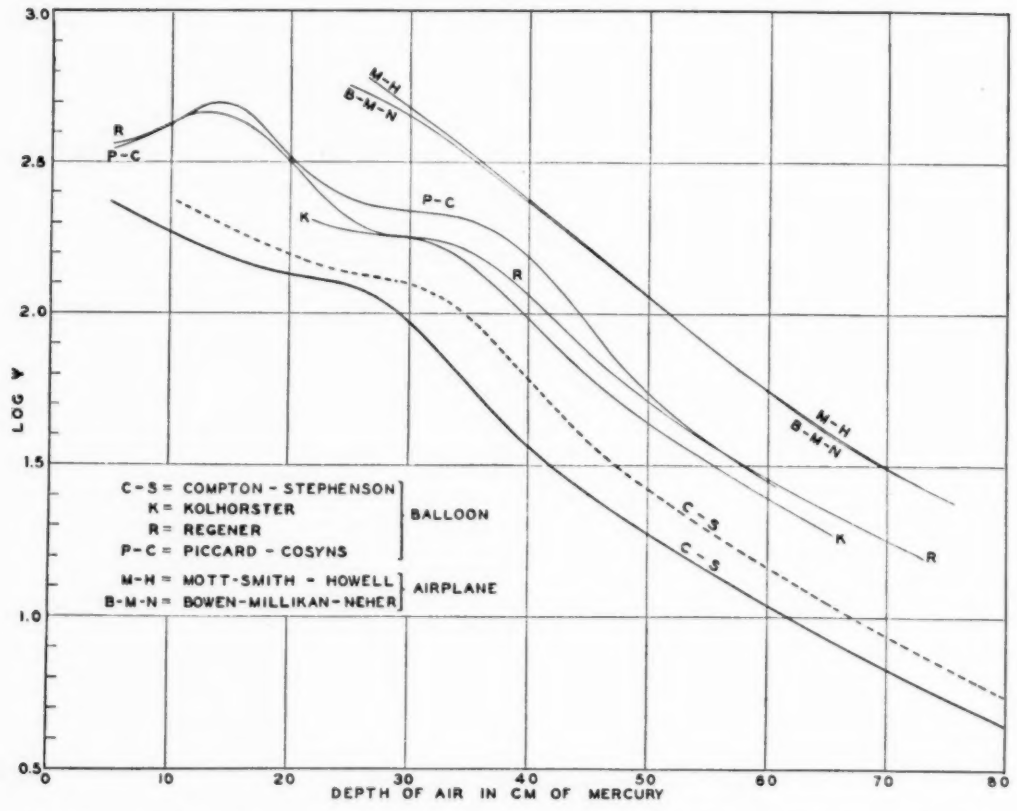

FIG. 6. Intensity of radiation coming vertically through atmosphere (ψ) as found by various observers.

into the atmosphere, whereas I is the observed intensity for the rays which enter from all directions. In Fig. 6 the solid curve C–S represents our experimental data thus transformed. The absorption by our chamber walls is equivalent to a layer of 5.4 cm of mercury in the path of a parallel beam of cosmic rays,[14] so in the dotted line C–S we have plotted the same data for a pressure $P+5.4$. This should be comparable with data obtained from an unshielded chamber after transformation by Eq. (8).

Curve R of this figure is a logarithmic plot of Regener's sounding balloon data as similarly transformed by Gross.[15] Curve K represents Kolhörster's early balloon data[16] similarly calculated, and curve P–C shows the measurements from Piccard and Cosyn's second stratosphere flight.[17] The occurrence of the hump in all four independent experimental curves at about 35 cm pressure would seem to establish its reality.

Two recent series of airplane observations have a somewhat different shape. Curve M-H of Fig. 6 represents the data thus transformed got by Mott-Smith and Howell with no lead shield,[18] and curve B–M–N is that of Bowen, Millikan and Neher[19] at geomagnetic latitude 42°N. All the other curves in this figure represent

[14] 6 cm of lead is equivalent in mass to 5 cm of mercury. A calculation by C. Eckart shows that for our case the absorption by a 5 cm spherical wall is equivalent to that by a 5.4 cm plate placed normally to the beam.

[15] B. Gross, reference 3, p. 218.

[16] Data taken from Hess, *Electrical Conductivity of the Atmosphere* (1928), p. 133, with $I_0=3$ ions.

[17] A. Piccard and M. Cosyns, C. R. **195**, 605 (1932). Curve P of Fig. 6 is based not on the curve given in their paper, which falls markedly below their datum at 34 cm, but upon a smooth curve averaging all of their experimental points.

[18] Mott-Smith and Howell, reference 12. Data taken from their average curve.

[19] I. S. Bowen, R. A. Millikan and H. V. Neher, Phys. Rev. **44**, 248 (1933). Data taken from their smooth curve in Fig. 2.

data from about 51°N geomagnetic latitude. (Curves M–H and B–M–N are shifted upward by a factor of $10^{\frac{1}{2}}$ to avoid overlapping.) These curves give only a slight indication of a hump at 30 cm pressure, though both show an extended portion which is slightly concave downward. The airplane flights were not sufficiently high to extend the cosmic-ray measurements beyond the hump. This probably accounts for the failure of these data to reveal the presence of the hump more clearly.

5. Significance of the Data

A very remarkable fact shown by the data given in Fig. 5 is that over the range from 10 to 40 cm of mercury the log I *vs.* P curve is concave downward. This, as our discussion of Fig. 2 shows, is inconsistent with the assumption that the cosmic rays are absorbed like photons. In fact, the broken curve of Fig. 5, which represents a two component "Gold integral" curve, is approximately the best fit that is possible, assuming cosmic rays of the photon type, if we take the values at 5 cm, 45 cm and 70 cm pressure as experimentally fixed. The departures of this curve from the solid line representing the experimental data become as great as 30 percent, which is much larger than the experimental error.

It has been noted above that the wall of our ionization chamber was thick enough to reduce the transition effects almost to zero. It is worthy of note that Schindler's transition effect measurements extended to thicknesses of lead up to 36 cm, and showed no irregularity such as that appearing in our intensity data at 20–30 cm of mercury. There thus appears no reason to ascribe the downward curvature of our experimental log I *vs.* P curve in this region to a transition effect.

On the other hand, the experimental curve can be completely accounted for in terms of ionization by particles of the r-type. Gross notes[20] that the range distribution of the r-particles necessary to account for the ionization I is given by

$$R = -d\psi/dP, \tag{9}$$

where R is defined as in Eq. (6) and ψ as in Eq. (8). By using the dotted curve of Fig. 6 for ψ, which has been corrected for absorption in the chamber wall, Fig. 7 shows the corresponding range distribution as calculated by Eq. (9). That is, this curve (Fig. 7) represents the range

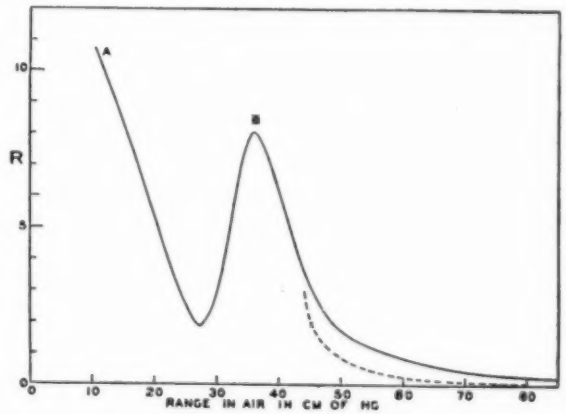

Fig. 7. Range distribution of ionizing particles entering atmosphere required to give observed ionization *vs.* altitude curve. Broken line, range distribution for component of cosmic rays deflected at equator by earth's magnetic field.

distribution of the r-particles entering the atmosphere which would give the experimental ionization pressure curve.

A straightforward analysis of our data in terms of r-particles thus shows, even after due allowance for the uncertainty of graphic differentiation, the presence of two sharply distinct range groups. One group A appears to have ranges of all values, with a maximum for very short ranges (less than 10 cm of mercury). In the other group B there appear to be no rays of range less than about 27 cm and a strong maximum at about 36 cm.

6. Origin of Range Group B

Clay's latitude effect, as confirmed and extended by our survey expeditions, has revealed a component of the cosmic rays which, being magnetically deflectable, must consist of electrically charged particles (more specifically, positively charged, in view of the Johnson-Alvarez-Rossi directional experiments). The theories of

[20] B. Gross, reference 3, p. 217. We use expression (9) instead of (7) to calculate R because the derivation applies to a thin walled chamber. The R *vs.* r curve is deformed due to the effect of the wall if Eq. (7) is used.

Störmer,[21] Rossi,[22] Lemaitre and Vallarta[23] and others have shown that at a given latitude, particles with less than a certain speed are so deflected by the earth's magnetic field that they cannot reach its surface. Peak *B* of Fig. 7 can thus be explained as due to electrically charged particles which occur in space with a wide range of energies, of which however only those with kinetic energy equivalent to a range in air of more than about 27 cm of mercury are able to penetrate the magnetic barrier at a latitude of 52 degrees.

According to Lemaitre-Vallarta's Fig. 1, the intensity *vs.* latitude curve which is steepest at 52 degrees is that for which their function $x_0 = 2.1$. This value should correspond approximately to the peak of our range curve (Fig. 7). By their Table VI, the value of the function $x_0 = 2.1$ corresponds to the following energies:

Electrons or positrons,	2.6×10^9 e.v.
Protons,	1.9×10^9 e.v.
Alpha-particles,	2.6×10^9 e.v.

The energy that a particle must have for a range of 36 cm (peak *B*) can be estimated most directly from experiments such as those of Anderson, which measure the energy loss of cosmic-ray particles on traversing plates of lead. He finds[24] that for electrons with energies of the order of 3×10^8 volts the average rate of energy loss in lead is 3.5×10^7 electron-volts per cm. He has preferred to use however a calculated value of 2.0×10^7, and has told us in conversation that later experiments indicate that the value 3.5×10^7 is too high. We shall use the mean of these values, 2.8×10^7 electron-volts per cm of lead. Following Anderson's procedure, this corresponds to 5500 volts/cm in standard air, or 4.4×10^9 electron-volts to penetrate vertically through the atmosphere. To penetrate to 36 cm of mercury this means, for electrons, positrons or protons, an energy of about 2.1×10^9 electron volts. For alpha-particles the energy would need to be about 4 times greater, or 8.4×10^9 electron-volts.

[21] C. Störmer, Zeits. f. Astrophysik **1**, 237 (1930).

[22] B. Rossi, Acc. d. Lincei **15**, 62 (1932).

[23] G. Lemaitre and M. S. Vallarta, Phys. Rev. **43**, 87 (1933).

[24] C. D. Anderson, Phys. Rev. **44**, 409 (1933).

Comparison of these values with those required by the magnetic deflection shows close agreement if the range group *B* is due to protons, an impossibly great difference in the case of α-particles, and a difference which is within the limits of error in the case of positrons or electrons. Noting that electrons are ruled out by the directional experiments, this means that the particles responsible for range group *B* are most probably protons. They cannot be alpha-particles. It is possible, but less probable, that they are positrons.

7. Ionization due to Cosmic-Ray "Protons"

The difference between the ionization measured at the geomagnetic latitude of our present experiments (52°N) and at the geomagnetic equator represents the ionization due to magnetically deflectable charged particles. If the above analysis is correct, these must be a part of those appearing in range group *B*. By comparing our present data with those which we obtained with similar apparatus on equatorial mountains we can determine the variation with altitude of the ionization due to this electrically charged component. In Fig. 8 are plotted *A*, the cosmic-ray ionization at geomagnetic latitude 52°N (from Fig. 5), *B* that at 3°S (from Fig. 6, reference 11, corrected for wall radiation of 0.14 standard ions), and curve *C* the difference

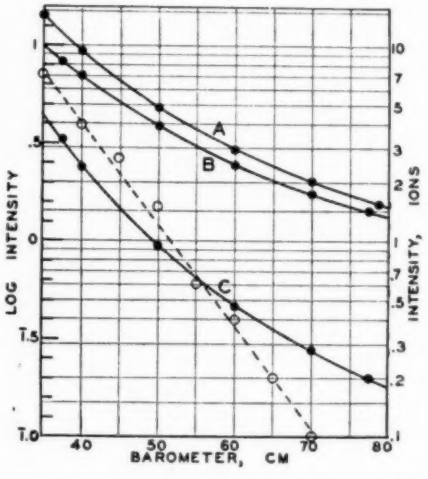

FIG. 8. Intensity *vs.* barometer curves for, *A*, high magnetic latitudes, *B*, magnetic equator, *C*, difference between *A* and *B*, showing that equatorial rays *B* are absorbed in same manner as magnetically deflectable rays *C*.

between the two ionizations. Curve C thus represents the ionization at different altitudes by rays which are known to be electrically charged, ionizing particles, and which are probably protons.

A similar comparison is possible from the airplane data recently published by Bowen, Millikan and Neher.[19] The dotted curve of Fig. 8 shows the difference between their values near the equator and at 42°N (geomagnetic). The differences between this and our curve C are partly ascribable to the different latitude range involved, and partly to the fact that our chamber was shielded by heavy lead walls. The curves however agree in showing an ionization altitude relation of an approximately exponential type. Since curve C is known to be due to charged particles, it is thus evident that we should err if we inferred from an exponential type of curve that it was due to photons.

Analysis of curve C according to expressions (8) and (9) gives the dotted line of Fig. 7. Since curve C is itself a difference curve, and since it is twice differentiated to obtain this dotted curve, slight experimental errors are greatly magnified. Nevertheless the trend of the curve is in good accord with the view that it is these magnetically deflectable particles which are responsible for the range group B.

Though the directional experiments of Johnson[25] and Rossi[26] have shown magnetically deviated particles at the equator, these must have ranges greater than the depth of the atmosphere. We should accordingly predict the absence of a hump due to the range group B appearing in high altitude measurements near the geomagnetic equator. The same reasoning indicates that the range corresponding to the maximum of this group should be shorter and the peak more prominent at high latitudes than at low latitudes.[27] High altitude experiments at different latitudes should thus give an important test of our interpretation of the origin of this peak.

[25] T. H. Johnson, Phys. Rev. **44**, 856 (1933).

[26] B. Rossi, Phys. Rev. **45**, 212 (1934).

[27] Examination of the data collected in Fig. 6 offers some support of this prediction.

8. Origin of Range Group A

From the shape of the curve of Fig. 7 it would appear possible that the radiation which is responsible for range group A may be almost completely absorbed in the upper part of the atmosphere. If this is true, we should need to account for the cosmic rays received at the equator as well as those at high latitudes in terms of the higher energy protons (or positrons) of group B, with the addition of the more penetrating radiations which do not show in this analysis. The strong directional effects observed near the equator by Johnson and Rossi lend support to this view.

That the nature of the cosmic rays at the equator is similar to that of the magnetically deflectable particles of group B is also shown by their similar absorption and transition effects. We have noted above the similarity in form of the absorption curves B and C of Fig. 8, which are due respectively to equatorial and to magnetically deviable cosmic rays. The similarity of their transition effects is shown by experiments made by our associated expeditions at various latitudes comparing the ionization with 1 and with 2 shields of 2.5 cm lead. The value of this ratio varies from 1.15 at sea level to 1.49 at 5800 meters, but shows no systematic variation with latitude. The measurements[28] given in Table I are typical. Since the fraction of magnetically deviable rays present in the cosmic rays is much greater at the higher latitudes, the constancy of this ratio i_1/i_2 means that the transition effect is substantially the same for the rays unaffected by the earth's magnetic field as it is for those which are thus affected.

Table I.

Place	Geomag. Lat.	Barometer	i_1/i_2
Mt. McKinley	67°N	50.0 cm	1.312
Jungfraujoch	49°N	50.0	1.302
Mt-aux-Sources	30°S	54.5	1.300
Chicla	1°S	48.6	1.312

The short range values of R (Fig. 7) are consistent with the assumption either that group A is electrically neutral (since no lower range

[28] A. H. Compton, reference 11, Table III.

limit appears), or that it is due to particles of large ratio of mass to charge, such as α-particles or heavier nuclei. If these rays do not penetrate the atmosphere, we do not find any existing data on which to base a choice between these hypotheses. The graphic differentiation leading to Fig. 7 is however not sufficiently reliable to justify extrapolating range group A to zero. It is not impossible that they may constitute an important part of the rays at sea level which are not found to be appreciably affected by the earth's magnetic field. If this is the case, the similarity between the equatorial and the magnetically deviable cosmic rays would suggest that these neutral rays may consist of hydrogen atoms, which on entering the atmosphere are broken into their component protons and electrons. It would be difficult to reconcile this similarity with the assumption of any considerable photon or neutron radiation in the equatorial cosmic rays as observed at the earth's surface.

On this view the photons which occasionally show themselves in cloud expansion experiments would be secondary rays, of the nature of x-rays produced by the passage of the high speed protons and electrons through the matter above the expansion chamber. Some of Anderson's recent experiments[29] which indicate showers of photons from a common source give direct indication of such an origin. Rossi[26] has also felt the need of some such catastrophic act in the stopping of charged cosmic-ray particles. X-ray experiments, which show in the range of x-ray voltages an increase in efficiency of x-ray production proportional to the energy of the cathode rays, suggest that such a transformation of a cosmic-ray particle's energy into x-ray photons may be a highly probable event.

9. The Apparent Nature of the Cosmic Rays

Our ionization-altitude curve obtained on the Settle-Fordney stratosphere flight is thus found to be inconsistent with the view that the cosmic rays enter the atmosphere as photons. It is however explicable in terms of ionizing particles with a definite range. Direct analysis of the data shows the existence of a group of rays with ranges greater but not less than the air equivalent of about 27 cm of mercury. Comparison with the effect of the earth's magnetic field shows that these rays are probably protons, or possibly positrons. The remaining rays (group A) show no lower range limit, and are thus either electrically neutral, or have a large ratio of mass to charge. These rays seem to be more strongly absorbed than those of group B, and may be confined to the upper atmosphere. Our measurements would be consistent with the view that some of the cosmic rays which reach the earth's surface enter the atmosphere as hydrogen atoms. The similarity in properties of the equatorial cosmic rays with those which are magnetically deflectable, however, leaves no room for any considerable admixture of photons in the primary cosmic rays which reach the earth. These conclusions are in complete accord with the various coincidence experiments which have seemed to demand a corpuscular character for the cosmic rays.

10. Acknowledgments

Without the cordial, careful and skillful cooperation of Lt. Commander T. G. W. Settle and Major C. L. Fordney in flying the balloon and handling the instruments these data could not have been obtained. To the sponsors of the flight, A Century of Progress Exposition, the *Chicago Daily News*, the National Broadcasting Company, the Union Carbide and Carbon Corporation and the Dow Chemical Company, we are indebted for the use of the balloon and for supplying needed equipment. Professor A. Piccard gave us helpful suggestions regarding the design of our instruments and equipment. Professor C. Eckart has helped us with the mathematical analysis. Most of the cost of the scientific work was borne by A Century of Progress Exposition and the Carnegie Institution of Washington.

[29] C. D. Anderson and S. H. Neddermeyer, Phys. Rev. **45**, 295 (1934).

The Influence of the Ionization Chamber on the Form of the Cosmic-Ray Depth-Ionization Curve

CARL ECKART, *Ryerson Laboratory, University of Chicago*

(Received February 23, 1934)

On the assumption that cosmic rays are absorbed exponentially, it is shown that the absorption of an homogeneous beam in the wall of a spherical ionization chamber can be approximately represented by a factor $\exp(-kd)$, where k is the absorption coefficient and d is an effective wall-thickness which is independent of k. This having been established, it is possible to treat the transition effects occurring in the atmosphere and the wall of the chamber. It appears that if the effective wall-thickness is great enough, the depth-ionization curve should be concave upward at every point. Since this has been shown not to be the case (Compton and Stephenson) the assumption of exponential absorption is not capable of accounting for the facts in their entirety.

THE following calculations are based on the assumption that an homogeneous unidirectional beam of cosmic rays is absorbed according to an exponential law, similar to electromagnetic radiation of lower penetrating power. They were intended to be used in the interpretation of the high altitude data obtained by Compton and Stephenson[1] but these authors concluded that it was not possible to reconcile the data with the calculations, and that the assumption is therefore very dubious. This paper arrives at the same conclusion, but considers the theory in more detail.

1. The Effective Wall-Thickness of a Spherical Ionization-Chamber

Let the ionization chamber have an inner radius r, an outer radius R, and set $s=R-r$. Suppose an homogeneous unidirectional beam of rays to be incident upon the chamber and consider an elementary cylinder of the rays, whose axis passes through the center of the chamber and whose radii are ρ and $\rho+d\rho$ (see Fig. 1). These rays will traverse a thickness ξ of wall and ionize a path of length 2η inside the chamber; their amount will be proportional to $2\pi\rho d\rho$. From this it follows that the average ionization per unit volume of the chamber is proportional to

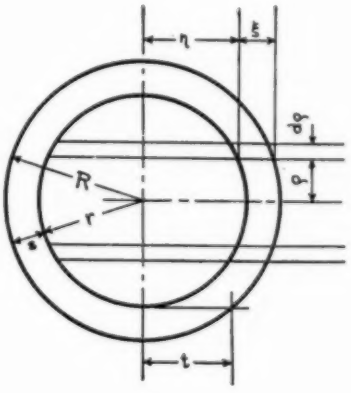

FIG. 1.

$$H(k, r, R)=(3/r^3)\int_{\rho=0}^{r}\exp(-k\xi)\cdot\eta\rho d\rho, \quad (1)$$

k being the absorption coefficient of the rays in (cm wall material)$^{-1}$. On introducing the new variable $z=\eta/r$, this integral becomes

$$H=3\int_{z=0}^{1}\exp(-k\xi)\cdot z^2dz, \quad (2)$$

and

$$\xi=(l^2+r^2z^2)^{\frac{1}{2}}-rz, \quad l^2=R^2-r^2. \quad (3)$$

Other transformations suggest themselves, but do not lead to essential simplifications; it has not been found possible to evaluate the integral except as a cumbersome series obtained as follows. The function $\exp(-k\xi)$ has singularities for $z=\pm it/r$, but for no other finite values of z. It may therefore be expanded as a power series

[1] A. H. Compton and R. J. Stephenson, Phys. Rev. **45**, 441 (1934).

in $(z-1)$ which will converge for $|z-1|<R/r$, and hence converge uniformly for $0\leq z\leq 1$, so that the series may be substituted in the integral. It is easily seen that the series has the form

$$\exp(-k\xi)=\exp(-ks)\{1+a_1(z-1)/1! +a_2(z-1)^2/2!+\cdots\} \quad (4)$$

and the coefficients a_n are readily calculated by means of Taylor's theorem: letting

$$\kappa=kr,\quad \sigma=s/R,\quad \gamma=t/R,\quad \beta=r/R, \quad (5)$$

the first four are

$$\begin{aligned} a_1&=\kappa\sigma,\\ a_2&=\kappa^2\sigma^2-\kappa\beta\gamma^2,\\ a_3&=\kappa^3\sigma^3-3\kappa^2\beta\gamma^2\sigma+3\kappa\beta^3\gamma^2, \quad (6)\\ a_4&=\kappa^4\sigma^4-6\kappa^3\beta\gamma^2\sigma^2+3\kappa^2[\beta^2\gamma^4+4\beta^3\gamma^2\sigma]\\ &\quad +3\kappa\beta^3\gamma^2[\gamma^2-4\beta^2]. \end{aligned}$$

On noting that

$$3\int_0^1 z^2(1-z)^n dz=3!n!/(n+3)! \quad (7)$$

the series for II is found to be

$$II=\exp(-ks)\{1-(a_1/4)+(a_2/20) -(a_3/120)\cdots\}. \quad (8)$$

This series was evaluated numerically for the two ionization chambers described by Compton and Stephenson[1] and Millikan.[2] It was unexpectedly found that the results could be represented by

$$II=\exp(-kd) \quad (9)$$

where d, the thickness of an equivalent plane parallel screen, was independent of k. No theoretical reason for this has been found, but the result was verified for four widely spaced values of k for each of the two chambers. The dimensions of the chambers and the values of d obtained follow:

	R	r	s	t	d	
Compton-Stephenson	12.5	4.7	7.8	11.6	8.5	cm
Millikan	16.0	15.7	0.3	3.1	0.41	cm

While Eq. (9) is sufficiently accurate for most purposes, Eq. (8) must be used when high precision is needed.

[2] R. A. Millikan, Phys. Rev. **39**, 397 (1932).

2. The Ionization as a Function of Barometric Height and Wall-Thickness

Suppose homogeneous radiation of unit intensity be incident from all directions upon the top of the atmosphere and let it be required to calculate the ionization produced in a spherical chamber of effective wall-thickness d, located at a place where the barometric height is h. In order to enter the chamber, the rays must traverse various thicknesses of air and wall. In so doing they will be diminished in intensity and secondary rays will be formed, both in the air (air-secondaries) and in the wall (wall-secondaries). This process has been discussed by Johnson[3] in connection with the transition effects investigated by Schindler[4] and others. The present discussion is different only in that the directional distribution is taken into account, which is formally equivalent to replacing exponential functions by Gold functions, G.

Let p, a, w be the numbers of primaries, air-secondaries, and wall-secondaries entering the chamber per second. Then it is readily seen from Johnson's equations that

$$\begin{aligned} p&=G(\nu_a h)\exp(-\nu_w d),\\ a&=\alpha_a[G(\nu_a h)-G(\mu_{aa}h)]\exp(-\mu_{wa}d), \quad (10)\\ w&=\alpha_w[\exp(-\nu_w d)-\exp(-\mu_{ww}d)]G(\nu_a h), \end{aligned}$$

where

ν_a, ν_w are the absorption coefficients of primaries in air and wall,

μ_{aa}, μ_{wa} are the absorption coefficients of air-secondaries in air and wall,

μ_{ww} is the absorption coefficient of wall-secondaries in the wall,

α_a, α_w are the efficiencies of production of secondaries in air and wall.

If I_p, I_a, I_w, are the ionizing powers of the three types of radiation, the measured ionization will be

$$I=pI_p+aI_a+wI_w. \quad (11)$$

It is obvious that the three terms of this expression will depend on d and h in various manners. The nature of the differences produced by varying d can best be understood by con-

[3] T. H. Johnson, Phys. Rev. **41**, 545 (1932).

[4] H. Schindler, Zeits. f. Physik **72**, 625 (1931).

sidering two limiting cases: thus if $d=0$, the ionization is given by

$$I_{\text{thin}}=AG(\nu_a h)-BG(\mu_{aa}h), \qquad (12)$$

where A and B are positive constants. A typical graph of this function is given in Fig. 2; the curve is convex upward for smaller values of h and does not become concave until $\mu_{aa}h$ is considerably greater than 1. Fig. 2 was constructed

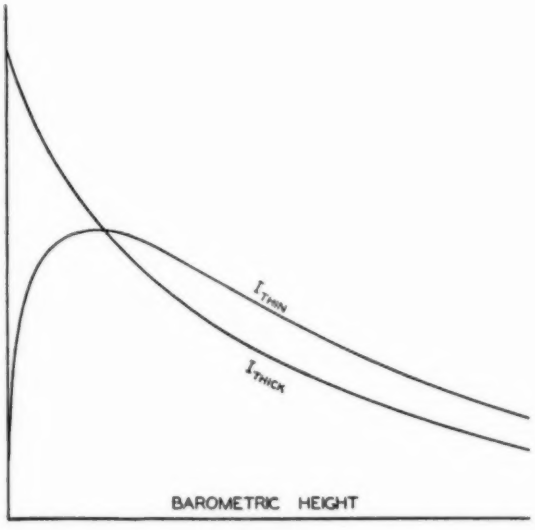

FIG. 2.

for the case of small I_p, most of the ionization being due to the secondaries. As these are formed only in air (the wall being thin) and none are present when $h=0$, the ionization at this point is small and proportional to I_p. The curve rises as the number of secondaries accompanying the primaries increases and does not become concave until the ratio a/p has sensibly attained its limiting value of α_a. It is very probable that the Millikan ionization chamber approximates closely to this limiting case, although numerical data to make a really satisfactory calculation are lacking.

The other limit is that of a thick-walled chamber: if the secondary rays are less penetrating than the primaries, it is always possible to filter them out by choosing d so great that $\exp(-\mu d) \ll \exp(-\nu d)$. Then the ionization is given by

$$I_{\text{thick}}=CG(\nu_a h)\exp(-\nu_w d), \qquad (13)$$

where C is again a *positive* constant. The graph of this function is also shown in Fig. 2; it is very important to note that the graph is everywhere concave upward. No maximum occurs in this case because no air-secondaries can enter the chamber, and the ratio w/p is independent of h. Thus even for $h=0$ the ionization will be due largely to wall-secondaries, and since these are more powerful ionizing agents than the primaries, the curve I_{thick} is initially higher than I_{thin}. It is not until the air-secondaries have begun to approach equilibrium with the primaries that this paradoxical situation disappears and the stopping power of the wall causes the curves to assume the expected configuration. The depth at which the intersection occurs will be strongly dependent on the properties of the air- and wall-secondaries. It is probable that the Compton-Stephenson chamber approximates this case.

The actual cosmic radiation is undoubtedly not homogeneous, but this merely results in the superposition of functions like (12) or (13). It is probable that any depth-ionization curve could be fitted by functions like (12) having both positive and negative coefficients, but *only curves which are everywhere concave upward* can be fitted by functions like (13) with *positive* coefficients. Since the curve obtained with the Compton-Stephenson chamber exhibits a convex range,[1] it follows that one of the assumptions in the foregoing discussion is not in agreement with the facts. The peccant assumption is undoubtedly the one mentioned in the introduction.

The author desires to acknowledge his indebtedness to Professor A. H. Compton for many stimulating comments and to Mrs. G. S. Monk for carrying out the numerical computations involved.

Confirmation of Crystal Wave-Length Measurements and Determination of $h/e^{4/3}$

PAUL KIRKPATRICK AND P. A. ROSS, *Stanford University*

(Received January 29, 1934)

By observation of x-ray continuous spectrum isochromats the potential necessary for the production of general radiation capable of reflection from calcite at a known Bragg angle θ has been determined. By using a double spectrometer and tungsten source, and reflecting at the Bragg angle for Ag $K\alpha_1$ the value $V'\sin\theta = 2035.3 \pm 0.2$ international volts has been obtained. This is very close to Feder's value, 2036.0. In agreement with Feder it is concluded that Wagner's "low" value is in error because of experimental conditions and that this error can not now be rectified. It is shown that the "high" value of Duane, Palmer and Yeh is subject to certain calculable corrections which lower it to 2034.6, in much closer agreement with present results. The wave-length of Ag $K\alpha_1$ as given by the law of Duane and Hunt is found to be in agreement with the value obtained from crystal measurements and at variance with ruled grating results. Utilizing crystal wave-length measurements by Bragg's law the present results yield $h/e^{4/3} = (1.7559 \pm 0.0002) \times 10^{-14}$ if Birge's (1929) auxiliary constants are employed, and 1.7563 with more recently determined values of five of these constants. Assuming the 1930 oil drop value $e = (4.770 \pm 0.005) \times 10^{-10}$ e.s.u. this investigation gives $h = (6.546 \pm 0.006) \times 10^{-27}$ erg·sec.

INTRODUCTION

SINCE the equations which are useful for determining the values of the more fundamental physical constants frequently contain more than one such constant it is advantageous to evaluate the several constants together, as in the method of Bond[1] for e, h and m, by using numerical data from a variety of experiments, each concerned with the investigation of some one of the several available relations which connect these constants. In this situation it is very desirable that all such relations which are to participate in a final evaluation be known with something like comparable accuracy, as otherwise the superior accuracy of some will not be fully effective.

Among the relations connecting h and e the value of $h/e^{5/3}$, obtained from the Rydberg constant, is known with outstanding accuracy, a fact which makes it very desirable to improve the precision of the other accessible relations. The x-ray experiment presently to be described offers this possibility and has been performed to this end several times in the past, but unfortunately these past investigations (to be discussed in a later section) are not in good agreement. Kirchner[2] has recently emphasized the desirability of new work upon the relation between h, and e by this method.

The minimum wave-length of the continuous x-ray spectrum is related to the cathode electron potential fall by the equation $Ve = hc/\lambda$. Upon measuring corresponding values of V and λ one obtains a numerical value of a relation between h and e. If λ has been measured by an absolute method, for example with a ruled grating, this relation is simply h/e. However, if the value of λ is got by crystal reflection it is dependent upon the crystal grating constant which, at present, can be evaluated only through a process involving e in such a way that one obtains finally a numerical value of the ratio $h/e^{4/3}$. The existing discrepancy between wave-length measurements by grating and crystal methods makes a premature commitment to either method inadvisable and we shall defer this decision and state experimental results in terms of the more directly measured quantity $V'\sin\theta$, the product of electron potential fall (in international volts) by the sine of the Bragg angle employed in our experiment. Since the V' and θ thus combined are associated with vanishing x-ray intensity we cannot realize them by a direct observation but only by extrapolating to zero intensity a curve of intensity against either θ or V'. We have employed the latter method, that is, θ has been maintained at a single fixed value and curves of

[1] Bond, Phil. Mag. **10**, 994 (1930); **12**, 632 (1931).
[2] Kirchner, Ann. d. Physik **13**, 59 (1932).

reflected intensity against tube potential (isochromats) have been observed through a voltage range including V'.

Experimental Procedure

A double spectrometer with large polished calcite crystals was used. Very little incoherent scattering comes through the double spectrometer so the backgrounds of the isochromats were kept quite faint. The x-ray tube used in preliminary runs had not been outgassed by heating, and was operated in continuous connection with its pumps. It was found impossible to keep the target of this tube sufficiently clean to avoid electron retardation in the contaminating surface layer. Upon starting with a clean target this layer steadily increased in thickness, as evidenced by a steady shift of successive isochromats toward higher voltages. It is true that the initial voltage for a given wave-length should be independent of the target material, whether metal or grease residue. The *slopes* of the isochromats are very different in these two cases, however, so that the effect of a dirty target is to produce a shifted isochromat from the underlying metal with a small foot of very much reduced slope, vanishing at the true critical voltage for the wave-length received. Since in all cases isochromats possess feet due to other causes it is out of the question to try to interpret quantitatively the effect of the target uncleanliness and the only alternative is to eliminate it. We have therefore obtained all final isochromats from a G.E. deep therapy tube. These tubes are baked out for several hours while under load in the process of manufacture and even old tubes show no visible contamination on the focal spot. The tungsten target also furnishes a relatively strong continuous spectrum.

Tube potential was supplied by rectified and filtered 580 cycle a.c. with an approximately sinusoidal ripple of less than 5 volts under our conditions of operation. Voltage was controlled by a rheostat in the field circuit of the 580 cycle generator. For voltage measurement a resistance was connected in parallel with the x-ray tube consisting of about 6 megohms of "copnic" wire (R_M) with a manganin-wound decade box (R_B), cut in at its center. The resistance of this central box was adjusted to be a known fraction (about 1/10,000) of that of the remaining 6 megohms and the potential drop across the central box was measured with a potentiometer. Whenever a spectrometer observation was in progress an assistant kept the potentiometer in balance at a preselected setting by manipulating the generator field rheostat. The magnitude of the fluctuations of the potentiometer galvanometer indicated that the high potential fluctuations were kept within 2 volts of the desired value throughout any one spectrometer observation.

This method of high potential measurement does not require knowledge of the absolute values of any resistances but does call for precise adjustment of the ratio of the resistances R_M and R_B. This adjustment was accomplished in two steps by Wheatstone bridge operations, making use of a pair of standard resistances as ratio arms whose nominal values were 100 and 10,000 ohms and whose more exact values were given by Bureau of Standards certificates. The purpose of the first bridge was to adjust a box resistance R_S, to a value one rth that of R_M, where r is the ratio of the larger standard resistance to the smaller. Similarly the second bridge permitted R_B to be adjusted to one rth of R_S or $1/r^2$ times R_M. The sensitivity of the bridge was such that a change of one part in 50,000 in the variable arm of the balanced bridge resulted in a readable deflection of the potentiometer galvanometer from its null position. Due precautions against thermal e.m.f.'s and resistance changes in the bridges were observed. The bridge balancing operations were performed before and after each set of isochromat observations. The dial readings of the boxes making up R_B were usually identical to one part in 50,000 for the two balances taken before and after a run, but from day to day these readings varied from their mean as much as one part in 10,000. If this resulted from a real change in R_M it does not impair the accuracy of the voltage measurement, and the fact that no significant correlation exists between the residuals of R and of V' for the several isochromats tends to indicate that this is the case. Nevertheless this variation presents the largest single source of uncertainty in our final voltage determination.

Corrections

The potential difference V' is not identical with the measured drop across R_M and R_B, and the several essential corrections will now be described. As Fig. 1 shows, a choke coil R_C, provided for protective purposes is inserted in such a position that it carries the target current of 22.0 m.a. The resistance of the choke coil and milliammeter is 3270 ohms so it is necessary to *subtract* from V_M, the drop across R_M, the 71.9 volt drop across the choke and meter. All other high tension line drops were shown by direct resistance measurements to be negligibly small.

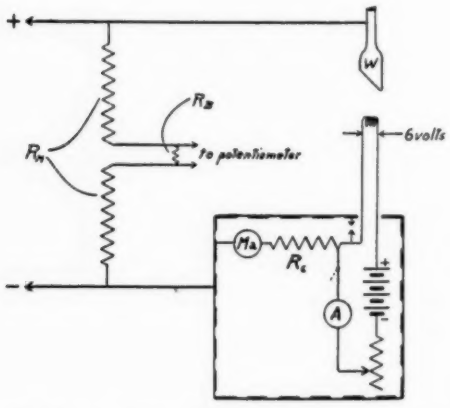

FIG. 1. Wiring diagram. The potentiometer is approximately at ground potential.

The electrons effective in producing x-rays may be emitted from any part of the filament, and since a potential drop (6 volts) occurs along the filament the potential fall from filament to target will not have a common value for all electrons. Assuming uniform emission along the filament Feder[3] has shown that the straight part of the isochromat obtained under these conditions is characteristic of the electrons from the center of the filament. Taking account of the current direction in our filament this means that 3 more volts must be *subtracted* from V_M. The adoption of an even 3 volts for this correction depends upon the assumption that the effective center of electron emission coincides with the potential center of the filament. In view of possible temperature non-uniformity along the filament and differential space charge limitations it is impossible to claim that this assumption is entirely correct. It seems unlikely, however, that the error which results is greater than a few tenths of a volt.

The electrons leaving the filament are emitted with velocities which correspond on the average to about 0.2 volt. This voltage is to be *added* to V_M.

Upon arriving at the target and entering the metal the electrons are subject to attractive forces which confer upon them an increment of energy corresponding to the work function of the target material. We therefore *add* to V_M the work function[4] of tungsten or 4.5 volts.

The potential applied to the tube was, as stated, slightly rippled. It can be shown that the isochromat produced by a potential with a small symmetrical ripple is, in its straight portion, identical with that produced by constant potential having the same average value. Since the potential measuring system measures average voltage the existence of ripple may be ignored.

A similar conclusion may be drawn regarding the effect of the finite wave-length band reflected by the spectrometer crystals. In the double spectrometer the width of this band is not determined by the slit system but is characteristic of the nature and treatment of the crystals themselves. The width and shape of the band of radiation passed by our spectrometer is known, and we have analyzed its effect upon the isochromat (a term which strictly speaking is here a misnomer) in a thorough study which is withheld here only for reasons of economy. The conclusion obtained is that the straight part of the isochromat so produced is indistinguishable (except perhaps in absolute ordinate scale) from the isochromat produced by an indefinitely narrow wave-length band at the peak (center) of the spectrometer transmission band. While as stated above this is not a slit problem the argument and conclusions are closely analogous to those which apply to slit effects, a subject to which we shall return in a later section of this paper.

[3] Feder, Ann. d. Physik [5] **1**, 497 (1929).

[4] We are indebted to Mr. R. H. Varian for bringing to our attention the necessity for including this correction.

Determination of θ

Errors in the measurement of the angle of reflection, θ, have been all but eliminated through the use of the Bragg angle of reflection of Ag $K\alpha_1$. This angle has been determined with great care in several different laboratories and is certainly known with higher precision than we are at present able to utilize. The mean of determinations by Leide,[5] Lang,[6] Kellström,[7] Cooksey,[8] Bearden[9] and Ross[10] when adjusted to the working temperature of this investigation (20°C) gives $\theta = 5°\ 17'\ 13.7'' \pm 0.4''$, or $\sin\theta = 0.092147 \pm 0.000002$, the index of precision being the statistical probable error of the six determinations.

To obtain this angle a silver target tube was mounted before the spectrometer, the $K\alpha_1$ line found and a setting made on its peak. The symmetry of the line was excellent and the peak could readily be located within 0.3''. After this setting the silver tube was replaced by the tungsten target therapy tube and the spectrometer was left untouched during the observation of isochromats. When these data were complete the silver line was observed again and found to be unchanged in position by any amount as large as the uncertainty of location of the peak.

Determination of V' and $V' \sin\theta$

Eleven isochromats (see Fig. 2) were obtained in a series of runs extending over five days. Room temperatures during these observations varied between 19 and 21°C. Observations were taken at intervals of ten or in a few cases twenty volts. The background, the curved foot and the linear isochromatic portion are sufficiently evident in the figure. In obtaining the critical voltage corresponding to the angle θ the linear portion was produced downward to its point of intersection (P) with the extrapolated background. The abscissa of P is the desired potential. Both extrapolations (for all isochromats) were

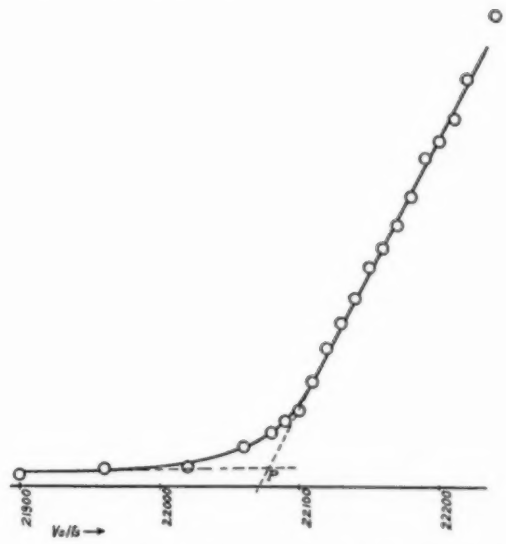

Fig. 2. One of eleven isochromats used in this investigation. Ordinates are ionization currents in arbitrary units.

performed by least squares assuming the background to be parabolic and the upper segment linear. It is unprofitable to extend these curves upward to higher voltages since the isochromat undergoes a rather abrupt decrease in slope at about 150 volts above its excitation potential, as Wagner[11] and others have shown.

The weighted mean value of V' from all data is $V' = 22087.5 \pm 1.5$ volts. The probable error attached includes the statistical probable error of the eleven values (0.005 percent) and the probable errors of all quantities entering into the calculation of the voltage and voltage corrections. Combining this result with the mean value of θ one obtains $V' \sin\theta = 2035.3 \pm 0.2$ international volts.

Before proceeding to discuss the effect of this determination upon the values of e or h it will be of interest to note (Table I) that the present

Table I. *Results of determinations of V' sin θ.*

Determined by	As determined	Adjusted
Duane, Palmer and Yeh	2039.9 ± 0.9	2034.6 ± 0.9
Wagner	2031.5 ± 3.0	
Feder	2036.0 ± 1.0	2036.0 ± 1.0
Kirkpatrick and Ross	2035.3 ± 0.2	

[5] Leide, Diss. Lund. (1925).
[6] Lang, Ann. d. Physik **75**, 489 (1924).
[7] Kellström, Zeits. f. Physik **41**, 516 (1927).
[8] Cooksey, Phys. Rev. **36**, 85 (1930).
[9] Bearden, Phys. Rev. **43**, 92 (1933).
[10] Ross, Phys. Rev. **44**, 977 (1933).
[11] Wagner, Ann. d. Physik **57**, 401 (1918).

value is in rather good agreement with that of Feder and stands about midway between the widely discrepant values given by Wagner[12] and by Duane, Palmer and Yeh.[13]

Critique of Former Determinations

All previous determinations are, we believe, subject to certain corrections and fortunately they can in some cases still be applied. In the work of Duane, Palmer and Yeh the effect of work function was not considered, the potential drop was measured to one end rather than to the center of the filament, thermal emission velocities were omitted from consideration, and the effect of finite slit widths was incorrectly treated. In applying Feder's conclusions to Duane, Palmer and Yeh's cathode potential drop the magnitude of this drop should be known. Since it is stated that a Coolidge cathode was used it is probably safe to assume a drop of six volts, and this assumption in connection with Fig. 1 of Duane, Palmer and Yeh permits the correction (3 volts) to be applied. The effect of electron emission energy is much smaller than the probable error in V' and need not be considered. Analysis[14] of the effect of spectrometer slits upon the isochromat shows that the effective angle θ determining the position of the upper or linear part of the isochromat is the angle between the crystal face and the *center line* of the slit system. The argument in this reference refers explicitly to a system in which the two slits are used to define the *incident* beam, but with trifling modifications it will apply to a system like that of Duane, Palmer and Yeh in which one slit is on the side of incidence and the other on the side of reflection.

One finds therefore that the angle θ employed in calculation by Duane, Palmer and Yeh is too large by 46″, and that their stated value of V' is too small by 1.5 volts. Recalculating we obtain $V' \sin\theta = 2034.6 \pm 0.9$ international volts.

The low value obtained by Wagner has been discussed by Feder who ascribes the result to a shift of the isochromat caused by wide slits but does not attempt to explain the effect. We have performed special experiments to test this effect and have obtained single crystal isochromats like Feder's Fig. 4, confirming his statement that the wide slit isochromat apparently meets the voltage axis (or the background) at a smaller V' than does the corresponding curve obtained with narrow slits. We do not, however, find the shift proportional to slit width (which Feder assumes), and over a range of sufficiently narrow slits no shift appears. Our observations lead to the conclusion that the effect depends upon the existence of the knee of the isochromat. The point V' is found by extrapolating downward the apparently straight segment between foot and knee. As the narrow slits are gradually widened this segment does not shift but becomes shorter due to the upward extension of the enlarging foot. When the foot has broadened and risen until it reaches the knee the straight segment upon which V' depends no longer exists, and one makes the natural mistake of extrapolating to the voltage axis the segment of the isochromat *above* the knee, thus obtaining too small a value. The stages in this process are illustrated in a somewhat formalized manner in Fig. 3.

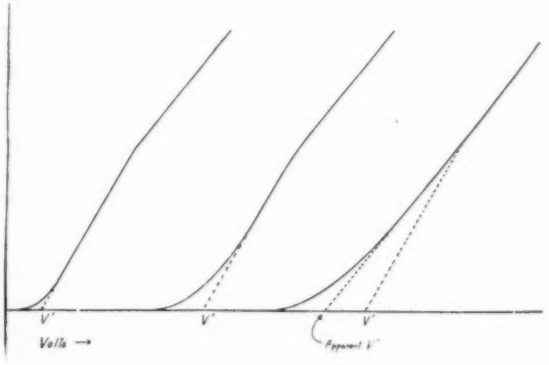

Fig. 3. Single crystal isochromats somewhat idealized. From left to right they represent curves taken with progressively wider slits.

In this situation there is no possibility of reinterpreting Wagner's data and obtaining a correct result, since the position of the knee and its associated change in slope are not known with sufficient exactness.

It remains to discuss Feder's own determination. This work was done with a rocksalt crystal

[12] Wagner, Phys. Zeits. **21**, 621 (1920).
[13] Duane, Palmer and Yeh, J. O. S. A. **5**, 376 (1921).
[14] Kirkpatrick and Miyake, R. S. I. **3**, 1 (1932).

but since the ratio of the grating constants of rocksalt and calcite is accurately known[15] the results are readily placed upon a calcite basis. Having assumed the isochromat shift proportional to slit width Feder corrects for the supposed shift in his case by adding a small quantity to his measured potentials. His slits were so narrow as to make the curve foot quite small so, as shown above, the correction is not required. Upon removing this supposed correction and taking account of the work function of the tungsten target, Feder's original value is found unchanged, due to the cancellation of the two corrections.

The revised values are entered in the third column of Table I, and it will be seen that revision has resolved this long-standing uncertainty by bringing the usable values so close together that their probable errors all overlap. The mean of the three determinations is 2035.3 ± 0.2, which is identical with the result of the present investigation. We have also retained a probable error for this mean which is the same as that of our own work since it is not apparent upon a basis of either external or internal consistency that the older determinations can be effective in reducing this figure. In spite of this, the agreement of these former determinations (as adjusted) with the present work is of the greatest service in indicating the probable freedom of our results from large undetected systematic errors.

Determination of X-Ray Wave-Lengths from the Law of Duane and Hunt

The application of the above results to a determination of the relation between h and e is obstructed by the systematic disagreement between crystal and grating wave-lengths which was mentioned above. Fortunately a reasonable choice between these two methods of wave-length measurement may now be effected by appeal to a third method which is potentially accurate and completely independent of the other two. We find such a method in the law of Duane and Hunt, according to which the minimum wave-length of the continuous spectrum $\lambda = (h/e)c^2/pqV' \times 10^8$. If a value of h/e derived independently of continuous spectrum observations be employed in this equation in combination with our experimental V' the wave-length of the $K\alpha_1$ line of silver is obtained.

Data collected and discussed by Birge[16] furnish values of h/e determined by five suitable independent methods. Assigning weights in accord with Birge's stated probable errors these values lead to the weighted average value $h/e = (1.3720 \pm 0.0004) \times 10^{-17}$ erg.sec./e.s.u. The resulting wave-length value for Ag $K\alpha_1$ as determined from the law of Duane and Hunt is 558.0 ± 0.2 X.U. The most probable crystal value is obtained by using in Bragg's law the mean θ discussed in an earlier section of this paper and Bearden's[17] value of the grating constant of calcite. This gives a result which is slightly lower than the value adopted by Siegbahn (0.55828A) but the latter is based upon a grating constant which is in part frankly conventional. The $K\alpha_1$ line of silver has not yet been measured by the grating method but grating measurements[18] on other lines, when taken collectively, show a percentage difference between grating and crystal values which increases slightly with wave-length in such a way as to indicate that a good grating measurement of Ag $K\alpha_1$ would give a result 0.21 ± 0.01 percent higher than the Siegbahn value. The various determinations (to four significant figures) are assembled in Table II.

Table II. *Wave-length of silver* $K\alpha_1$.

Most probable crystal value (mean θ and Bearden's d)	558.0 X.U.
As given by Siegbahn[19] (conventional d)	558.3
Ruled grating value (calculated)	559.5
By law of Duane and Hunt	558.0 ± 0.2

The complete agreement of the results of the new method with the crystal measurements compels us to accept the latter as essentially correct.

[15] Siegbahn, *Spektroskopie der Röntgenstrahlen*, p. 42, (1931).

[16] Birge, Phys. Rev. **40**, 228 (1932).

[17] Bearden, Phys. Rev. **38**, 2089 (1931).

[18] Cork, Phys. Rev. **35**, 1456 (1930); Bearden, Phys. Rev. **37**, 1210 (1931); Witmer and Cork, Phys. Rev. **42**, 743 (1932); Purdom and Cork, Phys. Rev. **44**, 974 (1933).

[19] Siegbahn, reference 15, p. 185.

Values of $h/e^{4/3}$ and h

Replacing λ in the equation $Ve=hc/\lambda$ by its Bragg's law expression (with the correcting factor 0.999865 for crystal refraction), expressing the grating constant (of calcite) in the form

$$d=\left\{\frac{\frac{1}{2}Me\ 0.0111800}{\rho\varphi Aqc}\right\}^{1/3}$$

and changing from electrostatic to international potential units we have

$$\frac{h}{e^{4/3}}=\frac{(2.\times 0.999865)pq^{2/3}10^{8}}{c^{7/3}}\left[\frac{M\ 0.0111800}{2\rho\varphi A}\right]^{1/3}\times V'\sin\theta, \quad (1)$$

in which p = international ohm/absolute ohm, q = international amp./absolute amp., c = speed of light, M = molecular weight of calcite, ρ = density of calcite, φ = a known function of the angle between the crystal edges, A = atomic weight of silver, θ = external Bragg angle (calcite cleavage face), V' = minimum electron potential fall (international volts) capable of exciting radiation reflectable at angle θ.

With the constants recommended by Birge[20] in 1929 and the new value $V'\sin\theta=2035.3\pm0.2$ we obtain $h/e^{4/3}=(1.7559\pm0.0002)\times10^{-14}$.

Recent work on c, ρ, φ, p and q makes advisable certain slight changes in the adopted values of these constants. The new values, together with their sources, are as follows:

$c=2.99774\times10^{10}$ cm/sec.,[21] $\rho=2.71030\pm0.00003$ g/cm^3,[22] $\varphi=1.09594\pm0.00001$,[17] $p=1.000460\pm0.000020$,[23] $q=0.999900\pm0.000040$.[23]

With these constants we obtain from (1) the result $h/e^{4/3}=(1.7563\pm0.0002)\times10^{-14}$.

The deduction of most probable individual values of e and h from the results of this paper in combination with other known relations between these constants is a critical task which we are content to leave to others. It is of much interest, however, to combine the above value of $h/e^{4/3}$ with an independent value of e and thus determine h. Since Birge's most probable values of e are based in part upon the x-ray determinations quoted above in support of our finally adopted $V'\sin\theta$ it appears more appropriate to employ here Millikan's[24] 1930 oil drop value $e=(4.770\pm0.005)\times10^{-10}$ e.s.u. Recent work upon c and pq is without effect upon this value as given. This calculation yields

$$h_{\text{crystal}}=(6.546\pm0.006)\times10^{-27}\ \text{erg}\cdot\text{sec.},$$

which is presented as the most probable present value of h as obtained by the x-ray method alone.

[20] Birge, Phys. Rev. Suppl. **1**, 1 (1929).

[21] Work of Michelson, Pease and Pearson, reported by *Science Service* in Science **78**, Dec. 29 (1933).

[22] Bearden, Phys. Rev. **43**, 92 (1933).

[23] Curtis, Bull. Nat. Res. Council, No. 93 (1933).

[24] Millikan, Phys. Rev. **35**, 1231 (1930).

Extension of the Dirac Vector Model to Include Several Configurations

ROBERT SERBER, *Department of Physics, University of Wisconsin*

(Received January 23, 1934)

The vector model for the electrostatic interactions of a system of n electrons, as originally given by Dirac and as used by J. H. Van Vleck, suffers from the restriction that it allows the energy matrix to be set up completely only for a single spatial configuration. In the present paper this restriction is removed. It is shown how the complete energy matrix may be found by means of the vector model, whatever the number of configurations involved. As an example of the method, the energies of the two ^2D states arising from the atomic configuration d^3 are calculated. Calculations by this method are simpler than the corresponding calculations using Slater wave functions in that the energy matrix factors according to characteristic values of S.

DIRAC[1] has given a very elegant method for determining the energy levels due to a single configuration of an n electron system, all other configurations being neglected. This method leads in a simple way to the vector model used by J. H. Van Vleck[2] in a previous paper in this journal. However, the restriction to a single configuration is a serious one; for example, if there is degeneracy other than spin degeneracy Dirac's method may give only the mean energy of a number of states. In the present paper this restriction will be removed; it will be shown how, by a simple extension of Dirac's argument, the inter-configurational elements of the energy matrix may be obtained.

Suppose we have a configuration A, specified by n orthogonal orbits, $(\alpha_1|xyz)$, $(\alpha_2|xyz)$, $\cdots(\alpha_n|xyz)$, which are all different. We can obtain $n!$ wave functions of the system by applying in turn all the permutations of the orbits (i.e., α's) among themselves to the wave function

$$\psi^A=(\alpha_1|x_1y_1z_1)(\alpha_2|x_2y_2z_2)\cdots(\alpha_n|x_ny_nz_n).$$

Consider any one of these wave functions, $P\psi^A$. It is clear that the same result is obtained if, instead of applying the permutation P to the orbits, we apply the reciprocal permutation to the coordinates x_i, y_i, z_i, that is

$$P\psi=(P^x)^{-1}\psi. \tag{1}$$

The superscript x indicates a permutation which operates on the coordinates.

The portion of the energy matrix in which the states arising from the given configuration intersect each other is a matrix, H^{AA}, of $n!$ rows and columns, whose elements are given by

$$(P_a\alpha|H|P_b\alpha)=\int(P_a\psi^A)^*HP_b\psi^A d\tau=\int(P^x{}_a{}^{-1}\psi^A)^*HP^x{}_b{}^{-1}\psi^A d\tau=\int(P^x{}_a{}^{-1}\psi^A)^*P^x{}_b{}^{-1}H\psi^A d\tau$$
$$=\int(P^x{}_bP^x{}_a{}^{-1}\psi^A)^*H\psi^A d\tau=\int(P_aP_b{}^{-1}\psi^A)^*H\psi^A d\tau=(P_aP_b{}^{-1}\alpha|H|\alpha), \tag{2}$$

as can be seen from (1), from the fact that the Hamiltonian function H is invariant under $P^x{}_b{}^{-1}$ and so commutes with it, and from the unitary property of the operator $P^x{}_b$. It is to be understood that the operator preceding ψ^{A*} acts only on ψ^{A*}, and not on the remainder of the integrand. Let $H_P{}^{AA}=(P\alpha|H|\alpha)$. Then it is seen from (2) that the coefficient of $H_P{}^{AA}$ in the energy matrix is itself a matrix, whose elements are zero except when $P=P_aP_b{}^{-1}$, in

[1] P. A. M. Dirac, *The Principles of Quantum Mechanics*, Chapter XI. The connection between the energy matrix of a single configuration and the representations of the permutation group has also been given by E. Wigner, Zeits. f. Physik **40**, 883 (1927).

[2] J. H. Van Vleck, Phys. Rev. **45**, 405 (1934). This paper will be referred to as *I*.

which case they are unity. But the elements of the matrix representing P are given by $(P_a\alpha|\mathbf{1}|PP_b\alpha)$, and so are zero except when $P_a=PP_b$, i.e., when $P=P_aP_b^{-1}$, in which case they also are unity. Thus the coefficient of $H_P{}^{AA}$ is simply the matrix representing P, and H^{AA} can be written

$$H^{AA}=\sum_P H_P{}^{AA}P. \tag{3}$$

Similarly, the portion of the energy matrix arising from a configuration B, specified by the orbits $(\alpha_1'|xyz)$, $\cdots(\alpha_n'|xyz)$, is

$$H^{BB}=\sum_P H_P{}^{BB}P. \tag{4}$$

If the states $P\psi^B$ are ordered in the same way as the states $P\psi^A$, as we shall always suppose done, the matrix P in (3) is identical with P in (4).

We must now consider the portion of the energy matrix, H^{AB}, in which the states $P\psi^A$ intersect the states $P\psi^B$. The argument which leads to (2) now gives the result

$$(P_a\alpha|H|P_b\alpha')=(P_aP_b^{-1}\alpha|H|\alpha'). \tag{5}$$

Let $H_P{}^{AB}=(P\alpha|H|\alpha')$. Then, comparing (2) and (5) and remembering that the states $P\psi^A$ and $P\psi^B$ are similarly ordered, we see that the coefficient of $H_P{}^{AB}$ in H^{AB} is the same as the coefficient of $H_P{}^{AA}$ in H^{AA}, i.e., is the same as the matrix representing P. In this sense we can write

$$H^{AB}=\sum_P H_P{}^{AB}P. \tag{6}$$

Eq. (6) has been established using a particular representation. We must now show that it holds whatever the representation, provided always that P is represented by the same matrix in (4) as in (3). If we apply a canonical transformation S_A to H^{AA}, which then becomes $S_A^{-1}H^{AA}S_A$, and a transformation S_B to H^{BB}, which becomes $S_B^{-1}H^{BB}S_B$, then H^{AB} becomes $S_A^{-1}H^{AB}S_B$. The proviso stated above requires that $S_A=S_B$; in consequence H^{AB} transforms in the same way as H^{AA} and H^{BB}, and (6) remains valid in the new representation.

Restrictions Imposed by the Exclusion Principle

Not all of the $n!$ states arising from a given configuration are permitted by the exclusion principle. In general, the degree of the secular equation which must be solved to find the energy levels can be greatly reduced if only the states allowed by the exclusion principle are considered. To do this we must obviously take into account the spin variables, as well as the positional variables. For an n electron system there exist 2^n linearly independent functions of the spins. Using these 2^n functions as a basis, we can construct the matrices representing the operators, P^S, which permute the spins among themselves. It has been shown by Wigner[3] that the representations of the P's allowed by the exclusion principle are obtainable from the representations of the P^S's by means of the matrix equation

$$P=\pm P^S, \tag{7}$$

the plus or minus sign being taken according as the permutation in question is even or odd.

Dirac has shown that $P^S{}_{ij}$, which permutes the spins of electrons i and j, can be expressed in terms of the spins by the relation

$$P^S{}_{ij}=\tfrac{1}{2}(1+4\mathbf{s}_i\cdot\mathbf{s}_j);$$

hence we can write

$$P_{ij}=-\tfrac{1}{2}(1+4\mathbf{s}_i\cdot\mathbf{s}_j), \tag{8}$$

and any permutation P can be expressed in terms of the spins by writing it as a product of interchanges.

Modifications Required when the Orbits are not Different

We must now consider the modifications required in the foregoing arguments when the orbits of a configuration are not all different.

For brevity let us refer to the orbits of any configuration, α_1, α_2, $\cdots\alpha_n$, simply by the numbers 1, 2, $\cdots n$. Suppose the orbits 1 and 2 of configuration B are identical. In this case we will say we have a pair of filled orbits. The permutation P_{12} satisfies the equation $P_{12}{}^2=1$, hence P_{12} has the characteristic values ±1. But if orbits 1 and 2 are identical, any wave function is left unaltered by P_{12}, and so the only non-vanishing states are those for which $P_{12}=1$. In terms of the vector model, this is simply the

[3] E. Wigner, *Gruppentheorie*, p. 277.

statement that the spins of two electrons in identical orbits must be anti-parallel (see reference 2, § 1).

It has been shown[2] in *I* that if the perturbations due to other configurations are not considered, the energies of the states arising from the configuration *B* are the same, except for an additive constant, as if we disregarded the orbits 1 and 2 entirely, and calculated the energy for the remaining $(n-2)$ electron problem. However, if we wish to include other configurations we must adopt a different attack.

In order to use the formula for the interaction of configurations, (6), we must formally consider the orbits 1 and 2 as different, that is, we must distinguish between them. The states $P\psi^B$ will no longer be orthogonal, for if $P'=P_{12}P$ the states $P'\psi^B$ and $P\psi^B$ are actually identical. The modification in the secular equation required when the states are not orthogonal is a familiar one; we must calculate the matrix elements of $H-W$ rather than the matrix elements of H. Thus (4) must be replaced by

$$(H-W)^{BB}=\sum_P(H-W)_P{}^{BB}P. \qquad (9)$$

A similar modification is not required in (6), as the states arising from the configuration *B* will still be orthogonal to those arising from any other configuration, *A*.

Suppose the orbits of *A* are all different. Let g be the degree (number of rows and columns) of the matrices representing the *P*'s. The complete energy matrix for both configurations, *A* and *B*, is of degree $2g$. Its form differs from that shown in Fig. 1 only in that it consists of four squares, each of degree g. Let us use a representation of the *P*'s in which P_{12} is diagonal. In such a representation there will be a number of rows, r in number, for which P_{12} has the characteristic value 1, while for the remaining $(g-r)$ rows P_{12} has the characteristic value -1. But we have seen that when orbits 1 and 2 are identical the only permissible states are those for which $P_{12}=1$. The $(g-r)$ rows and columns arising from *B* for which $P_{12}=-1$ must accordingly be struck out of the energy matrix, which then takes the form shown in Fig. 1. The symbol P^{BA} will be used to denote the matrix obtained from *P* by deleting the improper $(g-r)$ rows, and

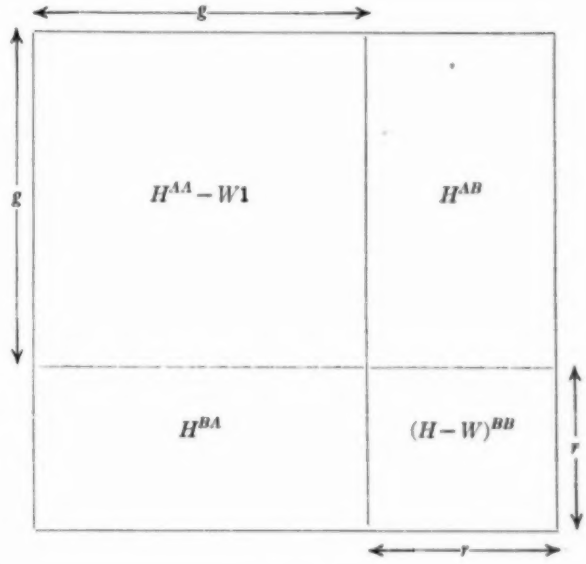

FIG. 1.

P^{BB} will denote the matrix obtained by deleting the improper $(g-r)$ rows and columns. In place of (6) and (9) we now have

$$\left.\begin{aligned} H^{BA}&=\sum_P H_P{}^{BA}P^{BA};\\ (H-W)^{BB}&=\sum_P(H-W)_P{}^{BB}P^{BB}.\end{aligned}\right\} \qquad (10)$$

If the permutations P' and P are connected by the relation $P'=P_{12}P$, we obviously have

$$(H-W\delta_{BC})_{P'}{}^{BC}=(H-W\delta_{BC})_P{}^{BC}, \quad (C=A, B).$$

Moreover $P'^{BC}=P^{BC}$, since

$$P'(i;j)=\sum_k P_{12}(i;k)P(k;j),$$

and in the r rows we have retained $P_{12}(i;k)=\delta_{ik}$. The contribution of P' and P to the energy is accordingly

$$(H-W\delta_{BC})_{P'}{}^{BC}P'^{BC}+(H-W\delta_{BC})_P{}^{BC}P^{BC}$$
$$=2(H-W\delta_{BC})_P{}^{BC}P^{BC}.$$

The entire group of $n!$ permutations can be divided into one set of $n!/2$ "independent" permutations, and a second set of $n!/2$ permutations which can be obtained by multiplying each permutation of the first set on the left by P_{12}. For example, the six permutations P_1, P_{12}, P_{13}, P_{23}, P_{123}, P_{132}, can be divided into an "independent" set P_1, P_{13}, P_{23}, and a "dependent" set $P_{12}=P_{12}P_1$, $P_{123}=P_{12}P_{23}$, $P_{132}=P_{12}P_{13}$. Instead

of (10) we can write

$$\left.\begin{aligned} H^{BA} &= 2\sum{}'_P H_P{}^{BA} P^{BA}, \\ (H-W)^{BB} &= 2\sum{}'_P (H-W)_P{}^{BB} P^{BB}, \end{aligned}\right\} \quad (11)$$

where the sum is taken only over the $n!/2$ permutations of an "independent" set. As all the exchange and higher order permutation integrals of unity appearing in (11) are clearly zero, the second expression in (11) is simply

$$(H-W)^{BB} = 2\sum{}'_P H_P{}^{BB} P^{BB} - 2W\mathbf{1}.$$

The matrix H^{AB} can be obtained from H^{BA} by use of the Hermitian character of the energy matrix, $H^{AB} = H^{BA\dagger}$. The entire energy matrix has the form shown in Fig. 2, if we put $a = b = 2$.

$\Sigma_P H_P{}^{AA} P - W\mathbf{1}$	$a(\Sigma'_P H_P{}^{BA} P^{BA})^\dagger$
$a\Sigma'_P H_P{}^{BA} P^{BA}$	$b(\Sigma'_P H_P{}^{BB} P^{BB} - W\mathbf{1})$

FIG. 2.

It is often inconvenient to have $-2W$ appear on the diagonal, for example if we wish to use the spur theorem. This difficulty can be avoided by renormalizing the energy matrix, which we can do by dividing each row and each column arising from the configuration B by $\sqrt{2}$. The final form of the energy matrix is given by Fig. 2 with $a = \sqrt{2}$, $b = 1$.

The problem arising when there are two pairs of filled orbits in the configuration B can be handled in the same way. If the orbits 3 and 4 are identical, as well as 1 and 2, we must use a representation in which both P_{12} and P_{34} are diagonal. The only rows and columns arising from B which are retained in the energy matrix are those for which both P_{12} and P_{34} are 1; all others must be struck out. The contribution of any permutation P to the energy matrix will be the same as the contribution of each of the permutations $P_{12}P$, $P_{34}P$, $P_{12}P_{34}P$. In place of (11) we now have

$$\left.\begin{aligned} H^{BA} &= 4\sum{}'_P H_P{}^{BA} P^{BA}; \\ (H-W)^{BB} &= 4\sum{}'_P H_P{}^{BB} P^{BB} - 4W\mathbf{1}, \end{aligned}\right\} \quad (12)$$

where the summation is to be taken over $n!/4$ permutations which do not differ merely by interchanges of identical orbits of B. The matrices P^{BA} in (12) will of course have a smaller number of rows, and the matrices P^{BB} a smaller number of rows and columns, than the corresponding matrices in (11). In order to renormalize the energy matrix each row and column arising from B must be divided by 2. The final form of the energy matrix is given by Fig. 2 with $a = 2$, $b = 1$.

The above arguments are readily generalized. Suppose we have any set of configurations R_1, R_2, $\cdots R_k$. Let r_j be the number of pairs of filled orbits in the configuration R_j. We shall always denote the first pair of filled orbits by 1,2, the second by 3,4, and so forth, and employ a representation in which P_{12}, P_{34}, $\cdots$ $P_{2p-1\,p}$, $\cdots$ are diagonal. This is possible, since these permutations all commute. Then if $r_i \geq r_j$, the matrix $H^{R_iR_j}$, in the normalized form, is given by

$$H^{R_iR_j} = \sqrt{2}^{\,r_i - r_j} \sum{}'_P H_P{}^{R_iR_j} P^{R_iR_j}, \quad (13)$$

where the summation is taken only over $n!/2^{r_i}$ permutations which do not differ merely by interchanges of identical orbits of R_i. The matrices $P^{R_iR_j}$ are obtained from the matrices P by striking out the rows which violate the condition that an interchange of identical orbits of R_i has the characteristic value 1, and striking out the columns which violate the condition that an interchange of identical orbits of R_j has the characteristic value 1. The matrix $H^{R_jR_i}$ is obtained from the relation $H^{R_jR_i} = H^{R_iR_j\dagger}$. Eq. (13) is the desired generalization of Dirac's result, (3). Eq. (13) is the same as (3) when $i = j$, $r_i = 0$.

Orthogonal and Non-Orthogonal Orbits

If the different orbits are orthogonal, as we have so far supposed to be the case, the number of terms which it is necessary to consider in setting up the matrix $H^{R_iR_i}$ can be considerably reduced by taking into account the fact that the Hamiltonian function representing the electrostatic interactions between electrons contains no terms involving the coordinates of more than two electrons. It is evident from the form of the Hamiltonian function that if in the integral $H_P{}^{R_iR_i}$ more than two electrons are in different orbits, the integral will be zero. But this will surely be the case if P is any permutation involving more than two orbits, i.e., any permutation other than the identity, P_1, or a simple interchange, P_{kl}. It should be noted in this connection that permutations involving an interchange of identical orbits do not appear in (13). When $i=j$, (13) may accordingly be written

$$H^{R_iR_i}=[H_{P_1}{}^{R_iR_i}\mathbf{1}+\sum_{k<l}H_{P_{kl}}{}^{R_iR_i}P_{kl}{}^{R_iR_i}]. \tag{14}$$

Interchanges of identical orbits are to be omitted from the summation. Here $H_{P_1}{}^{R_iR_i}$ is the ordinary "Coulomb" energy, while the coefficients $H_{P_{kl}}{}^{R_iR_i}$ are the usual exchange integrals.

When the orbits are not orthogonal, as in molecular problems, (13) is still valid if we write $H-W$ in place of H. The method for solving the resulting secular equation has been discussed in I.

Calculation of the Matrices Representing the P's

We have seen that any permutation P can be expressed in terms of the spin variables by means of (8). From the form of (8) it is evident that P is invariant under a rotation of spin axes. The P's, and the energy, which is a function of the P's, can accordingly have no matrix elements between states of different S or M_S, and for each characteristic value of S we obtain a representation of the P's which is independent of M_S.

The first task in finding these representations is to express the spin wave functions belonging to a given S and M_S, for an n electron system, in terms of one-electron spin functions. The representative of any P^s, i.e., any permutation of spin orbits, can then be calculated, and P obtained by use of (7).

The wave functions are found by repeated application of the familiar formula for the compounding of two vectors S_1, S_2 to a resultant S,

$$\psi^{S_1S_2}{}_{SM_S}=\sum_\mu s^{S_1S_2}{}_{S\mu M_S-\mu}\psi_{S_1\mu}\psi_{S_2M_S-\mu}.$$

General formulas for the coefficients $s^{S_1S_2}{}_{S_\mu M_S-u}$ have been given by Wigner.[4] The matrices P_{12}, P_{34}, $\cdots$ will be diagonal if we begin by compounding s_1 and s_2 to a resultant S_{12}, s_3 and s_4 to a resultant S_{34}, etc., and then proceed to compound S_{12} and S_{34} to S' and so forth until the total spin, S, is diagonal. Only one value of M_S need be considered; it is simplest to take $M_S=S$. For the single state with $S=n/2$ all the electron spins are parallel, and it follows directly from the vector model, (8), that any odd permutation is represented by -1, any even permutation by $+1$.

The case $n=4$ will serve as an example of the method, and also of some devices which considerably shorten the labor in more complicated cases. From four electrons we obtain one quintet state, three triplet states, and two singlet states, as can be seen from Fig. 1 of reference 2. The wave functions, $\psi^{S_{12}S_{34}}{}_{11}$, of the three triplet states can be expressed in terms of two-electron spin wave functions as

$$\begin{aligned}&\psi^{11}{}_{11}=(1/\sqrt{2})[\psi_{11}(s_1s_2)\psi_{10}(s_3s_4)-\psi_{10}(s_1s_2)\psi_{11}(s_3s_4)],\\&\psi^{10}{}_{11}=\psi_{11}(s_1s_2)\psi_{00}(s_3s_4),\qquad\psi^{01}{}_{11}=\psi_{00}(s_1s_2)\psi_{11}(s_3s_4).\end{aligned}\tag{15}$$

The two electron wave functions are given by

$$\psi_{11}(s_is_j)=\xi_i\xi_j;\qquad\psi_{10}(s_is_j)=(1/\sqrt{2})(\xi_i\eta_j+\eta_i\xi_j);\qquad\psi_{00}(s_is_j)=(1/\sqrt{2})(\xi_i\eta_j-\eta_i\xi_j),\tag{16}$$

[4] E. Wigner, reference 3, p. 206.

where ξ_i is the spin wave function of the ith electron for $m_s=\frac{1}{2}$, and η_i is the spin wave function for $m_s=-\frac{1}{2}$.

For the first and second of the states (15), the spins of electrons 1 and 2 are parallel, so $P_{12}=-1$; for the third they are anti-parallel, so $P_{12}=1$. Similarly, the characteristic values of P_{34} are $-1, 1, -1$. This is a rather trivial illustration of a fact which is very useful when n is greater than 4; if we have found the P's for the cases $n=r$ and $n=p$ we can immediately write down, for the case $n=r+p$, all the P's which involve only the first r or the last p orbits. The labor involved in calculating the matrix elements of the remaining P's can be greatly reduced by taking advantage of relations between the P's, obvious symmetry properties of the wave functions, and the fact that the matrices representing simple interchanges are both Hermitian and unitary. For example, from (15) and (16) we find

$$P^S{}_{13}\psi^{01}{}_{11}=-(1/\sqrt{2})\psi^{11}{}_{11}+\tfrac{1}{2}\psi^{10}{}_{11}+\tfrac{1}{2}\psi^{01}{}_{11}. \tag{17}$$

This equation determines the last column of the matrix representing $P^S{}_{13}$. If both sides of (17) are multiplied by P^S, the left side becomes $P^SP^S{}_{13}\psi^{01}{}_{11}=P^S{}_kP^S\psi^{01}{}_{11}$, with $P^S{}_k=P^SP^S{}_{13}P^{S-1}$. Choose $P^S=P^S{}_{(13)(24)}$. Then $P^S{}_k=P^S{}_{13}$, and inspection of (15) immediately shows that $P^S{}_{(13)(24)}\psi^{01}{}_{11}=\psi^{10}{}_{11}$, $P^S{}_{(13)(24)}\psi^{10}{}_{11}=\psi^{01}{}_{11}$, $P^S{}_{(13)(24)}\psi^{11}{}_{11}=-\psi^{11}{}_{11}$. Hence

$$P^S{}_{13}\psi^{10}{}_{11}=(1/\sqrt{2})\psi^{11}{}_{11}+\tfrac{1}{2}\psi^{10}{}_{11}+\tfrac{1}{2}\psi^{01}{}_{11},$$

and the second column of the matrix representing $P^S{}_{13}$ is determined. The third column can now be found by using the fact that $P^S{}_{13}$ is unitary and Hermitean. The matrix representing $P^S{}_{23}$ is found by means of the relation $P^S{}_{23}=P^S{}_{12}P^S{}_{13}P^S{}_{12}$, which, in view of the diagonal form of $P^S{}_{12}$, shows how $P^S{}_{23}$ may be obtained by simply changing certain signs in $P^S{}_{13}$. Similarly, $P^S{}_{14}$ is determined by $P^S{}_{14}=P^S{}_{34}P^S{}_{13}P^S{}_{34}$, and $P^S{}_{24}$ by $P^S{}_{24}=P^S{}_{34}P^S{}_{23}P^S{}_{34}$.

Using (7), we find for $n=4$, $S=1$,

$$P_{12}=\begin{vmatrix}-1 & 0 & 0\\ 0 & -1 & 0\\ 0 & 0 & 1\end{vmatrix},\qquad P_{34}=\begin{vmatrix}-1 & 0 & 0\\ 0 & 1 & 0\\ 0 & 0 & -1\end{vmatrix},\qquad P_{13}=\begin{vmatrix}0 & -\sqrt{\tfrac{1}{2}} & \sqrt{\tfrac{1}{2}}\\ -\sqrt{\tfrac{1}{2}} & -\tfrac{1}{2} & -\tfrac{1}{2}\\ \sqrt{\tfrac{1}{2}} & -\tfrac{1}{2} & -\tfrac{1}{2}\end{vmatrix},$$

$$P_{14}=\begin{vmatrix}0 & \sqrt{\tfrac{1}{2}} & \sqrt{\tfrac{1}{2}}\\ \sqrt{\tfrac{1}{2}} & -\tfrac{1}{2} & \tfrac{1}{2}\\ \sqrt{\tfrac{1}{2}} & \tfrac{1}{2} & -\tfrac{1}{2}\end{vmatrix},\qquad P_{23}=\begin{vmatrix}0 & -\sqrt{\tfrac{1}{2}} & -\sqrt{\tfrac{1}{2}}\\ -\sqrt{\tfrac{1}{2}} & -\tfrac{1}{2} & \tfrac{1}{2}\\ -\sqrt{\tfrac{1}{2}} & \tfrac{1}{2} & -\tfrac{1}{2}\end{vmatrix},\qquad P_{24}=\begin{vmatrix}0 & \sqrt{\tfrac{1}{2}} & -\sqrt{\tfrac{1}{2}}\\ \sqrt{\tfrac{1}{2}} & -\tfrac{1}{2} & -\tfrac{1}{2}\\ -\sqrt{\tfrac{1}{2}} & -\tfrac{1}{2} & -\tfrac{1}{2}\end{vmatrix}.$$

In a similar way we obtain for $n=4$, $S=0$,

$$P_{12}=P_{34}=\begin{vmatrix}-1 & 0\\ 0 & 1\end{vmatrix},\qquad P_{13}=P_{24}=\begin{vmatrix}\tfrac{1}{2} & \sqrt{\tfrac{3}{4}}\\ \sqrt{\tfrac{3}{4}} & -\tfrac{1}{2}\end{vmatrix},\qquad P_{14}=P_{23}=\begin{vmatrix}\tfrac{1}{2} & -\sqrt{\tfrac{3}{4}}\\ -\sqrt{\tfrac{3}{4}} & -\tfrac{1}{2}\end{vmatrix}. \tag{18}$$

The representation of higher order permutations can be found by multiplication of these representations of the interchanges.

The representations of P_{12}, P_{13}, and P_{23} which we have just found for $n=4$, $S=0$ are also the representations of these permutations for $n=3$, $S=\frac{1}{2}$, for, on removing the fourth electron, a state $S=0$ of the four electron problem evidently goes over into a state $S=\frac{1}{2}$ of the three electron problem.

Application to the Atomic Configuration d^3

As an example of the use of (13) we shall calculate the energies of the two ^2D levels arising from the atomic configuration d^3. It has been shown[2] in I how the vector model can be used, as an alternative to Slater's method, to find the energies of the other levels arising from this configuration, but of

course either method gives only the mean energy of the ^2D states. To separate them we must set up the complete secular determinant for $M_L=2$.

The orbits having $m_l=2, 1, 0, -1, -2$ will be denoted by $d\delta, d\pi, d\sigma, d-\pi, d-\delta$, respectively. The four configurations which have $M_L=2$ are

$$A: (d\pi, d-\pi, d\delta), \quad B: (d\sigma, d\sigma, d\delta), \quad C: (d\pi, d\pi, d\sigma), \quad D: (d\delta, d\delta, d-\delta).$$

All the orbits of A are different, so the matrices $P_{ij}{}^{AA}$ are simply those given in (18). The orbits 1 and 2 are the same in B, C, D, so $P_{ij}{}^{XA}$, $(X=B, C, D)$, is the second row of P_{ij}, and $P_{ij}{}^{XY}$, $(X, Y=B, C, D)$, is the element in the second row, second column of P_{ij}. The energy matrix for the doublet states is shown below.

$H_1{}^{AA}-H_{12}{}^{AA}+\frac{1}{2}H_{13}{}^{AA}+\frac{1}{2}H_{23}{}^{AA}$	$\sqrt{\frac{3}{4}}[H_{13}{}^{AA}-H_{23}{}^{AA}]$	$\sqrt{\frac{3}{2}}[H_{13}{}^{BA}-H_{23}{}^{BA}]$	$\sqrt{\frac{3}{2}}[H_{13}{}^{CA}-H_{23}{}^{CA}]$	$\sqrt{\frac{3}{2}}[H_{13}{}^{DA}-H_{23}{}^{DA}]$
$\sqrt{\frac{3}{4}}[H_{13}{}^{AA}-H_{23}{}^{AA}]$	$H_1{}^{AA}+H_{12}{}^{AA}-\frac{1}{2}H_{13}{}^{AA}-\frac{1}{2}H_{23}{}^{AA}$	$\sqrt{2}[H_1{}^{BA}-\frac{1}{2}H_{13}{}^{BA}-\frac{1}{2}H_{23}{}^{BA}]$	$\sqrt{2}[H_1{}^{CA}-\frac{1}{2}H_{13}{}^{CA}-\frac{1}{2}H_{23}{}^{CA}]$	$\sqrt{2}[H_1{}^{DA}-\frac{1}{2}H_{13}{}^{DA}-\frac{1}{2}H_{23}{}^{DA}]$
$\sqrt{\frac{3}{2}}[H_{13}{}^{BA}-H_{23}{}^{BA}]$	$\sqrt{2}[H_1{}^{BA}-\frac{1}{2}H_{13}{}^{BA}-\frac{1}{2}H_{23}{}^{BA}]$	$H_1{}^{BB}-\frac{1}{2}H_{13}{}^{BB}-\frac{1}{2}H_{23}{}^{BB}$	$H_1{}^{CB}-\frac{1}{2}H_{13}{}^{CB}-\frac{1}{2}H_{23}{}^{CB}$	$H_1{}^{DB}-\frac{1}{2}H_{13}{}^{DB}-\frac{1}{2}H_{23}{}^{DB}$
$\sqrt{\frac{3}{2}}[H_{13}{}^{CA}-H_{23}{}^{CA}]$	$\sqrt{2}[H_1{}^{CA}-\frac{1}{2}H_{13}{}^{CA}-\frac{1}{2}H_{23}{}^{CA}]$	$H_1{}^{CB}-\frac{1}{2}H_{13}{}^{CB}-\frac{1}{2}H_{23}{}^{CB}$	$H_1{}^{CC}-\frac{1}{2}H_{13}{}^{CC}-\frac{1}{2}H_{23}{}^{CC}$	$H_1{}^{DC}-\frac{1}{2}H_{13}{}^{DC}-\frac{1}{2}H_{23}{}^{DC}$
$\sqrt{\frac{3}{2}}[H_{13}{}^{DA}-H_{23}{}^{DA}]$	$\sqrt{2}[H_1{}^{DA}-\frac{1}{2}H_{13}{}^{DA}-\frac{1}{2}H_{23}{}^{DA}]$	$H_1{}^{DB}-\frac{1}{2}H_{13}{}^{DB}-\frac{1}{2}H_{23}{}^{DB}$	$H_1{}^{DC}-\frac{1}{2}H_{13}{}^{DC}-\frac{1}{2}H_{23}{}^{DC}$	$H_1{}^{DD}-\frac{1}{2}H_{13}{}^{DD}-\frac{1}{2}H_{23}{}^{DD}$

For brevity we have written $H_{12}{}^{AA}$ in place of $H_{P_{12}}{}^{AA}$, and so forth. The coefficients $H_P{}^{R_iR_j}$ can readily be expressed in terms of the integrals

$$(\alpha\beta;\ \gamma\epsilon)=\int(d\alpha\,|\,x_1y_1z_1)^*(d\beta\,|\,x_2y_2z_2)^*r_{12}{}^{-1}(d\gamma\,|\,x_1y_1z_1)(d\epsilon\,|\,x_2y_2z_2)d\tau_1d\tau_2,$$

and these in turn in terms of the Slater-Condon parameters F_0, F_2, F_4. To quote a few examples,

$H_1{}^{AA}=(\pi-\pi;\ \pi-\pi)+(\pi\delta;\ \pi\delta)+(-\pi\delta;\ -\pi\delta)$; $H_{12}{}^{AA}=(\pi-\pi;\ -\pi\pi)$; $H_1{}^{BB}=(\sigma\sigma;\ \sigma\sigma)+2(\sigma\delta;\ \sigma\delta)$; $H_{13}{}^{BB}=H_{23}{}^{BB}=(\sigma\delta;\ \delta\sigma)$; $H_1{}^{BA}=(\sigma\sigma;\ \pi-\pi)$; $H_{13}{}^{BA}=H_{23}{}^{BA}=0$; $H_1{}^{CB}=0$; $H_{13}{}^{CB}=H_{23}{}^{CB}=(\pi\pi;\ \sigma\delta)$.

Three of the five characteristic values of the energy matrix are already known; namely ^2H, ^2G, ^2F. The mean of the two ^2D levels can be found by subtracting the known characteristic values from the spur of the energy matrix. In a similar way, the mean square of the ^2D levels can be found by subtracting the squares of the known characteristic values from the spur of H^2. This spur is $\mathrm{Sp}\,H^2=\sum_{ij}|H_{ij}|^2$, i.e., it is simply the sum of the squares of the elements of the energy matrix. The energies of the two ^2D states are then given by

$$^2D_\pm=\tfrac{1}{2}\alpha\pm\tfrac{1}{2}(2\beta-\alpha^2)^{\frac{1}{2}} \quad \text{with} \quad \alpha=^2D_+ +{}^2D_-, \quad \beta=(^2D_+)^2+(^2D_-)^2.$$

On carrying out the arithmetic we check the result previously obtained by Shortly and Ufford[5] by means of Slater wave functions. One advantage of the present method is that the secular determinant factors according to characteristic values of S; the Slater wave functions do not lead to such a factorization.

I wish to thank Professor J. H. Van Vleck for his very kind advice and aid.

[5] C. W. Ufford and G. H. Shortley, Phys. Rev. **42**, 167 (1932).

The Nuclear Spin of Sodium

JOSEPH JOFFE, *Department of Chemistry, Columbia University*

(Received February 1, 1934)

The alternation of intensities in absorption in the band spectrum of sodium was investigated for the purpose of determining the spin of the sodium nucleus. Measurements were confined to the (0,2) band in the $^1\Pi \leftarrow {}^1\Sigma$ transition, which alone is reasonably free from overlapping bands. Relative absorption coefficients for the Q branch lines, with $J=48$ to $J=73$ inclusive, were calculated. These yielded an average value for the alternation of intensities of 1.71, the average being obtained from 5 different plates. These results agree best with the theoretical alternation ratio of 1.67 corresponding to a nuclear spin of 3/2.

INTRODUCTION

ALTHOUGH alternation of intensities in band spectra does not offer a method of great precision in the determination of nuclear spins, the present state of knowledge makes it highly desirable that as many different methods as possible be used to determine these constants. Especially is this true for sodium, for which previous experimenters have obtained widely differing results. Hyperfine structure investigations have given $i=1/2$, 1, 3/2 for the spin.[1, 2, 3, 4, 5, 6] The polarization of resonance radiation indicates $i=1$, according to Ellett.[7] Band spectral observations by Loomis and Wood[8] suggested $i \geq 3/2$.[9] Atomic beam pattern investigations by Rabi and Cohen have recently yielded a reliable value of 3/2 for the nuclear spin.[10] Urey previously showed that the sodium nucleus obeys the Fermi-Dirac statistics.[11] As band spectral observations[8, 9] appeared to disagree with the values of i obtained by other methods, we undertook a quantitative investigation of alternating intensities in absorption in sodium bands.

In this connection it was found impossible to use the methods of Harvey and Jenkins[12] and of Van Wijk and Van Koeveringe,[13] who obtained the alternation of intensities in the lithium bands without determining directly absorption coefficients of lines. In our case, the number of lines available for intensity measurements was too small and the deviations in line intensities produced by background irregularities were too large to use these methods. It was found necessary to measure relative absorption coefficients of lines after the manner of the work of Elliott[14, 15] on chlorine bands and the work of Childs and Mecke[16] on the acetylene bands.

APPARATUS AND PROCEDURE

The absorption spectrum was photographed in the second order of a 21-foot concave grating, having 14,500 lines to the inch and six inches wide. The photographic plates were Eastman Spectroscopic Plates Type 3J. A 500-candle-power lamp, with an arc between tungsten electrodes served as a continuous source.* The light

[1] H. Schüler, Naturwiss. **16**, 513 (1928).
[2] H. Schüler and J. E. Keyston, Zeits. f. Physik **68**, 174 (1931).
[3] R. deL. Kronig and S. Frisch, Phys. Zeits. **32**, 457 (1931).
[4] Frisch and Ferchmin, Naturwiss. **18**, 866 (1930).
[5] K. Murakawa, Inst. Phys. and Chem. Research Sci. Papers No. 398, p. 1–12 (Dec. 1932).
[6] C. M. Van Atta and L. P. Granath, Phys. Rev. **44**, 60 (1933); **44**, 935 (1933).
[7] Heydenburg, Larrick and Ellett, Phys. Rev. **40**, 1041 (1932).
[8] F. Loomis and R. Wood, Phys. Rev. **32**, 223 (1928).
[9] A. Ellett, Phys. Rev. **35**, 594 (1930), footnote.
[10] I. Rabi and V. Cohen, Phys. Rev. **43**, 582 (1933).
[11] H. Urey, Phys. Rev. **38**, 1074 (1931).
[12] A. Harvey and F. Jenkins, Phys. Rev. **35**, 789 (1930).
[13] Van Wijk and Van Koeveringe, Proc. Roy. Soc. **A132**, 98 (1931).
[14] A. Elliott, Proc. Roy. Soc. **A123**, 629 (1929).
[15] A. Elliott, Proc. Roy. Soc. **A127**, 638 (1930).
[16] W. Childs and R. Mecke, Zeits. f. Physik **64**, 162 (1930).

* This was the Point-o-Lite lamp manufactured by James G. Biddle, Philadelphia, Pa.

from the incandescent electrode was focussed by means of a condensing lens, placed between the lamp and the absorption tube, onto the slit of the spectrograph.

The iron absorption tube is shown diagrammatically in Fig. 1. Nitrogen gas, freed from

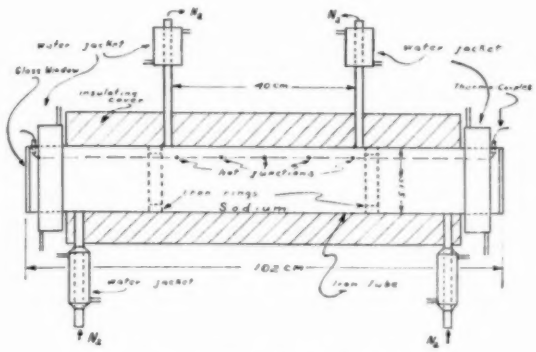

FIG. 1. The absorption cell.

oxygen and water vapor, was admitted into the absorption tube through two side pipes at the ends of the tube, while two more centrally located pipes served to draw it away. Metallic sodium could be placed in a 40 cm central portion of the tube and its vapor kept in that region by the flow of nitrogen gas from the ends of the tube towards the central outflow pipes. Two cylindrical iron rings were placed inside the tube (see Fig. 1) to assist in keeping the gaseous and liquid sodium confined in the central region. Glass windows were cemented to each end of the tube with de Khotinsky cement. Two chromel resistance coils, imbedded in alundum cement and asbestos, heated the tube electrically. One of the coils heated the tube along its whole length, while the other was short-circuited along the 40 cm central portion and heated the ends. By adjusting the current in each coil to the proper value, it was possible to obtain a uniform temperature in the 40 cm central portion of the tube, to which the sodium vapor was confined. Five iron-constantan thermocouples were strung through the tube with their hot junctions spaced at 10 cm intervals in the central 40 cm column. The heating of the tube was so regulated that the thermocouples showed a variation in temperature of only about two degrees and also no more than a two-degree variation in the course of the thirty-minute exposures. The suitable working temperature for the sodium vapor was found to be 347°C. Different nitrogen gas pressures up to atmospheric pressure were used in order to study the effects of possible line broadening on intensity ratios.

A comparison iron spectrum, the absorption spectrum, and sets of calibration marks were photographed at the top, middle and bottom of the plate respectively. A screen placed in front of the plate in its mounting, was used to give the three different exposures on the plate. The screen was supported by the arrangement shown diagrammatically in Fig. 2, and could be moved up

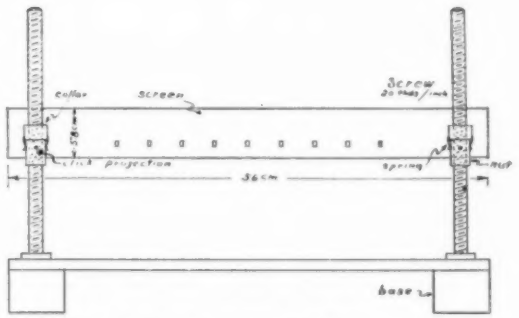

FIG. 2. The photographic plate screen.

and down by a pair of clicking nuts. Small rectangular openings in the lower half of the screen served to produce sets of calibration marks on the plate, a set of different wave-length for each opening. This was accomplished by moving the plate in its rack a few mm between exposures for density marks and keeping the screen stationary. To produce density marks of different relative intensities for each exposure, a tungsten ribbon filament lamp and rotating copper oxide screens were used according to the procedure described by Harrison.[17] The plates were microphotometered on a Moll microphotometer.

CALCULATION OF RESULTS

Three sets of calibration marks in the region of the band under investigation were microphotometered, yielding three characteristic curves for each plate, each corresponding to a different wave-length. The curves for plate *C* are shown

[17] G. R. Harrison, J. O. S. A. and R. S. I. **18**, 492 (1929).

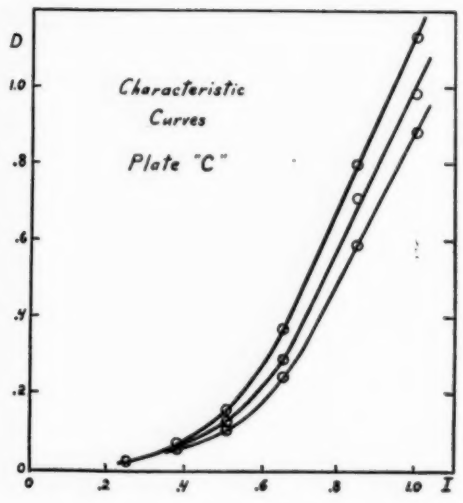

FIG. 3. Characteristic curves for Plate *C*.

in Fig. 3. The absorption band spectrum was also microphotometered, a portion of a tracing being shown in Fig. 4.

The density D of any point on the plate is given by $D=\log_{10}(F_m/F)$, where F_m is the height of the clear plate deflection on the microphotometer curve above the dark point line, and F is the height of the given point above the dark point line. The characteristic curves, which represent a plot of D against I, where $I=\log_{10} i$ (i is here the relative intensity), could then be used to translate densities into relative intensities.

We notice that the band lines occur in groups of three with an irregular background between each group. The designations of the lines as assigned by Loomis and Wood[8] are shown in Fig. 4. Measurements were confined to the (0,2) band in the $^1\Pi \leftarrow {}^1\Sigma$ transition, which alone was sufficiently free from overlapping bands to be used for intensity measurements. It was found that, besides the P, Q and R branch lines of the band, irregularities occurred throughout the spectrum. These could not be attributed either to the light source or to the optical system, since the same irregularities appeared on the microphotometer tracings from a plate by Loomis and Wood,[8] who used a different source (carbon arc) and grating. All attempts to systematize these irregularities or to trace them to impurities or to any overlapping Na_2 bands failed. Since these apparently random irregularities could underlie the band lines and thus affect their intensities, the problem of determining the true value of the latter became a difficult one.

Of the three branches, the Q branch is the most intense and hence it is affected least by background irregularities. Moreover, the range over which the Q lines were resolved from the P and R companions was larger than the corresponding range for either the P or R lines. Therefore, intensity measurements were limited to the Q lines, with $J=48$ to $J=73$ inclusive. For $J<48$, the Q line was not sufficiently resolved from its companions to warrant intensity measurements. For $J>73$ the background irregularities became so large that large errors would be introduced into intensity measurements. The following method was devised to compensate for the disturbing effect of background irregularities: it was assumed that the background irregularities can be treated as a random phenomenon and that the background occurring between band line groups is a representative sample of the entire background. The heights of the background occurring between each two band line groups were measured at small regular intervals yielding about 7 readings in each case, and the average of these was taken as the height of a representative background point between two such groups. To prove

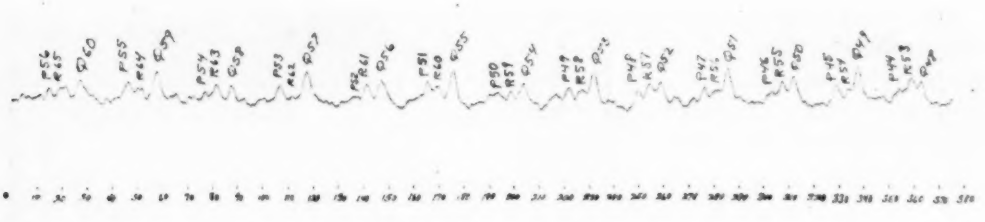

FIG. 4. Portion of microphotometer tracing of absorption band.

that averaging background heights (galvanometer deflections) is equivalent to averaging background intensities, we calculated in several instances the intensity corresponding to each reading and averaged the intensities. In each case the same value was obtained for the average point as by the first method. Since the first method is much the shorter one, it was adopted throughout the calculations.

Let the calculated deflection corresponding to each such average point be F_0. A plot of $\log_{10} F_0$

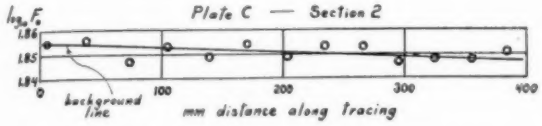

FIG. 5. Plot of $\log_{10} F_0$ against position along tracing.

against position along the tracing was made for each microphotometer tracing. Fig. 5 shows one such graph. It was found that in every case a straight line drawn through the plotted points was the best representative simple curve for the background density distribution. An interpolated value for the background density, D_0, could then be obtained from the graph for the background occurring directly under each absorption line. This method of calculating the background under a line removes a systematic error which would result if we referred the line intensities to the lowest points in the background. The density at the peak of each absorption line is given by $D=\log_{10} F_m/F$ where F_m and F are defined as above, and F refers to the line peak.

The calculation of intensities from corresponding densities was carried out with the aid of three characteristic curves which had been obtained for each plate. Thus, for two of the plates these curves were obtained for the wave-lengths of 4985, 5035 and 5085A, whereas the lines whose intensities were measured are located between 5019 and 5039A. To each curve was fitted an equation of the type: $D=a+bK+cK^2$, where $K=I-$constant, and then the values of a, b and c were interpolated for the wave-length of each absorption line whose intensity was to be found. By this method values of I and I_0, corresponding to values of D and D_0 respectively, were obtained for each absorption line in question. We desire in the case of each line, the quantity

$$\alpha=I_0-I=K_0-K. \tag{1}$$

This method of analytical interpolation for a value of α for each absorption line was checked by graphical interpolation for α directly from the three characteristic curves.

Further calculations follow from the following theoretical arguments: the intensities of the incident and transmitted light in absorption are given by

$$i_\nu=i_0e^{-\beta_\nu l} \tag{2}$$

where i_0 is the intensity of light in the background, i_ν is the intensity of light in the absorption line at wave-length ν, β_ν is the coefficient of absorption at wave-length ν, and l is the thickness of the absorbing layer, which is a constant for all the lines.

The coefficient, β_ν, will have a different form, depending on whether the shape of the line is determined by Doppler or "Dispersion" broadening.[18] For absorption at the center of the line, we have

$$i=i_0e^{-\beta l} \tag{3}$$

where all quantities are referred to the center of the line. It can be shown, irrespective of whether the shape of the line is determined by Doppler or "Dispersion" broadening, that the coefficient of absorption at the center of the line, β, becomes directly proportional to Einstein's coefficient of absorption and the number of molecules in the initial state.[18] If the observed intensity of the peak of the absorption line be taken as a measure of the true intensity, i, of the center of the line, we have for the center of the line

$$\beta l=\log_e 10\ (\log_{10} i_0-\log_{10} i). \tag{4}$$

Letting $\alpha=\log_{10} i_0-\log_{10} i=I_0-I=K_0-K$, we see that α will obey the same proportionality relation as that stated above for β. More explicitly, we have

$$\alpha \propto h\nu_{mn}B_{mn}g_m \exp\ (-E_m/kT). \tag{5}$$

Using Einstein's coefficient of spontaneous emission, A_{nm}, instead of B_{mn}, we have from the relation:

$$B_{mn}=A_{nm}(g_n/g_m)(C^3/8\pi h\nu^3) \tag{6}$$

[18] R. Ladenburg and Levy, Zeits. f. Physik **65**, 189 (1930).

that

$$\alpha \propto \nu^{-2} A_{nm} g_n \exp(-E_m/kT). \quad (7)$$

The theoretical relative values of the intensity factor $A_{nm}g_n$ for the lines in a band are given for our case by Dennison.[19] For the Q lines of our band, the intensity factor is $c(2J+1)g_i$ where c is a constant for all the lines in the branch and g_i is the statistical weight factor due to the spin of the nucleus. Variation in ν over the range of lines measured is very small. Therefore we will assume that, very nearly, we have

$$\alpha \propto (2J+1)g_i \exp(-E''/kT), \quad (8)$$

where E'' is the rotational energy of the lower state of the absorbing molecule, which is usually given as:

$$E'' = BhcJ(J+1)/kT + DhcJ^2(J+1)^2/kT. \quad (9)$$

The values for B and D are given by Loomis and Wood[8] and are: $B=0.15255$ and $D=-0.5954\times10^{-6}$. For our purposes the D term may be neglected. We may then write:

$$\alpha = C(2J+1)g_i \exp[-BhcJ(J+1)/kT] \quad (10)$$

where C is a constant for all the lines in question. This equation is equivalent to

$$[\alpha K_{00}/(2J+1)] \exp[BhcJ(J+1)/kT] = Cg_iK_{00}, \quad (11)$$

where K_{00} is a constant used for purposes facilitating computation.

Letting $Cg_iK_{00}=M$, we can obtain from Eq. (11) one set of experimentally observed values of M for the strong lines and another set for the weak lines, each M being computed from the experimentally known values of α and T. The calculated values of M for all plates are given in Table I. An average of all the M's for the strong lines, M_A (strong), is considered as the best value for Cg_iK_{00} for the strong lines, and similarly M_A (weak) for the weak lines. It is clear that:

$$\frac{M_A(\text{strong})}{M_A(\text{weak})} = \frac{g_i(\text{strong})}{g_i(\text{weak})} = \frac{i+1}{i}, \quad (12)$$

i.e., $M_A(\text{strong})/M_A(\text{weak})$ gives us the best value for the alternation of intensities. From this i, the spin of the sodium nucleus, is found. Calculated values of $(i+1)/i$ are listed in Table II. In Fig. 6 is shown a plot of M against J for plate C, the horizontal straight lines representing M_A(strong) and M_A(weak) respectively for that plate.

[19] D. Dennison, Phys. Rev. **28**, 318 (1926).

TABLE I.

J	B	C	D	D'	F	G
48	0.276	0.261	0.357	0.330	0.417	0.420
49	.455	.493	.633	.639	.678	.698
50	.397	.411	.448	.474	.510	.545
51	.491	.446	.629	.594	.736	.711
52	.322	.250	.352	.359	.435	.410
53	.522	.517	.605	.687	.689	.793
54	.448	.355	.337	.478	.481	.504
55	.574	.509	.638	.626	.677	.804
56	.412	.340	.422	.495	.502	.475
57	.459	.472	.606	.601	.739	.710
58	.274	.231	.316	.349	.337	.350
59	.534	.441	.626	.664	.646	.795
60	.379	.276	.415	.405	.541	.572
61	.477	.464	.522	.592	.703	.782
62	.321	.338	.293	.382	.478	.473
63	.585	.550	.660	.749	.826	.941
64	.178	.197	.219	.224	.284	.316
65	.551	.432	.561	.594	.712	.738
66	.205	.197	.237	.277	.447	.319
67	.591	.502	.586	.805	.760	.892
68	.323	.322	.239	.418	.365	.393
69	.410	.334	.524	.537	.639	.630
70	.274	.240	.271	.285	.301	.305
71	.542	.404	.501	.579	.623	.718
72	.299	.242	—	.308	.323	.420
73	.542	.503	—	.544	.588	.752

TABLE II.

Plate No.	N_2 Pressure	Temperature	$(i+1)/i$	Probable Error (P.E.)
B	2.5 mm	347°C	1.64	±0.09
C	27.4 mm	348°C	1.66	± .08
D†	103 mm	346°C	1.77*	± .08 (estimat.)
F	185 mm	347°C	1.66	± .07
G	185 mm	348°C	1.81	± .08

Average = 1.71

* Note: The value, 1.77, is an average obtained from two different tracings of the same plate, D, which yielded 1.82 ±0.09 and 1.72±0.08 respectively. Since this plate lacked a comparison iron spectrum, it presented special difficulties in alignment for microphotometry. Hence, the plate was microphotometered twice.

† Lines $J=72$ and $J=73$ were not measured on the first tracing of plate D.

DISCUSSION

Undoubtedly, a serious possible source of error in our calculations is the assumption that the observed intensity at the peak of an absorption

line is a measure of the true intensity at the center of the line. The finite slit widths in our optical system and the finite resolving power of the grating both influence the observed intensity and change the observed shape of the line from its true shape. Especially may this effect be disturbing in the case of absorption lines, whose shape varies with the percentage of the light absorbed. This effect will become more important as the amount of absorption increases. However, when we consider Table I, and Fig. 6, we notice

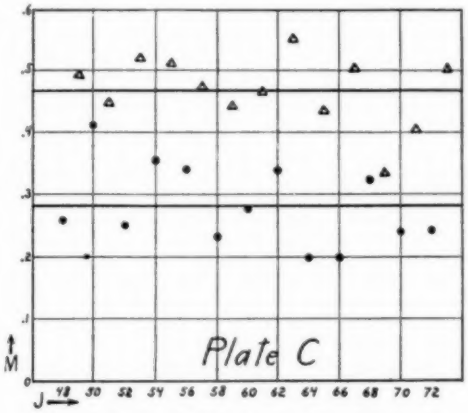

FIG. 6. Plot of M against J for Plate C.

that M (odd lines) is a good constant over our range of observations in spite of the fact that the magnitude of the absorption coefficients varies from one end of the graph to the other by a factor of 2.5. This, obviously, would not be the case if the above-mentioned source of error were present. That M (even lines) is not as good a constant as M (odd lines) is explained by the fact that background irregularities introduce a larger variation into the observed values of the α's for the weak than for the strong lines, and that smaller absorptions are known with smaller precision.

Another serious possible source of error in our calculations is the disturbing effect of background irregularities. Our method of construction of an average background line, presupposes that background irregularities occur in a random fashion. It is clear that the true relative absorption coefficients of the lines will differ from those calculated by this method, depending on whether the actual background under the absorption line happens to be lower or higher than the average background line, and the deviations from the true values will be random if the background irregularities occur in a random way. This partly accounts for the scattering of the points in Fig. 6. Other effects tending to scatter the observed values from the average are grain in the plate, dust particles, developer effects, galvanometer vibrations and other limitations in accuracy inherent in photometric determinations of intensities. Since these effects may be treated as largely random, we see that, as far as such errors go, the large number of observations available makes the final average much more reliable than the ratio of intensities as calculated from a single pair of lines on a single plate. The P.E. measure obtained for each plate is a good measure of the reliability of the mean for that plate as far as accidental and random errors go. The reliability measure of the mean for all plates should not be much better than that for a single plate, since the effect of background irregularities is the same on all plates. Hence, we consider a P.E. $= \pm 0.08$ to be a good measure of the reliability of the mean for all plates, as far as random errors are concerned. We must, however, call attention to the fact that the values of M (even lines) show a trend in Fig. 6. That this trend is not real and is the effect of a random distribution of errors is suggested by the fact that M (odd lines) shows no such trend; and we would hardly expect the odd and even lines to follow different laws. Still, the possibility remains that the trend is produced by a systematic background disturbance affecting mainly the even lines. In that case, the reliability of our results would be considerably less than that indicated by the above P.E. value.

RESULTS

The average value for $(i+1)/i$ computed from all the plates is 1.71 with a P.E. $= \pm 0.08$, assuming no systematic error. Since, as pointed out in an earlier paragraph, there is a possibility of systematic errors, we estimate the reliability of the above ratio to be considerably less than that indicated by the above P.E. The above average value agrees best with the value 1.67, the theoretical value corresponding to a spin of 3/2 for the sodium nucleus. We conclude therefore from these results that the most probable value of the

spin is 3/2, but that the values of 1 and 2 are not excluded as highly improbable.

In addition, it may be stated that the observation of Urey,[11] that the sodium molecule obeys the Fermi-Dirac statistics, has been confirmed by our present investigation. In all other cases, where both the spin of the nucleus and statistics are known, it has been found that in the case of nuclei with integral spins, the Bose-Einstein statistics are obeyed, while in the case of nuclei with half-integral spins, the Fermi-Dirac statistics are obeyed. Our results are in agreement with this experience.

In conclusion, I wish to express my sincere appreciation to Professor Harold C. Urey, who inspired this investigation, for his constant help and advice throughout this research. I also wish to thank the Physics Department at Columbia University for the use of their grating, and to express my appreciation to Dr. Gorman and Mr. Shriver of New York University for their work in making the microphotometer tracings, and to Professor F. W. Loomis of the University of Illinois for the loan of his note-books covering the analysis of the spectral region used in this investigation.

Fine-Structure Analysis of $H^1\alpha$ and $H^2\alpha$

R. C. WILLIAMS AND R. C. GIBBS, *Department of Physics, Cornell University*

(Received January 31, 1934)

Methods employed in applying corrections to an observed "doublet" interval to find the true interval and in relating the position of an intensity maximum to that of the components of which it is composed are critically discussed. The need for clearly distinguishing between the position of the center of gravity of even a nearly symmetrical intensity complex and that of its maximum is emphasized. A Fabry-Pérot interferometer was used to examine the fine structure of the $H^1\alpha$ and the $H^2\alpha$ lines. The interval between the main components of the "doublet" is found to be 0.308 cm^{-1} for $H^1\alpha$ and 0.321 cm^{-1} for $H^2\alpha$ as compared with 0.328 cm^{-1} indicated by theory. The relative intensities of the components as revealed by the analysis are approximately in agreement with theory.

THE Balmer lines of hydrogen are commonly referred to as "doublets," each of the two members of which, according to theory, is composed of two or more single symmetrical lines or components. The fine structure of these "doublets" has been studied by numerous investigators. Although roughly concordant results have been obtained experimentally in recent years for the $\Delta\nu$ interval between the two members of the doublets, the positions and relative intensities of the various components, especially the weaker ones, have been determined with only moderate accuracy and reliability. It is the purpose of this paper to discuss the methods of obtaining an analysis of the fine structure of the hydrogen lines, and to give the results of such an analysis for both $H^1\alpha$ and $H^2\alpha$.

The latest extensive paper upon the fine structure of H^1 lines was published by Kent, Taylor and Pearson.[1] They used crossed Lummer plates and an echelon grating as the resolving instruments, and a liquid-air-cooled Wood tube as a source. The crossed Lummer plates gave patterns which had to be measured visually, while the echelon grating gave patterns which could be measured both visually and with microphotometer curves. Corrections for the "shrinking effect"[2] were applied to the microphotometer curve results. Combining such corrected results with the visual measurements they obtained for $H^1\alpha$ a weighted average of 0.318 cm^{-1} for the "doublet" interval. Further, they analyzed the microphotometer curves to show the components predicted by theory.

In commenting upon their methods and results it may be pointed out that their microphotometer curves show grain variations comparable with the intensities of the weaker components, and that in their corrections and analyses these curves were used in their original form without reduction to intensity. Their shrinking effect correction amounted in some cases to as much as 9.6 percent of the measured interval. Both the size of this correction and their method of applying it are open to question. This correction is one to be made to the observed separation of intensity maxima of an incompletely resolved doublet composed of two similar and symmetrical components having approximately the same intensities. It is computed from the relative *intensity* of the "saddle" to that of either of the peaks, and when applied, changes the observed separation between intensity maxima to the true separation between two such components. For a given doublet, the relative saddle intensity and therefore the shrinking correction will be independent of photographic exposure. Kent, Taylor and Pearson made a shrinking correction on their *unreduced* curves, and hence obtained corrections that varied with the density of the photographic image. After applying this correction, they interpreted the interval thus determined as representing that between the centers of gravity of the two sets of components that form the "doublet." Several objections can

[1] Kent, Taylor and Pearson, Phys. Rev. **30**, 266 (1927).
[2] Hansen, Ann. d. Physik **78**, 558 (1925).

be raised to such a procedure. As can be seen from their curves the "doublet" is not of the type to which such a correction can suitably be applied. If theory is at least approximately correct, the main components do not overlap each other sufficiently to produce any measurable shrinking. Whatever shifts occur in the maxima, so as to displace them from the peaks of the main components, are due to the minor components, and these shifts are in the same direction for both maxima. As a matter of fact, our results show that the *total saddle intensity*, made up of contributions from both major and minor components, is not sufficient to produce an appreciable correction of the type treated by Hansen, even if a correction of this sort were applicable. Since they used the original microphotometer curves from which to obtain fine-structure analyses, they were able to obtain results in harmony with theory only from plates having a limited range of blackening.

Kent and his colleagues gave values of the $\Delta\nu$ they obtained and compared them favorably with the theoretical values of the $\Delta\nu$ between the centers of gravity of the "doublet." Yet the $\Delta\nu$ measured was in reality that between maximum intensity peaks, to which interval, as has already been noted, a shrinking correction was erroneously applied in the case of measurements from the microphotometer records. However, when an intensity complex is made up of two or more simple components of such relative positions and intensities as is indicated by theory for each member of the H$^1\alpha$ "doublet," the position of the maximum intensity does not coincide with the center of gravity of that complex.

For a complex of n symmetrical spectral components, of intensity I_0, I_1, I_2, $\cdots$ I_n, the displacement x_c of the *center of gravity* of the components from the I_0 component is defined by the equation:

$$x_c = -(1/I_0)\{I_1(x_c - x_1) + \cdots + I_n(x_c - x_n)\}$$
$$= -(1/I_0)\sum_{k=1}^{k=n} I_k(x_c - x_k) \quad (1)$$

where x_1, x_2, $\cdots$ x_n are respectively the distances of the center of each component from that of the component chosen as I_0.

Let us now consider the displacement of the *position of maximum intensity* of the complex composed of similar and symmetrical components from the component chosen as I_0. Let the distance of the center of each component from that of I_0 be respectively x_1, x_2, $\cdots$ x_n as before, and the corresponding intensities be I_1, I_2, $\cdots$ I_n. Then the resultant intensity curve of the complex will be:

$$I = I_0 e^{-cx^2} + I_1 e^{-c(x-x_1)^2} + \cdots + I_n e^{-c(x-x_n)^2}, \quad (2)$$

where c is defined by the equation $\log_e 2 = c(\text{half-line-width}/2)^2$. The stationary points of the complex are obtained by differentiating the above expression with respect to x, and equating the result to zero. Then the displacements x_m of the maxima and minima, from I_0, are given by the values of x_m which satisfy the equation:

$$x_m = -(e^{cx_m^2}/I_0)\sum_{k=1}^{k=n} I_k(x_m - x_k)e^{-c(x_m - x_k)^2}. \quad (3)$$

By using the theoretical positions and intensities of the components of the high frequency member of the H$^1\alpha$ "doublet" as an illustration, it is found from Eqs. (1) and (3) that the center of gravity of the two components is displaced 0.014 cm^{-1} from the stronger one while the intensity maximum, with a value of c determined from our half-line-width, is shifted 0.007 cm^{-1}. This clearly indicates that in a doublet, either member of which contains one or more components, the position of maximum intensity cannot be identified in general with the position of the center of gravity. A careful analysis of an experimental intensity curve, an illustration of which will be given later, for H$^1\alpha$ fine structure will yield information to which Eq. (3) can be applied as a check.

In obtaining the H$^1\alpha$ interference fringes the source of radiation was a liquid-air-cooled Wood tube bent in the form of a modified U, with suitable precautions to insure the complete immersion in liquid air of the portion of the tube from which light was taken. The radiation was analyzed by a Zeiss three-prism spectrograph, with a Fabry-Pérot etalon in the collimated beam. The discharge in gaseous hydrogen was maintained by a 3000-volt transformer, and the pressure and current were held at such values

that the discharge was maintained only very weakly. The exposures were from 30 seconds to 1 minute of actual exposure time, the discharge being run only 5 seconds in every 20. Intensity marks were placed on the plates by using a continuous uniform source and varying the slit widths.

Eastman 4-C and 5-C plates, which are very fine grained and quite sensitive in the Hα region, were used. As an example of the type of record obtained from these plates, an original microphotometer curve taken of $H^2\alpha$ with a 3 mm etalon on a 4-C plate is shown in Fig. 1.

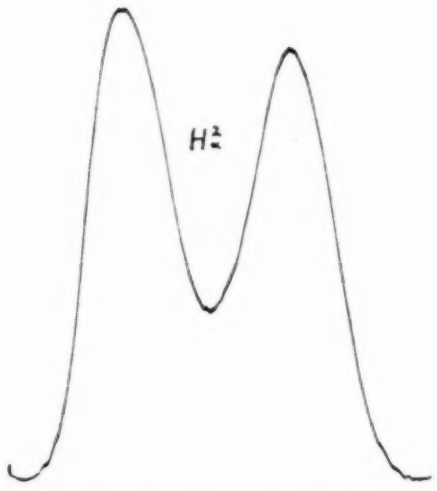

FIG. 1. Microphotometer curve of $H^2\alpha$ (3 mm etalon).

Such curves together with the intensity mark records were obtained on a Moll microphotometer. These curves were then enlarged fourfold upon cross-section paper by a transmission projector, the uniformity of whose field had been checked. The curves were next reduced to densities by the usual logarithmic formula, and were further reduced to intensities by the density-intensity curve obtained from the intensity mark records. A satisfactory check on this procedure was obtained by drawing intensity curves for both an overexposed and an underexposed pattern. Although the original microphotometer curves were quite unlike, the intensity curves of the two were practically identical.

The intensity curves were analyzed for fine structure as will be later explained, and after this analysis the $\Delta\nu$ between the centers of the main components could be obtained as follows. It is readily seen that the position of a maximum on the microphotometer record coincides with the position of the corresponding maximum on the intensity curve. For a particular plate the displacements of the centers of the two main components from the positions of the respective intensity maxima were obtained from a fine-structure analysis, and checked by Eq. (3). These displacements being known, the interval between the peaks of the original microphotometer curve of that plate could be used in determining the $\Delta\nu$ between main components. Of course a fine-structure analysis had to be made for each plate in order to discover whether any change in relative intensities occurred due to changing discharge conditions, for this would affect the displacements mentioned above. However, in the results here reported there were noted no relative changes of intensity of sufficient size to affect the displacements appreciably. By using the curves obtained from several plates, an average interval between main components was determined with an estimated error of not more than 0.002 cm^{-1}.

Some investigators have used an etalon spacing such that the members of the "doublet" are spaced just one-half of an interference order apart, in order to neutralize the Eberhard and shrinking effects. The Eberhard effect can be minimized by rapid brush development or by the use of light exposures on fine-grained plates as were used in this study. The shrinking effect, which is not readily corrected for in the case of visual measurements, must be taken into account when the interval between resolved components is small, but as has been already pointed out, it is negligible for the Hα "doublets." Accordingly, since in this study a positive analysis of the intensity curves was desired, an etalon spacing such as to reduce the intensity between successive interference orders to a very low value was used. Thus, in the light of the theoretical analysis, the intensity distribution on the high frequency side of the "doublet" pattern coincides with the true intensity curve of the corresponding main component over most of its high frequency side, which makes it possible to determine the constant in the intensity equation of all com-

ponents for any chosen position and maximum intensity of this component. Consequently a 5 mm etalon spacing was selected for $H^1\alpha$.

The analysis of the experimental intensity curve was performed as follows. As already explained, all but the top portion of the high frequency side of the pattern is the actual shape of the intensity curve for one of the main components. A center position and a height for this component were tentatively chosen. From these the half-line-width and the related constant c in the equation $I = I_0 e^{-cx^2}$ could be found. Then the approximate position of the low frequency main component (which was restricted within relatively narrow limits by the shape of the intensity distribution), was tentatively chosen. The separation of each minor component from its major component was taken so that the ratio of such intervals to that between the two main components was approximately the same as the corresponding ratio predicted by theory. This choice of intervals will be discussed later. All the components were then drawn in, in such a way as to satisfy the three simultaneous conditions: (a) The curve for each component had to satisfy the intensity equation with the same value for c; (b) the component curves had to add up to the original intensity distribution at every point; (c) the positions of all the maxima and minima of the complex as fixed by the tentative analysis had to satisfy Eq. (3). Successive trials were made until these conditions were all closely fulfilled.

Fig. 2 shows the analyzed intensity curve for $H^1\alpha$, with an interval[3] between intensity peaks of 0.304 cm^{-1}, which is an average value obtained from several microphotometer curves. The observed half-line-width is 0.180 cm^{-1}. The theoretical separations and intensities for $H^1\alpha$ are shown in Fig. 3. The analysis, made as described above, gives $\Delta\nu = 0.308$ cm^{-1} as the separation of the main components, while $\Delta\nu = 0.328$ cm^{-1} is expected theoretically. The theoretical intensities have been computed by Sommerfeld and Unsold,[4] by Saha and Banerji[5] and by Kupper.[6] The analysis was not sufficiently critical to establish either the existence or nonexistence of the 5th component which theory predicts to be very weak. Accordingly in Figs. 2 and 4 no attempt has been made to show this component.

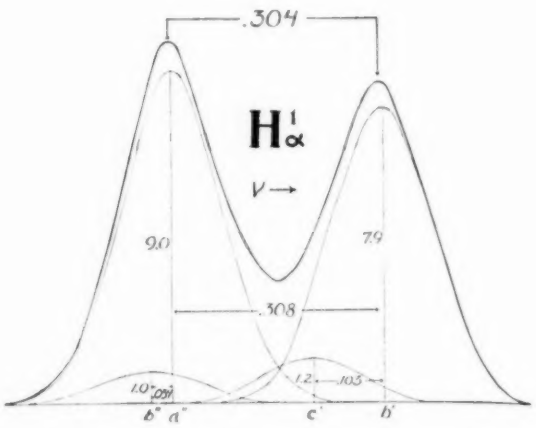

FIG. 2. Analysis of $H^1\alpha$ (intervals in cm^{-1}).

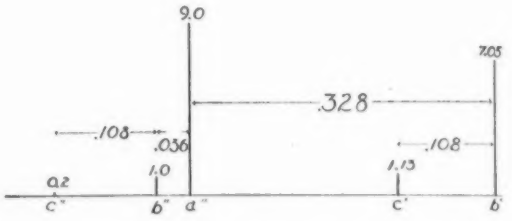

FIG. 3. Theoretical structure of $H^1\alpha$ (intervals in cm^{-1}).

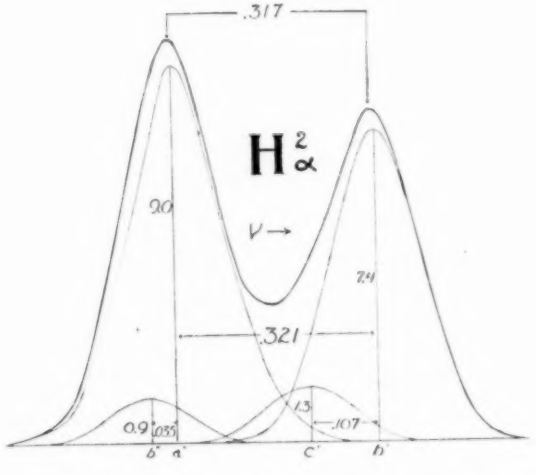

FIG. 4. Analysis of $H^2\alpha$ (intervals in cm^{-1}).

Experimental work on $H^2\alpha$ was started with a sample of hydrogen containing about 1 part

[3] Gibbs and Williams, Phys. Rev. **45**, 221 (1934).
[4] Sommerfeld and Unsold, Zeits. f. Physik **38**, 237 (1926).
[5] Saha and Banerji, Zeits. f. Physik **68**, 704 (1931).
[6] Kupper, Ann. d. Physik **86**, 511 (1928).

in 80 of H^2, kindly supplied by Professor H. C. Urey of Columbia University. Later a sample of water, whose hydrogen content was nearly 50 percent H^2, was generously furnished by Professor G. N. Lewis of the University of California. A discharge in the water vapor of this latter sample actually produced the $H^2\alpha$ line only about 1/3 as intense as the $H^1\alpha$ line, probably due to ordinary hydrogen contamination in the discharge tube. An etalon spacing of 3 mm was used, for this allowed the $H^2\alpha$ and $H^1\alpha$ fringes to be distinctly separated, although they were overlapped $2\frac{1}{2}$ orders of interference. This spacing has a resolving power of over 400,000 when the etalon plates have a reflectivity of 92 percent. With a resolution as great as this, or greater, the shape of the $H\alpha$ intensity curves is almost solely determined by the thermal Doppler effect, and consequently not much is to be gained from greater optical resolution. In order to determine whether much resolution is lost by the use of 3 mm plates, the $H^1\alpha$ fringes were photographed with etalon spacings of 3, 5 and 7 mm. No measurable decrease in half-width with increase in etalon spacing was observed.

Fig. 4 shows the analyzed intensity curve for $H^2\alpha$, with an averaged interval[3] between intensity peaks of 0.317 cm^{-1}. The observed half-width is 0.171 cm^{-1}. Had $H^2\alpha$ been observed from a discharge in gas, at the same temperature as was $H^1\alpha$, its half-width should have been 0.127 cm^{-1}. The maintaining of the water-vapor discharge in a liquid-air-cooled tube required an increased current and thus increased the effective temperature of the H^2 discharge.

The interval between main components for $H^1\alpha$ is about 6 percent below that expected theoretically. This is in approximate agreement with the most recent results of Houston and Hsieh.[7] Furthermore, the average of the intervals between intensity peaks given by Kent, Taylor and Pearson from direct measurements of their microphotometer curves, before any "shrinking-correction" was applied, is found to be 0.306 cm^{-1}. This is in close agreement with our value of 0.304 cm^{-1} for the same interval.

The observed interval between peaks is for $H^1\alpha$ considerably less and for $H^2\alpha$ somewhat less than that predicted by theory. This smaller interval may be due chiefly to a shift toward lower frequencies of the c' and b' components, each of which is made up in part of a radiated frequency involving a transition to the $2s\,^2S_{1/2}$ level, for of the levels involved in $H\alpha$ this level is most likely to be displaced by a departure from a coulomb field or from a spherically symmetrical field near the nucleus. These observations and considerations may perhaps suggest some modification in our choice of intervals between components b' and c' and between a'' and b''. However, before these questions can be definitely determined, it will be necessary to secure interference patterns with considerably smaller half-line-widths.

Spedding, Shane and Grace[8] have published microphotometer curves which by their asymmetry indicate the presence of the same components for $H^2\alpha$ as are revealed by this study.

---

[7] Houston and Hsieh, Phys. Rev. **45**, 132A (1934).

[8] Spedding, Shane and Grace, Phys. Rev. **44**, 58 (1933).

Bands in the Extreme Ultraviolet Emission Spectrum of the H^1H^2 Molecule

C. RULON JEPPESEN, *University of California*

(Received February 15, 1934)

By using a two meter grazing incidence vacuum spectrograph, the extreme ultraviolet emission spectrum of a mixture of about 60 percent ordinary hydrogen and 40 percent "heavy" hydrogen has been photographed. All together twelve bands have been identified as belonging to the $2p\,^1\Pi_{cd}-1s\,^1\Sigma$ system of the H^1H^2 molecule. Analysis of these bands indicates that the rotational and vibrational constants for the H^1H^2 molecule are the same to within experimental error as those derived from the theory of the isotope effect. *There is, however, an extremely large electronic isotope shift of 135 cm^{-1} units.* The apparent vibrational perturbation found previously in the $v=3$ level of the $2p\,^1\Pi_{cd}$ state of the H^1H^1 molecule has its counterpart in the same level of the H^1H^2 molecule where its magnitude is about 4.3 cm^{-1} units, compared to 10.4 cm^{-1} for H^1H^1.

INTRODUCTION

FOLLOWING the discovery of a hydrogen isotope of mass 2, many investigators have studied the various properties of this new atom and the molecules formed by its combinations with other atoms. The present paper deals with the results so far obtained in an investigation of the extreme ultraviolet spectrum of a mixture of about 60 percent ordinary hydrogen and 40 percent of the "heavy" isotopic hydrogen.

EXPERIMENTAL PROCEDURE

The spectrograph and the type of discharge tube used in the present study have been described previously.[1] A quantity of the heavy isotopic hydrogen was generously supplied by Professor G. N. Lewis of the chemistry department. Exposures of one hour duration using power from a one kw 25,000 volt transformer were sufficient to obtain more than 2500 lines in the spectrum between 800 and 1375A. Known lines in the spectrum of H^1H^1, the wave-lengths of which had been previously determined,[1] were used as standards for the reduction of the plates.

ANALYSIS

The well-known theory[2] of the isotope effect in band spectra allows the calculation of the rotational and vibrational constants for the molecule H^1H^2 from the known values of these constants for H^1H^1. The mass of H^2 has been found by Bainbridge[3] to be 2.01363. This leads to a value of the constant ρ equal to 0.86616. The equations given in the previously-mentioned[1] study of the H^1H^1 bands, together with this value of ρ, then lead to the following equations for the respective constants of the H^1H^2 molecule.

For the $1s\,^1\Sigma$ (normal) state of the molecule B_v from $v=0$ to $v=5$ is given in cm^{-1} units by the equation:

$$B_v{}^i = 45.668 - 1.99305(v+\tfrac{1}{2}) + 0.0384948(v+\tfrac{1}{2})^2 - 0.00316885(v+\tfrac{1}{2})^3. \quad (1)$$

Because of the extreme curvature of the $B_v : v$ function, another equation is necessary for the fitting of B_v for higher values of v. Accordingly for $v=6$ to $v=9$ the following equation may be used.

$$B_v{}^i = 45.350 - 1.81546(v+\tfrac{1}{2}) + 0.00590989(v+\tfrac{1}{2})^2 - 0.00117286(v+\tfrac{1}{2})^3. \quad (2)$$

For all observed values of v, $D_v{}^i$ is given by the equation:

$$D_v{}^i = -0.0261849 + 0.00065863(v+\tfrac{1}{2}). \quad (3)$$

[1] C. R. Jeppesen, Phys. Rev. **44**, 165 (1933).

[2] W. Jevons, *Report on Band Spectra of Diatomic Molecules*, Cambridge (1932).

[3] K. T. Bainbridge, Phys. Rev. **44**, 57 (1933).

F_v^i, which may be assumed equal to F_c^i, is found to be $F_v^i = 2.1876 \times 10^{-5}$ cm^{-1}. (4)

And finally, ΔG_v is given with sufficient accuracy from $v = -\frac{1}{2}$ to $v = 6\frac{1}{2}$ by the equation:

$$\Delta G_v^i = 3826.0 - 197.03(v+\tfrac{1}{2}) + 6.0733(v+\tfrac{1}{2})^2 - 0.42776(v+\tfrac{1}{2})^3. \quad (5)$$

For the $2p\ ^1\Pi_{cd}$ (C) state of the H^1H^2 molecule the corresponding equations, which are valid for all observed values of v, are as follows:

$$(B_c^x)_v^i = 23.473 - 0.85564(v+\tfrac{1}{2}) - 0.0673705(v+\tfrac{1}{2})^2 + 0.00800339(v+\tfrac{1}{2})^3, \quad (6)$$

$$(D_c^x)_v^i = -0.0117966 + 0.000403285(v+\tfrac{1}{2}), \quad (7)$$

$$(F_c^x)_v^i = 7.9813 \times 10^{-6}, \quad (8)$$

$$(B_d^x)_v^i = 23.8086 - 1.02035(v+\tfrac{1}{2}), \quad (9)$$

$$(D_d^x)_v^i = -0.0120466 + 0.00039199(v+\tfrac{1}{2}), \quad (10)$$

$$(F_d^x)_v^i = 8.31957 \times 10^{-6}. \quad (11)$$

The subscripts c or d as the case may be, indicate that the constant in question should be ascribed to the c or d component levels. The superscript x indicates that the values of B, D and F given are "effective" values of these constants to take account of the Λ-type doubling. The values of ΔG_v for the $2p\ ^1\Pi_{cd}$ state are given by the equation:

$$\Delta G_v^i = 2140.3 - 133.44(v+\tfrac{1}{2}) + 11.940(v+\tfrac{1}{2})^2 - 1.22607(v+\tfrac{1}{2})^3. \quad (12)$$

These equations not only allow the calculation of the rotational energy functions for each electronic state, from which the ΔF values may be obtained, but they may also be used to find the position of any band in the system.

A search for lines satisfying the conditions required by the above equations, assuming the origin of the $2p\ ^1\Pi_{cd} - 1s\ ^1\Sigma$ system to be the same in the case of the H^1H^2 molecule as in that of the H^1H^1 molecule, was entirely unsuccessful. However, twelve bands were found in which all the lines satisfy our theoretical equations, if we assume an electronic isotope shift of approximately 135 cm^{-1}. The electronic term value T_e of the $2p\ ^1\Pi_{cd}$ state in the H^1H^2 molecule is then found to be approximately 100,184 cm^{-1} units to be compared with 100,049 cm^{-1} for this same constant in the case of the H^1H^1 molecule.

So large an electronic shift is not, however, unreasonable for two isotopic molecules differing so greatly in mass. A simple calculation shows that the normal mass effect for a system consisting of a single electron and nucleus should give an electronic isotope shift of about 9 cm^{-1} at our observed ν_e for nuclei differing in the ratio of the masses of H^1H^1 and H^2H^1. The "specific effect" of Hughes and Eckart[4] in the case of the Li^6 and Li^7 atoms produces an additional shift of about 3.6 times the normal mass effect for these atoms. Hence if this same ratio holds for the hydrogen molecule, a total electronic shift of about 42 cm^{-1} is to be expected. Of course our observed shift is considerably greater than this, but it appears to be at least of the expected order of magnitude.

By using the observed frequencies of the lines, the origin of each band has been found by means of the calculated value of the rotational energy for each state. For any particular band the calculated origin, as determined from each individual line, was found to be the same to within the experimental error. With the origins thus found, the calculated value of the frequency of each line has been found. Table I gives the observed and calculated wave numbers of lines in each of the twelve bands. Lines marked with an asterisk are known blends. In some cases these blends are very wide on the photographic plate so that the measured values of their wave

[4] D. S. Hughes and Carl Eckart, Phys. Rev. **36**, 694 (1930).

TABLE I.

Branch	K''	I	Obs. (cm^{-1})	Calc. (cm^{-1})	$O-C$
		(0–2) Band ν_0 = 92,140.1 cm^{-1}			
R	0	5	92,182.0	92,182.3	−0.3
	1	6	92,193.3	92,193.4	−0.1
	2	3	92,167.7	92,169.3	−1.6
	3	2D	92,109.7	92,110.0	−0.3
P	2	4	91,936.9	91,938.0	−1.1
	3	8	91,787.2*	91,788.2	−1.0
	4	6	91,606.7	91,605.9	0.8
	5	7	91,388.2*	91,392.4	−4.2
Q	1	7	92,100.4	92,099.9	0.5
	2	8	92,029.0	92,029.1	−0.1
	3	4	91,923.0	91,923.4	−0.4
	4	8	91,787.2*	91,783.9	3.3
	5	6	91,606.7*	91,611.6	−4.9
		(0–3) Band ν_0 = 88,865.1 cm^{-1}			
R	0	6	88,908.0	88,907.7	0.3
	1	4	88,922.9	88,922.6	0.3
	2	6	88,908.0	88,905.8	2.5
	3	2	88,857.1	88,857.5	−0.4
	4	0D	88,779.5	88,778.6	0.9
P	2	7	88,671.9*	88,674.5	−2.6
	3	4	88,535.6	88,535.7	−0.1
	4	4	88,366.8	88,368.1	−1.3
	5	3D	88,168.2	88,172.7	−4.5
Q	1	7	88,828.7	88,829.1	−0.4
	2	7	88,765.5	88,765.6	−0.1
	3	7	88,671.9	88,670.9	1.0
	4	2D	88,545.6	88,546.1	−0.5
	5	3	88,390.3	88,391.9	−1.6
		(1–1) Band ν_0 = 97,617.1 cm^{-1}			
R	1	4	97,660.9	97,659.8	1.1
	2	3	97,622.7	97,622.1	0.6
	3	2	97,543.7	97,543.6	0.1
P	2	4	97,401.9	97,401.0	0.9
	3	3	97,234.9	97,235.9	−1.0
Q	1	5	97,571.4	97,570.6	0.8
	2		Hidden by 2nd Lyman Line		
	3	5	97,364.3	97,365.7	−1.4
		(1–3) Band ν_0 = 90,875.4 cm^{-1}			
R	0	4	90,915.6	90,915.7	−0.1
	1	4D	90,926.6	90,926.5	0.1
	2	2D	90,903.0	90,903.6	−0.5
P	2	5	90,683.3	90,682.5	0.8
	3	4	90,538.8	90,539.6	−0.8
	4	4	90,366.7	90,365.9	0.8
	5	3	90,161.5	90,162.5	−1.0
Q	1	7	90,837.6	90,837.3	0.3
	2	7	90,769.6	90,769.9	−0.3
	3	4	90,668.3	90,669.4	−1.1
	4	4B	90,538.8	90,537.0	1.8
		(1–4) Band ν_0 = 87,768.2 cm^{-1}			
R	0	10	87,807.5*	87,809.0	−1.5
	1	8	87,824.3	87,823.4	0.9
	2	10	87,807.5*	87,807.9	−0.4
	3	4	87,762.0	98,872.7	−0.6
	5	10	87,585.2*	87,585.2	0.0
P	2	10	87,585.2*	87,586.8	−1.6
	3	4	87,455.4	87,454.9	0.5
	4	8	87,296.3	87,295.6	0.7
	5	5	87,109.7	87,110.3	−0.6
Q	1	10	87,734.5	87,734.2	0.3
	2	10	87,674.9	87,674.2	0.7
	3	10	87,585.2*	87,584.7	0.5
	4	3	87,467.2	87,466.7	0.5
	5	1D	87,322.4	87,321.3	1.1
		(1–5) Band ν_0 = 84,829.2 cm^{-1}			
R	0	9	84,871.1*	84,870.5	0.6
	1	8	84,889.0	84,888.6	0.4
	2	8	84,880.7	84,880.4	0.3
	3	2	84,844.4	84,846.2	−1.8
P	2	4	84,661.6*	84,659.3	2.3
	3	4	84,540.6	84,538.5	2.1
	4	3	84,394.2	84,393.9	0.3
	5	1	84,225.9	84,226.7	−0.8

Branch	K''	I	Obs. (cm^{-1})	Calc. (cm^{-1})	$O-C$
		(1–5) Band ν_0 = 84,829.2 cm^{-1}			
Q	1	7	84,799.5	84,799.4	0.1
	2	6	84,747.3	84,746.7	0.6
	3	4	84,668.3*	84,668.3	0.0
	4	2D	84,562.8	84,565.0	−2.2
	5	1D	84,436.0	84,437.7	−1.7
		(2–2) Band ν_0 = 96,068.4 cm^{-1}			
R	0	5	96,108.3*	96,106.0	2.3
	1	5	96,108.3*	96,108.9	−0.6
P	2	3	95,861.4	95,861.7	−0.3
	3	3	95,703.9	95,703.7	0.2
Q	1	5	96,024.5	96,023.8	0.7
	2	2D	95,945.2	95,945.0	0.2
	3	3	95,826.6	95,827.4	−0.8
		(2–3) Band ν_0 = 92,787.6 cm^{-1}			
R	0	7	92,827.8*	92,825.6	2.2
	1	7	92,827.8*	92,832.3	−4.5
	2	3	92,803.1	92,803.4	−0.3
P	2	4	92,592.7	92,592.4	0.3
	3	6	92,445.8	92,445.4	0.4
Q	1	8	92,747.9	92,747.2	+0.7
	2	3	92,676.2	92,675.8	0.4
	3	3	92,569.9	92,569.1	0.8
	4	2D	92,428.4	92,428.6	−0.2
	5	3	92,253.6	92,255.0	−1.4
		(2–5) Band ν_0 = 86,741.7 cm^{-1}			
R	0	7	86,780.1*	86,780.7	−0.6
	1	7	86,793.9	86,794.7	−0.8
	2	7	86,780.1*	86,780.5	−0.4
P	2	7	86,569.2	86,569.5	−0.3
	3	7	87,445.4	86,444.6	0.8
	4	5	86,289.2	86,294.0	−4.8
	5	3	86,117.7	86,118.7	−1.0
	6	2D	85,926.7?	85,920.3	6.4
Q	1	7	86,710.3	86,709.6	0.7
	2	7	86,652.2	86,652.8	−0.6
	3	7	86,569.2	86,568.3	0.9
	4	1D	86,457.6	86,456.9	0.7
	5	3	86,321.0	86,319.5	1.5
		(2–6) Band ν_0 = 83,974.4 cm^{-1}			
R	0	7	84,014.8*	84,013.8	1.0
	1	6	84,031.2	84,031.5	−0.3
	2	7	84,014.8*	84,024.7	−9.9
P	2	5	83,814.6	83,813.7	0.9
	3	4	83,698.7	83,699.7	−1.0
	4	4	83,557.2	83,563.6	−6.4
Q	1	7	83,946.7	83,946.4	0.3
	2	7	83,898.0	83,897.0	1.0
	3	5	83,822.4	83,823.4	−1.0
	4	3	83,725.9	83,726.5	−0.6
		(3–4) Band ν_0 = 91,495.0 cm^{-1}			
R	0	5	91,541.3*	91,531.2	10.1
	1	5	91,541.3*	91,537.5	3.8
	2	3B	91,508.2	91,509.8	−1.6
	3	3D	91,453.7	91,448.4	5.3
P	2	2D	91,313.2	91,309.0	4.2
	3	4	91,175.7	91,169.0	6.7
	4	2D	91,002.4	90,997.5	4.9
	5	2D	90,800.5	90,796.1	4.4
Q	1	7	91,456.2	91,456.3	−0.1
	2	7B	91,388.2	91,388.1	0.1
	3	5	91,287.1	91,286.3	0.8
	4	2D	91,154.3	91,151.9	2.4
		(3–7) Band ν_0 = 83,190.1 cm^{-1}			
R	0	5	83,231.5	83,227.7	3.8
	1	6	83,246.6*	83,245.2	1.4
	2	6	83,246.6*	83,239.9	6.7
P	2	2	83,042.8	83,039.1	3.7
	3	3	82,936.2	82,932.4	3.8
	4	4	82,809.4*	82,805.2	3.8
	5	2	82,663.7	82,658.8	4.9
Q	1	7	83,164.0	83,164.0	0.0
	2	6	83,117.8	83,118.2	0.4
	3	4	83,049.8	83,049.7	0.1
	4	3	82,961.2	82,959.6	1.6
	5	3	82,847.5	82,848.9	−1.4

numbers have comparatively very large probable error. In other cases the probable error is about 2 cm^{-1} units or less.

The value of the origins of the bands as given in Table I allow the calculation of a number of the ΔG_v values for each of the two states in question. These values are given in Table II.

TABLE II. ΔG_v *values.*

v	For $1s\,{}^1\Sigma$ State Obs.	Calc.	For $2p\,{}^1\Pi_{cd}$ State Obs.	Calc.
$\frac{1}{2}$			2010.3	2017.6
$1\frac{1}{2}$	3466.8*	3453	1912.5	1911.4
$2\frac{1}{2}$	3277.8	3278	1814.3*	1804.6
$3\frac{1}{2}$	3107.2	3108		
$4\frac{1}{2}$	2939.0	2940		
$5\frac{1}{2}$	2767.3	2771		
$6\frac{1}{2}$	2598.7*	2599		

The probable error of measurement of the ΔG values is rather large (about 5 cm^{-1}) since the wave-length interval is larger than the range over which it has been possible to obtain consistent standards. It should be remarked also that the ΔG values marked with an asterisk in Table II could not be obtained directly and so may contain the sum of several errors of measurement.

A graphical representation of the $\Delta G_v : v$ data for the two states considered is shown in Fig. 1,

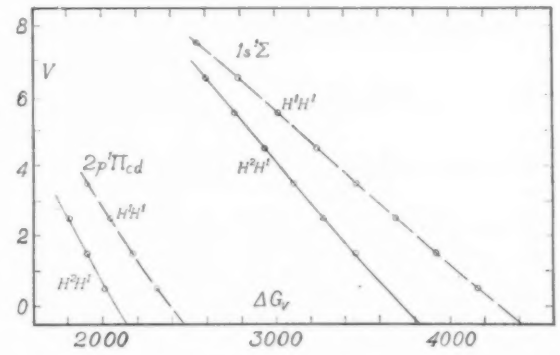

FIG. 1. Graphical representation of the $\Delta G_v : v$ data for the $1s\,{}^1\Sigma$ and $2p\,{}^1\Pi_{cd}$ states.

together with the corresponding data for the H^1H^1 molecule. In the case of the H^1H^2 data the curves drawn are those given by the theoretical Eqs. (5) and (12).

An additional check upon the identification of lines is afforded by a calculation of the term differences ΔT_K given by equations of the following type as suggested by Jenkins and McKellar.[5]

$$\begin{aligned}\Delta T_K &= R^{(1-3)}(K) - R^{(1-4)}(K)\\ &= P^{(1-3)}(K) - P^{(1-4)}(K)\\ &= Q^{(1-3)}(K) - Q^{(1-4)}(K)\\ &= \Delta G_{3\frac{1}{2}}'' - \alpha''(K+\tfrac{1}{2})^2 + \cdots. \qquad (13)\end{aligned}$$

Accordingly in the cases for which such calculations are possible, ΔT_K values have been found and fitted by least squares to equations of the form given by (13). In each of the four cases thus examined the observed values of ΔT_K and those calculated by the least squares equations have differences within the probable error of measurement (about 2 cm^{-1}), and the values of ΔG_v given by the constant terms of our least squares equations differ by an equally small amount from the ΔG_v values obtained by use of the band origins given in Table I.

A typical example of one of these $\Delta T_K : (K+\frac{1}{2})$ functions, as obtained from the 1–3 and 1–4 bands, is shown in Fig. 2, together with the same

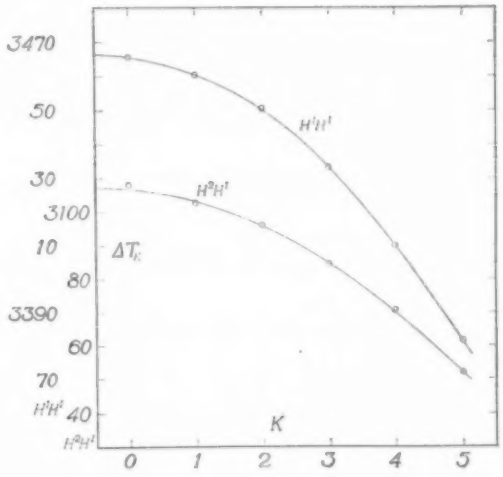

FIG. 2. Typical examples of $\Delta T_K : K$ relations as obtained from 1–3 and 1–4 bands for H^1H^1 and H^2H^1.

function as obtained from the data on the H^1H^1 molecule.[1] The curves drawn through the experimental data have been obtained from the least squares equations mentioned above.

The coefficients of $(K+\frac{1}{2})^2$ in these equations

[5] F. A. Jenkins and Andrew McKellar, Phys. Rev. **42**, 473 (1932).

are the slopes of the $B_v : v$ curve at the particular value of v for which any equation applies. Ordinarily this slope, α, is very nearly constant for low values of v but in the case of the normal state of hydrogen this has been shown[1] not to be true. Due to this fact we cannot determine an experimental value of α_e for this state of the H^1H^2 molecule, although we have the value of α for values of v between $2\frac{1}{2}$ and $5\frac{1}{2}$ inclusive. The ratio α_e^i/α_e, according to the theory of the isotope effect, equals ρ^3, but as just noted, we cannot unfortunately, obtain this ratio from the data at hand. However, α_v^i/α_v for $v=2\frac{1}{2}$ to $5\frac{1}{2}$, where the $B_v : v$ curve is almost a straight line, is found to be 0.610 as compared with the known $\rho^3=0.650$. The agreement is probably as good as might be expected, and furnishes an independent check upon the correctness of the assignment of lines.

Perturbations

As has been shown in a former paper[1] there exist a number of perturbations in the levels of the $2p\ ^1\Pi_{cd}$ state of the H^1H^1 molecule. Because of the comparatively small number of bands observed in the present study, not more than a few recognized lines originate on any one particular rotational level. Since any given line may happen to be an unrecognized blend, it is therefore difficult to establish with certainty any perturbations in the H^1H^2 spectrum. However, there is some evidence that a few of these levels may be perturbed. For example, the $K=3$ level of the $v=2$ state appears to have a perturbation of a few cm^{-1} units. It should be noted that although this level in the H^1H^1 spectrum is perturbed by -7.4 cm^{-1} units, one does not, in general, expect the same quantum states to be perturbed in the two systems because the energies are different.

It may be seen at once, however, from Table I that all of the lines of the P and R branches of bands having the $v=3$ state as their initial level are perturbed by about 4.3 cm^{-1}. This apparently is a vibrational perturbation and is very similar to the observed vibrational perturbation of 10.4 cm^{-1} in the same $v=3$ level of the H^1H^1 molecule. The term value, G_3, for this level in the H^1H^1 spectrum is 6526 cm^{-1}. In the H^2H^1 spectrum G_3 for the $2p\ ^1\Pi_{cd}$ state is 5734 cm^{-1} units and $G_4 = 7453$ cm^{-1}. It is very likely that the perturbing level has an isotope shift of an equally appreciable amount so that it is difficult to say whether or not we should expect adjacent levels to be perturbed also. It is seen, however, that the $v=3$ level in the H^2H^1 spectrum is nearer to the perturbed level of the H^1H^1 spectrum than is the $v=4$ state so that even were the perturbing level not shifted, the $v=3$ state should still be affected more than its adjacent levels. It may also be significant that the amount of the perturbation is less in the case of the H^2H^1 molecule than it is for H^1H^1.

In conclusion the writer wishes to thank Professor Lewis and Dr. MacDonald of the chemistry department for a supply of isotopic hydrogen which has made this investigation possible.

Doppler Displacements in the Spectrum of Hydrogen Canal Rays

ANNA I. MCPHERSON, *University of Chicago*

(Received November 13, 1933)

Hydrogen canal rays of uniform energy have been obtained by accelerating the hydrogen ions formed in a low voltage arc through a short electric field. The spectrum has been observed at $H\beta$ and $H\gamma$, in the direction of motion, and the Doppler displacements of the lines H_{31}, H_{21}, H_1, from atoms accelerated as H_3^+, H_2^+, H_1^+, agree acceptably with the values of the displacements calculated from the applied potentials between 7000 and 17,000 volts. H_{31} diminishes in intensity and H_{21} and H_1 increase with decrease of pressure. H_{31} and H_{21} are equal in intensity at 0.019 mm which is of the order of pressure expected if the numbers of H_3^+, H_2^+ are determined in the arc space. An apparent minimum velocity for excitation of radiation in the neutral hydrogen atom moving in hydrogen was observed at about 40 volts. In a helium-hydrogen mixture the hydrogen Doppler lines H_{21} and H_1 alone were perceptible, H_{31} not appearing.

IN general, the spectrum of hydrogen canal rays viewed in the direction of motion, shows each of the Balmer lines accompanied by three rather diffuse displaced Doppler lines, whose relative positions indicate their sources to be atoms which have passed the accelerating field as H^+, H_2^+, H_3^+ ions. The displacements are less than one would expect from the applied field, and this defect increases with the field.[1, 2, 3, 4]

With hydrogen canal rays of uniform energy, produced in the one case by magnetic deflection, in the other by acceleration of ions through a narrow condenser, Riezler,[5] and Batho and Dempster[6] have observed Doppler lines which were sharp, and whose displacements agreed well with the expected values. Batho and Dempster also found a variation in the relative intensities of the lines with the gas pressure.

In the present experiments, by using the method of Batho and Dempster, the variation of intensity of the lines with pressure has been studied, and displaced lines observed under various conditions.

APPARATUS

The apparatus was similar to that previously described.[7] Perforated aluminum electrodes were mounted with their adjoining parallel surfaces 1.5 mm apart. The hydrogen was purified by admission through a palladium thimble, and its pressure was measured with a McLeod gauge. The gas could be made to flow through the system continuously, or as was usually sufficient, could be renewed for each photograph. The Steinheil spectrograph with dispersion 58.3A per mm at $H\beta$, 32.4 Angstroms per mm at $H\gamma$ was used, with Eastman 40 plates.

The brightness of the beam increased with increasing voltage, and with increasing pressure. The upper limit of pressure, about 0.15 mm of mercury was reached when the displaced lines became very diffuse, the lower limit, about 0.003 mm necessitated very long exposures. The upper limit of voltage was set by the nature of the discharge tube, as occasional sparking took place between the electrodes at 17,000 volts; at 7000 volts the least displaced lines at $H\beta$ were not easily resolved. The voltage across the low voltage arc was kept at about 90 volts.

EXPERIMENTAL RESULTS

The plates showed $H\beta$, $H\gamma$, very brightly, with their shifted companion lines H_1, H_{21}, H_{31}

[1] J. Stark, Phys. Zeits. **6**, 892 (1905).
[2] F. Paschen, Ann. d. Physik **23**, 247 (1907).
[3] J. Stark and W. Steubing, Ann. d. Physik **28**, 974 (1909).
[4] H. Krefft, Ann. d. Physik **75**, 75 (1924).
[5] W. Riezler, Ann. d. Physik **2**, 429 (1929).
[6] H. F. Batho and A. J. Dempster, Astrophys. J. **75**, 34 (1932).
[7] A. I. McPherson, Phys. Rev. **44**, 711 (1933).

radiated from atoms formed from H_1^+, H_2^+, H_3^+ ions respectively, and the secondary spectrum of hydrogen fairly intense besides.

To compare the separations of the displaced lines with those calculated from the measured voltage, a series of pictures was taken, with pressures from 0.003 to 0.145 mm, voltages 7500 to 17,000 volts, and all plates were used on which at least three separations could be measured. The values $d\lambda/\lambda$, $d\lambda/\lambda\sqrt{2}$, $d\lambda/\lambda\sqrt{3}$ were computed from each voltage, and compared with $d\lambda/\lambda$ from the measured separations of H_1, H_{21}, H_{31}. The agreement is very good, thus for Plate No. 30 the values from the voltage are 0.00448, 0.00317, 0.00259, while measurements at Hβ give 0.00448, 0.0030, 0.00275, and at Hγ, —, 0.00303, 0.00259. Fig. 1 shows these results graphically, the observed $d\lambda/\lambda$ plotted against the calculated v/c. Points marked dot, plus, circle, are from measurements of H_{31}, H_{21}, H_1. The average percentage excess of the calculated over the measured value for the 124 measured separations is 3.5, which is well within the experimental error. All three ions show similar agreement over the entire range of speeds used.

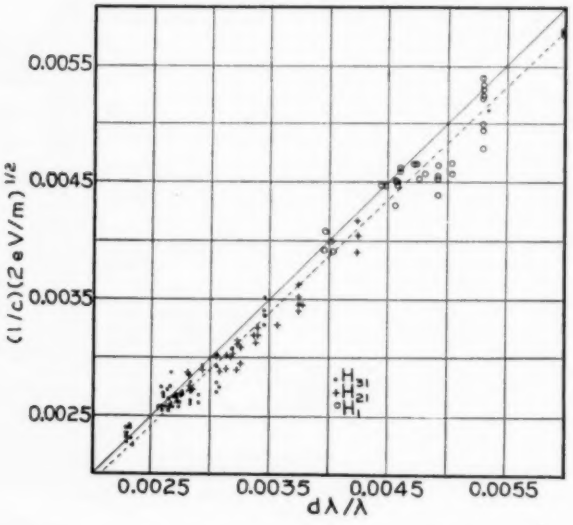

FIG. 1. Vertical. Displacements expected from voltage measurement $(1/c)(2eV/m)^{\frac{1}{2}}$. Horizontal. Observed displacements $d\lambda/\lambda$. The heavy line represents the theoretical equality, the broken line the average of the measured values, 3.5 percent low.

Krefft[4] observed displacements only 85 percent of those expected up to 3000 volts, still less for higher voltages, while Batho and Dempster for 20 displacements at 5300, 12,000 and 15,000 volts found agreement to better than 90 percent.

With the present experimental arrangement, the displacement of the Doppler lines in hydrogen is calculable from the applied potential, over the range of velocities from 7500 to 17,000 volts.

Dependence of intensity of displaced lines on pressure

Three sets of plates were taken at 11,800, 13,450 and 16,900 volts, at pressures 0.003, 0.007, 0.026, 0.04, 0.06, 0.105, 0.14 mm. At 0.14 mm the displaced lines were very diffuse, the line from the diatomic ion was missing, the lines H_{31} and H_1 were visible. As the pressure was reduced to 0.05 mm the shifted lines were less diffuse and consequently more intense, and the line H_{21} could be seen as a faint shadow. With further decrease of pressure the lines became definitely sharp, and as observed by Batho and Dempster, the intensity of H_{21} increased steadily, while that of the other lines decreased. The monatomic line H_1 is always faint, the lines H_{31}, H_{21}, at a pressure between 0.013 and 0.026 mm have equal intensities less than that of the rest line, but comparable to it. The number of radiating atoms in the beam which passed the field as H_3^+ is equal to the number which passed as H_2^+ at this approximate pressure of 0.019 mm, which is of the order of magnitude of that calculable from the results of very different positive ray experiments of Smyth[8] and Hogness and Lunn,[9] and Harnwell,[10] assuming that the distribution of the ions is principally determined by the pressure in the arc space.

From the known paths for neutralization of hydrogen ions[11] it may be shown that little change of charge takes place within the accelerating field at the lower pressures used; the displaced lines are sharp and as all the ions undergo the full acceleration the Doppler lines have the full displacement calculable from the field. At the higher pressures used, a considerable

[8] H. D. Smyth, Phys. Rev. **25**, 452 (1925).

[9] T. R. Hogness and E. G. Lunn, Phys. Rev. **26**, 44 (1925).

[10] G. P. Harnwell, Phys. Rev. **29**, 830 (1927).

[11] H. Bartels, Ann. d. Physik **6**, 957 (1930).

part of the ions change charge in the field, giving rise to the observed diffuse lines.

Minimum velocity for light excitation by neutral hydrogen atoms

At the higher pressures the H_{31} lines were decidedly less sharp on the side nearer the rest line, shading off to a faint fog which extended uniformly towards the rest line but broke off before reaching it. This fog decreased in both intensity and extent with decreasing pressure, becoming imperceptible at 0.01 mm. At the highest pressure used a similar fainter fog extended from H_1 to H_{31}. These effects may be due to radiation from atoms which traversed only a small part of the electric field as ions. An estimate of the width of the clear strip shows it to correspond to 40 volts, which may be compared with the minimum velocity of 50 volts for radiation by neutral hydrogen atoms, reported by Dempster.[12]

Doppler effect in helium-hydrogen mixtures

In observations of the Doppler effect in helium, as previously described,[7] at a total pressure of 0.02 mm, sufficient traces of hydrogen were present to show $H\beta$ and $H\gamma$ in considerable intensity, in each case accompanied by a relatively strong displaced line whose position identified it as H_{21}, and in two instances by a very faint line, H_1. H_{31} did not appear. These observations accord with those of Harnwell,[10] that the ratio H_3^+ to H_2^+ formed in hydrogen at partial pressure below 0.02 mm in presence of helium is negligible; indeed H_3 is necessarily a secondary product unlikely to be formed under these conditions.

No indication was seen of the helium hydride ions HeH^+ and HeH_2^+ reported by Hogness and Lunn.[9] If they were formed they did not decompose to produce hydrogen atoms in a perceptible number.

No radiation was observed from the unstable fourth hydrogen ion H_4^+, suggested by Döpel[13] and apparently confirmed by Ney-Valerius[14] at velocities of the order of 1000 volts, nor were there any variations in the relative positions of H_{21} and H_1 with change of pressure, as observed under certain conditions in the latter experiments. In the present experiments, the shifted lines lost their sharpness with the higher pressures, but as the measured separations for pressures to 0.1 mm show, the positions of the maxima were not observably affected. Also, change of velocity caused no perceptible change in the relative intensities of the lines.

Discussion

The secondary hydrogen spectrum was developed in considerable intensity. Comparison of the plates indicated no change in its intensity relative to the Balmer lines, with pressure or voltage, and none of its lines in the region between $H\beta$ and $H\gamma$ showed any Doppler displacement. Evidently the secondary spectrum is excited by the positive rays, in the gas at rest, no appreciable part of its intensity coming from molecules which have formed from the neutralization or decomposition of the molecular ions.

For particles in the positive ray beam the free path traversed before neutralization increases with the speed,[11] and the number of paths terminated in the observation space decreases. If the radiation were emitted mainly as a result of neutralizing collisions, the intensity should decrease with increasing speeds, but the observed intensity increases considerably with the speed, in similar degree for the rest lines and the displaced lines. It is probable that many collisions occur between the moving particles and the stationary, which result in excitation and radiation of either or both particles, without ionization. The increase of intensity with speed may then imply merely a greater probability of excitation of the colliding particles at high speeds.

These experiments were suggested and directed by Professor A. J. Dempster, to whom the writer expresses sincere thanks. The friendly advice and aid of fellow students is also gratefully acknowledged.

[12] A. J. Dempster, Phys. Rev. **8**, 651 (1916).
[13] R. Döpel, Ann. d. Physik **76**, 1 (1925).
[14] F. Ney-Valerius, Ann. d. Physik [5] **6**, 721 (1930).

Insulating Films Formed Under Electron and Ion Bombardment

R. LARIVIERE STEWART, *Ryerson Physical Laboratory, University of Chicago*

(Received December 18, 1933)

In an evacuated tube in which the slightest traces of organic vapors may occur, even with liquid air cooling, insulating layers are formed on surfaces subject to electron or canal-ray bombardment. These layers may be attributed to carbon compounds, and their formation is related to the polymerization of organic vapors by electrical discharges, α-particles, and ultraviolet light. The simple ion-deposition theory is inadequate as the layers are formed only at the point of impact of the rays on the surface. Electrical resistances and break-down potentials were observed for several films. The importance of these deposits in general experimental practice, such as the photometry of mass-spectra, is pointed out, and, amongst others, cases are cited of their influence producing contact potentials, pseudo high vacua, erroneous photographic recording and differential condensation of vapors upon previously bombarded surfaces.

AS is well known, metallic electrodes subjected to electron bombardment eventually become discolored if vacuum conditions are not sufficiently good. The purpose of this paper is, first, to point out the nature of the films which cause the surface to change and to discuss the importance of considering them in general experimental practice, and, second, to describe certain new features in the processes which occur in organic vapors subjected to a bombardment leading to polymerization.

In the present experiments, an electron gun, furnished with an oxide coated filament, was fixed in a vacuum tube to give a circular beam of electrons of $1\text{–}18\times10^{-6}$ amp., at a potential kept at 190–210 volts. The tube was connected through a stopcock to a mercury diffusion pump which, with accompanying liquid air trap, produced a vacuum of about 10^{-5} mm Hg. The beam formed upon the target a circular film with insulating properties, characterized by a circular distribution of interference colors.

Since a black deposit was obtained upon magnesium and deposits were formed upon glass targets, the films are not produced by oxidation. Moreover they are not soluble in any of the common solvents, but when deposited on glass, sometimes loosen in the liquids used and break up into very fine slivers.

The following facts are evidence that the deposit is a carbon compound. (1) When a platinum strip on which a colored film had been formed was heated in a vacuum the deposit turned black (enlarging slightly in area) instead of disappearing as it would in air. (2) Heating the platinum bright red *in vacuo* did not rid it of this black deposit. (3) This black film when tested with a telephone receiver was found to have become conducting. (4) It disappeared in air at the same temperature as an artificial film formed by charring a trace of stopcock grease put on platinum. (5) The films disappeared readily in air at 450°C to 470°C and more slowly at lower temperatures. Some turned black before diminishing noticeably, others merely grew thinner until they vanished.

At higher pressures, without liquid air, and with organic vapors present in quantity, solid films are not surprising, since solid polymers or compounds are commonly observed as products of organic vapors after bombardment by α-particles,[1] in various forms of electrical discharges,[2, 3, 4, 5] and even after exposure to

[1] S. C. Lind, *The Chemical Effects of Alpha Particles and Electrons*. Chemical Catalog Co., New York, 1928.

[2] J. C. McLennan, M. W. Perrin and H. J. C. Ireton, Proc. Roy. Soc. **A125**, 246 (1929).

[3] J. B. Austin and I. A. Black, J. Am. Chem. Soc. **52**, 4552 (1930).

[4] A. K. Brewer and P. D. Kueck, J. Phys. Chem. **35**, 1293 (1931).

[5] E. G. Linder and A. P. Davis, J. Phys. Chem. **35**, 3649 (1931).

ultraviolet light.[6, 7, 8] Spectrographic studies have been made of the intermediate products,[9, 10] and experiments are still in process to determine more fully the kinetics of the reactions. Also workers in the x-ray field find it difficult to avoid the K lines of carbon from the "'film de carbone'[11, 12] which results from the destruction by the cathode rays of the carbonized residual gases."

To test the simple ion-deposition theory of polymerization, a glass target was coated with fluorescent material, and a magnetic field was used strong enough to deflect the electrons just at the end of their path towards the edge of the target. The film then formed at the new point of impact only. Since such a magnetic field could not deflect the heavier ions as much as the electrons, the formation of the solid films at the point of impact only indicates the necessary conjunction of three factors: (1) The wall or target surface; (2) the organic vapor or its derivative; (3) the energizing particle.

Another new feature was the discovery that similar films were formed at the point of impact of hydrogen canal rays and also at the point of impact of neutral particles which had been accelerated when traversing the discharge tube in a charged state.

A self-deflection of the electron beam was observed which was probably due to charges accumulating upon the insulating deposit (on target or in gun). These deposits also altered the target current. This was shown by an increase in the reading whenever the electron beam was momentarily deflected from the center towards the cleaner edges. The thickness of the deposit, however, is not proportional to the time of running, for, though the deposition continued throughout, the rate varied. Resistance measurements were secured by the following device: a small drop of mercury was placed on the film and pressed upon it with a loop of platinum wire. Minimum values of the order of 10^6 ohms were obtained for the film beneath the drop, whilst corresponding rupturing voltages varied from 4–14 volts.

These films are likely to be an undetected disturbing factor in many types of experiment. A colorless layer extends beyond the colored center. (Under some conditions the whole film appears to be colorless.)[13]

When they form on fluorescent screens they render the original bright spot diffuse and "permanently fatigue" the spot bombarded.

When they produce contact potential differences they may quite frustrate the attempts of experimenters who by special method[14] or design[15] intend to avoid these potential differences.

In secondary electron experiments, copper oxide has been recommended for large secondary emission when the "oxide" referred to[16] was very probably a carbon compound deposit due to an unrecognized source of organic vapor.

They explain the phenomenon of the pseudo high vacuum, which has been ascribed to a changed condition of the cathode[17] or of the anode[18] or to a changed condition of the walls of the tube allowing them to collect a screening electric charge[19, 20]—that is exactly what these films would lead one to expect under differing experimental conditions; and also the case in photoelectric emission of a surface which was made insensitive by electron bombardment and remained so until restored to its former condition by heat.[21]

It is, however, in the case of photographic recording that the deposits have produced their most extensive though not their most important effects: They have been studied as a pseudo

[6] S. C. Lind and R. Livingston, J. Am. Chem. Soc. **54**, 94 (1932).

[7] A. R. Olson and C. H. Meyers, J. Am. Chem. Soc. **48**, 389 (1926).

[8] D. Berthelot and H. Gaudechon, Comptes Rendus **150**, 1169 (1910).

[9] W. D. Harkins and D. M. Gans, J. Am. Chem. Soc. **52**, 5165 (1930).

[10] W. D. Harkins and J. M. Jackson, J. Chem. Phys. **1**, No. 1, 37 (1933).

[11] A. Dauvillier, J. de Phys. et le Rad. **8**, 1 (1927).

[12] D. L. Webster, W. W. Hansen and F. B. Duveneck, Rev. Sci. Inst. **3**, 736 (1932).

[13] S. C. Lind, reference 1, page 159.

[14] F. G. Dunnington, Phys. Rev. **43**, 404 (1933).

[15] E. O. Lawrence, Phys. Rev. **28**, 947 (1926).

[16] L. E. McAllister, Phys. Rev. **21**, 122 (1923).

[17] S. Ratner, Phil. Mag. [6] **43**, 193 (1922).

[18] A. Janitsky, Zeits. f. Physik **31**, 277 (1925).

[19] A. Guntherschulze, Zeits. f. Physik **31**, 606 (1925).

[20] E. Heermant and R. Thaller, Zeits. f. Physik **39**, 130 (1926).

[21] R. Suhrmann, Phys. Zeits. **30**, 939 (1929).

photographic effect,[22] where the observer, using a magnetic spectrograph, reported that lines appeared upon the plate even before development, that lines could be obtained upon metals also and upon glass, and that they could be removed from the glass by heating above 450°C.

Also a number of experimenters have done work upon the differential condensation of vapors on parts of metal surfaces exposed to light,[23] to various discharges,[24, 25] and to cathode-ray bombardment,[26] where doubtless this effect was involved; and an attempt[27] was made to use the differential condensation due to the unrecognized occurrence of the organic deposits for the registration of cathode rays in daylight without developing process.

From the examples selected it can be seen how readily this effect may vitiate results wherever intensity measurements of refined accuracy are desired, as in the photometry of mass-spectra.[28] The deposit forms a layer between the plate and the impinging beam that is not necessarily proportional to the time of exposure and that has optical properties of its own, which need not be additive, superimposed upon those of the image. The effect is equally vicious in electrical and magnetic deflection measurements of such delicacy that insulating layers of this character cause uncompensated deflections. And wherever it is important that thin films subjected to bombardment should retain their original thickness this effect has to be contended with. Also in spectrographic work the films often cause a darkening of the window which limits the effective length of exposure.

In summation, these deposits may be considered a very insidious and prevalent source of error.

[22] J. E. Henderson, Phys. Rev. **29**, 360 (1927).

[23] W. W. Coblentz and E. W. Hughes, Science **60**, 64 (1924).

[24] M. E. Mascart, *Traité d'électricité statique*, Vol. 2, p. 177 (figures roriques), G. Masson éditeur, Boulevard St. Germain, Paris, 1876.

[25] H. M. Ollivier, J. de Phys. et le Rad. [6] **5**, 135 S (1924); **6**, 83 S (1925); **7**, 89 S (1926).

[26] P. H. Carr, Rev. Sci. Inst. **1**, 711 (1930).

[27] W. W. Nicholas and C. G. Malmberg, Bur. Standards J. Research **8**, 61 (1932).

[28] F. W. Aston, Proc. Roy. Soc. **A115**, 495 (1927).

Acknowledgments

The report of this work cannot be concluded without an expression of thanks to those who have furthered its accomplishment: First and particularly, to Dr. A. J. Dempster, who proposed the problem and made possible its solution by his generous interest and guidance; also to Dr. J. B. Hoag, Dr. Elmer Dershem and Dr. A. E. Shaw for helpful suggestions; and to Dr. F. L. Verwiebe for facilitating the extension of the research to include the effects of hydrogen canal rays and of accelerated neutral particles.

LETTERS TO THE EDITOR

Prompt publication of brief reports of important discoveries in physics may be secured by addressing them to this department. Closing dates for this department are, for the first issue of the month, the twentieth of the preceding month; for the second issue, the fifth of the month. The Board of Editors does not hold itself responsible for the opinions expressed by the correspondents.

A Slight Correction to the Rydberg Constant for H^1

The most accurate determination of R_{H^1}, the Rydberg constant for light hydrogen, was made by Houston[1] in 1927. He measured with a Fabry-Pérot interferometer the wave number of the $2p\,^2P_{3/2}-3d\,^2D_{5/2}$ component of $H^1\alpha$ and the $2p\,^2D_{3/2}-4d\,^2D_{5/2}$ component of $H^1\beta$, and by the use of Sommerfeld's equation for the fine structure of the hydrogen spectrum obtained the value of R_{H^1} directly.

For each line only the wave number of the position of the *maximum* of the low frequency member of the "doublet" could be measured directly, and to this, in order to obtain the wave number of the above designated major component of that member, was added a correction of $+0.0056$ cm^{-1} for $H^1\alpha$ and $+0.0024$ cm^{-1} for $H^1\beta$, based on the assumption that the center of gravity of the member as determined from theoretical data coincided with its position of maximum intensity. (Incidentally, according to theoretical data, these corrections, if valid, should have been 0.0063 cm^{-1} for $H^1\alpha$ and 0.0029 cm^{-1} for $H^1\beta$.) As shown on page 475 of this issue, this assumption is not valid for these Balmer lines of hydrogen. According to Eq. (3) of the article just mentioned, a computation of the correction to be made to the observed wave number of the maximum, using our value of 0.180 cm^{-1} for the half-line-width, and the theoretical intensities and positions of the components, gives $+0.0034$ cm^{-1} for $H^1\alpha$ and $+0.0024$ cm^{-1} for $H^1\beta$. Thus the $H^1\beta$ correction, computed from this equation, happens to agree with the correction applied by Houston, but the $H^1\alpha$ correction differs from his by 0.0022 cm^{-1}. According to the published report[1] of the discharge conditions in the hydrogen gas, there is good reason to believe the half-line-width was very closely that obtained by us. Computation shows, however, that for the theoretical positions and intensities of the components the maximum correction that could be applied for $H^1\alpha$ for any half-line-width is only about 0.0035 cm^{-1}. For successively larger half-line-widths components in the high frequency member are effective in reducing this correction and eventually in reversing it.

For $H^1\alpha$ the value of R_{H^1} is approximately 36/5 times the value of the wave number of the measured component, so that the error of 0.0022 cm^{-1} in the wave number produces an error of about 0.0158 cm^{-1} in R_{H^1}. For $H^1\beta$, as previously noted, no final error was made in the wave number. Upon subtracting this correction from the published[1] value of R_{H^1} found from $H^1\alpha$, the value obtained is 109,677.738 cm^{-1}. The average of this and R_{H^1} for $H^1\beta$, using Houston's weightings, is 109,677.747 cm^{-1} instead of the published[1] value of $109{,}677.759\pm0.008$ cm^{-1}, which value was later adopted by Birge.[2] In calling attention to this very small correction the authors wish chiefly to stress the importance of distinguishing between the location of the center of gravity of an intensity complex and the position of its maximum intensity, even when the complex appears quite symmetrical. Further adjustments in this correction may be necessary when the relative positions and the intensities of the components have been more precisely determined. Any marked departure from the theoretical positions of the components in this low frequency member of the "doublet" with respect to each other is, however, hardly to be anticipated. Shifts are more likely to occur for components involving the $2s\,^2S_{1/2}$ level.

R. C. Williams
R. C. Gibbs

Physics Department,
Cornell University,
February 8, 1934.

[1] Houston, Phys. Rev. **30**, 605 (1927).
[2] Birge, Rev. Mod. Phys. **1**, 1 (1929).

Incipient Arcs in Ionization Chambers

Millikan, Anderson and Neher[1] suggest that the "Hoffmann bursts" found in cosmic-ray studies are "merely instrumental accidents." This suggestion is based on the existence of a proposed "incipient arc" formed by the multiplication of ions by collision in high fields. These high fields are in turn supposed to result from space charges of ions set free by cosmic-ray showers. Since it is difficult to see how this form of arc could be initiated in a chamber filled with gas at 30 atmospheres pressure where a

[1] Millikan, Anderson and Neher, Phys. Rev. **45**, 141 (1934).

total potential of only a few hundred volts is involved it seems worth while to look at this suggestion quantitatively.

The proposed suggestion seems to describe accurately the action of the Geiger counter. In the ordinary type of this instrument a wire of about 0.025 cm diameter is stretched down a cylinder about 2.5 cm in diameter. Counting action is obtained with voltages of the order of 1000 when the pressure (for argon) is reduced to about 5 cm of mercury. The gradient at the wire under these conditions calculated from the geometry, amounts to about 17,000 volts per cm. Judging from the behavior of point counters,[2] a counter of this type would operate under atmospheric pressure at not less than 3000 volts, and at 5 atmospheres at not less than 9000 volts. At 30 atmospheres, judging from the studies of Hayashi[3] we should expect this counter to operate at certainly not less than 30,000 volts. The corresponding gradient at the surface of the wire would be about 5×10^5 volts per cm. Hence in order to get this sort of action in an ionization chamber working at pressures of 30 atmospheres we should expect to find fields of the order of five hundred thousand volts per cm. In the first and second types of instrument designed by Compton and Bennett[4, 5] fields of this magnitude would necessitate collecting voltages of at least 100,000 volts, while the most recent type[6] would require several hundred thousand volts.

The problem may be approached from another angle. The field strength necessary to produce ionization by collision (arcs or breakdown) in air at atmospheric pressure amounts to about 30,000 volts per cm. The values in argon and other gases are not far different. From the work of Hayashi mentioned above the value of this quantity at 30 atmospheres is nearly 700,000 volts per cm, in reasonable agreement with the values estimated from studies of Geiger counter action.

It is evident that the collecting voltages used in chambers of the Compton-Bennett type can make no significant contribution to the fields necessary to cause ionization by collision at high pressures. Yet the magnitudes and frequency of bursts observed in these instruments are comparable to those observed by Millikan. It is interesting to examine quantitatively possible effects of space charge.

In general the ions produced by a shower of fast particles will be distributed throughout a considerable portion of the volume of the chamber, with positives and negatives intermingled. The collecting field will separate the two kinds, those of one kind diverging toward the wall, while those of the other kind will converge toward the collecting electrode. In order to have any appreciable space charge fields it will be necessary to assume either that the ions are produced by the cosmic rays in a very limited volume, or that they are drawn together by the collecting field into a very limited volume.

Let us assume then the extreme case where all the ions of one sign observed in Millikan's largest burst are produced in one cubic millimeter of volume near the collecting electrode, the effect of the accompanying ions of opposite sign being neglected. The total charge of 7.5×10^7 ions is about 0.035 e.s.u. If all the lines of force of all the charges were directed from this cubic millimeter of space toward a nearby electrode by an induced charge of opposite sign on the electrode, then the corresponding field strength would amount to $4\pi(0.035)\div(0.1)^2=46$ e.s.u./cm $=13{,}800$ volts per cm. This falls short by a factor of more than thirty-fold of producing enough field strength to cause ionization by collision.

In instruments of the Millikan-Neher type where fine fibers which may have sharply pointed ends are exposed to the electric field very high gradients may be built up, even with low values of charging voltage. These gradients are so high that any reasonable concentration of space charge will make little contribution to their magnitude. A simple test of the relation between charging potential and ability to retain charge, carried on for convenience at low pressure, should indicate what values of voltage are safe from corona difficulties. The test could be made to simulate more nearly actual conditions by the use of x-rays or α-rays which are capable of building up enormously higher space charge densities than any rays yet found in cosmic-ray work.

The following conclusions seem justified: (1) No reasonable assumption of space charge density leads to field strengths comparable to those required for ionization by collision in the Compton-Bennett and other types of cosmic-ray ionization chambers. (2) There is a remote possibility that in ionization measuring devices of the Millikan-Neher type sharp points may produce gradients dangerously near the breakdown point. Such instruments can and should be tested in this respect before being used for statistical studies. (3) In general the discarding of very large cosmic-ray showers does not appear to be justified on the basis of "instrumental accidents" of the type described by Millikan, Anderson and Neher.

RALPH D. BENNETT

Massachusetts Institute of Technology,
March 2, 1934.

[2] R. D. Bennett, J.O.S.A. and R.S.I. **16**, 339 (1928).
[3] F. Hayashi, Ann. d. Physik **45**, 431 (1914).
[4] Bennett, Stearns and Compton, Phys. Rev. **41**, 119 (1932).
[5] A. H. Compton, Phys. Rev. **43**, 387 (1933).
[6] Compton and Bennett, Paper before meeting of Int. Ass'n of Terrestrial Magnetism and Electricity, Lisbon, Sept. 1933.

Proton Source for Atomic Disintegration Experiments

As part of the program of nuclear studies instituted here by R. Ladenburg we have been experimenting for some time in an effort to develop a satisfactory proton source to use in conjunction with our 400,000 volt transformer rectifier installation. The present source has proved so much more promising than any of the others tried that it seems worth while to describe it now, although due to an accident which will probably cause a delay of some

weeks, its behavior has not yet been studied at all thoroughly. We have been able to obtain a focussed beam of ions of 20 to 50 microamperes. These currents were measured with a Faraday cage, a magnetic field trapping secondary electrons. Checking by the disintegration yield from LiF bombarded at 250 kv showed that they must be largely protons. Under these circumstances the total current drawn from the arc was a little over one milliampere and the arc current itself was of the order of 0.2 amperes.

The source is a low voltage arc of the general form described by Lamar and Luhr,[1] with certain alterations suggested by Mr. Eugene W. Pike of this laboratory. Power supply for it and the associated solenoid is obtained from an aircraft radio generator driven by an insulating textolite shaft. The arc consists of an oil-cooled copper cylinder $2\frac{1}{2}''$ long and $1\frac{1}{2}''$ in diameter which is the anode, with a cylindrical oxide-coated cathode along its axis. The ends are closed by copper disks insulated from the cylinder by lavite rings. The end-plates are held slightly negative with respect to the cathode, the protons escaping through a 1/8" hole in the center of one plate while hydrogen is admitted through a tube fastened to the opposite end.

The whole is placed inside a solenoid which produces a field of about 400 gauss along the axis, sufficient to keep electrons from reaching the anode without making one or more collisions. The solenoid, wound with No. 10 enameled wire, is placed directly in the main vacuum tube and seems to give no trouble when 6 to 8 amperes flow through it. In some preliminary work at pressures of hydrogen as low as 5×10^{-3} an arc current of one ampere was obtained, the drop between anode and cathode being about 35 volts. At somewhat lower pressures the arc current drops sharply and the voltage rises, although the ion current does not seem to change as rapidly.

It seems possible that with better focussing conditions, which would bring a larger percentage of the ions leaving the arc to the target, currents of a considerable fraction of a milliampere may be obtained fairly easily.

S. N. Van Voorhis
J. B. H. Kuper
G. P. Harnwell

Palmer Physical Laboratory,
Princeton University,
March 14, 1934.

[1] Lamar and Luhr, Phys. Rev. **45**, 287 (1934). We are indebted to Dr. Lamar for communicating to us the details of this source before publication.

Disintegration of Boron by Deutons and by Protons

Using a method we have already described in some detail,[1] we have attempted to analyze the radiation obtained from boron bombarded with a mixed beam of deutons and protons. The absorption of the radiation in lead and in paraffin out to a thickness of 8.3 cm was measured by using both a lead and a paraffin lined ionization chamber. The four curves obtained are shown in Fig. 1. The large absorption obtained with small thicknesses of lead, when using a lead lined chamber (see curve IV), shows clearly that, in addition to neutrons, there is a large component of γ-radiation. The dotted line in this, as in our previous work, represents the intensity due to neutrons alone, as obtained by extrapolation, and the difference between this and curve IV is ascribed to γ-rays. The γ-ray intensities thus obtained are plotted on a log scale in Fig. 2, together with a curve obtained with a radium γ-ray source under the same conditions for comparison. The curve for the boron γ-rays is a straight line having the same slope as the curve for radium after 1.5 to 2.0 cm of lead filtration. It must therefore be concluded that the quantum energy of the γ-rays from boron here observed is close to 1.6×10^{6} e.v. By comparing the intensity of the boron γ-radiation with that of the radium, we were able to determine the number of quanta produced per second. This checks with the number of neutrons, to within the accuracy with which we are able to estimate the number of neutrons from the ionization they produced in the paraffin lined chamber. It is probable, then, that the γ-rays are associated with the same transformation

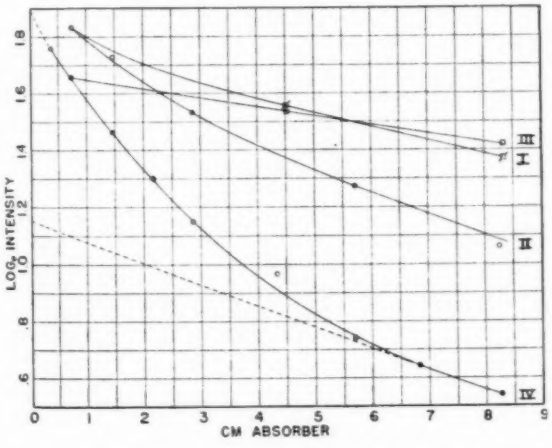

Fig. 1. Absorption of the boron-H^2 radiation. I, paraffin chamber, paraffin absorber: II, paraffin chamber, lead absorber; III, lead chamber, paraffin absorber; IV, lead chamber, lead absorber.

[1] Crane and Lauritsen, Phys. Rev. **45**, 226 (1933).

γ-rays and neutrons in approximately equal numbers were obtained from beryllium bombarded with deutons. Due to an error in plotting the absorption curve for the γ-rays, the absorption coefficient appeared to be only one-half its real value. After correcting this, and making a small correction for scattering, the linear absorption coefficient comes out to be 1.2, corresponding to a quantum energy of about 0.7×10^{6} e.v. This energy probably corresponds to an excitation level in the B^{10} nucleus.

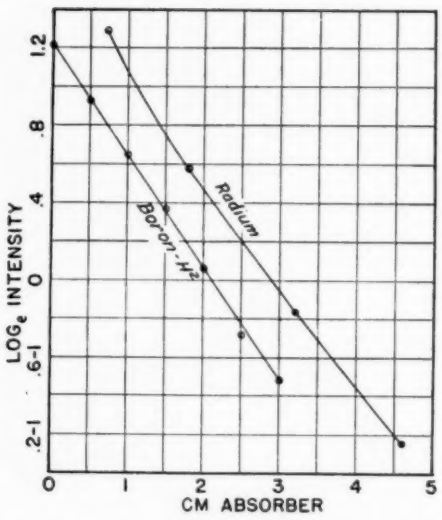

FIG. 2. Absorption of the boron γ-radiation in lead with the absorption of radium γ-radiation made under the same experimental conditions for comparison.

which produces the neutrons, which we assume to be

$$B^{11}+H^2\rightarrow C^{12}+n^1+\gamma, \qquad (1)$$

and that 1.6×10^6 e.v. corresponds to an excitation level in C^{12}.

The relative efficiency of production of the radiation from boron as a function of the energy of the deutons was investigated, and is shown in Fig. 3. An ion current of 10 microamperes was used—approximately 3 microamperes

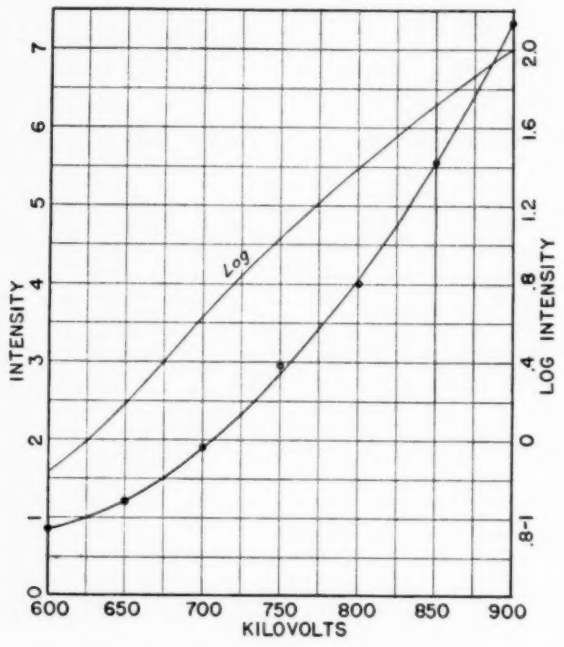

FIG. 3. Intensity for boron radiation as a function of the voltage used to accelerate the deutons.

due to deutons—and at 900,000 volts we estimate that about 2×10^6 neutrons (and an equal number of γ-ray quanta) per second were being produced.

Since the ion beam used consisted of at least as many protons as deutons, it seemed desirable to determine whether or not protons were responsible for any of the effect observed. In particular, γ-rays might be expected to accompany the α-particles produced in the disintegration of boron by protons on the basis of the work reported by Oliphant and Rutherford.[2] They assumed the reaction

$$B^{11}+H^1\rightarrow 3He^4 \quad (+11\times10^6 \text{ e.v.}), \qquad (2)$$

and treated the problem on the assumption that the α-particles of maximum energy represent those cases in which one of the α-particles gets 2/3 of the total energy, or in other words the cases in which two of the particles go off in one direction with equal energies, and the third in the opposite direction. On this hypothesis the maximum range they observed gave only 9×10^6 e.v. total energy for the three α-particles, or 2×10^6 e.v. less than expected from the energy balance in the above equation. This then might indicate a γ-ray quantum corresponding to that energy.

To test this possibility, boron (B_2O_3) was bombarded with 10 microamperes proton current at 900,000 volts, but no γ-rays were found, and the effect, if present at all can be said to be less than 1/50 that to be expected if there were one γ-ray quantum per disintegration.

It is natural, in view of this result, to consider the possibility of there being some restriction on the angles at which the three α-particles may be ejected with respect to one another, and that the case in which one of the particles gets 2/3 of the total energy may be excluded. This seems understandable if we reason as follows: As long as the three α-particles are so close together that they do not repel each other with the known Coulomb forces, we can say nothing of the way in which the energy is distributed among them. However, after they become separated far enough to repel each other according to the Coulomb law, they will still have considerable potential energy with respect to one another. It is known from experiments on the scattering of α-particles in helium that the inverse square law of force holds down to distances corresponding to potentials of the order of a million e.v. This means that, after complete separation, the relative velocity between any pair of the three particles resulting from the disintegration of the boron nucleus must correspond to the conversion of at least a million e.v. of potential into kinetic energy and that the case of two of the particles coming off in the same direction is ruled out. Taking Oliphant and Rutherford's value (5.96×10^6 e.v.) as the maximum observed energy of the α-particles, and 11×10^6 e.v. as the total energy available, the minimum kinetic energy any two α-particles can have with respect to each other is 2×10^6 e.v., an altogether reasonable figure, on the basis of the above argument. All this is on the assumption that the nucleus does break up into three separate

[2] Oliphant and Rutherford, Proc. Roy. Soc. **A141**, 259 (1933).

α-particles, and that two of them do not remain permanently associated together as in Be^8.

Since the discovery by Curie and Joliot of the delayed decomposition of some of the products of artificial transformations, we have observed such an effect from a target of B_2O_3 after deuton bombardment. A target of SiO_2 was also bombarded and no effect of comparable intensity was observed, so it is quite certain that the effect obtained with B_2O_3 is due to the boron. This means that in addition to the process described above, another process must take place to form a radioactive substance, and we suppose that the reaction is

$$B^{10}+H^2 \rightarrow C^{11}+n^1, \qquad (3)$$

the C^{11} being the radioactive product. From a comparison of the intensities of the two effects, we estimate that reaction (1) takes place about 200 times as frequently as reaction (3). Since there is only one-fifth as much B^{10} in the target as B^{11}, we may say that the ratio of the probabilities of reaction (1) and (3) taking place is about 40 to 1.

It is a pleasure to acknowledge our indebtedness to the Seeley W. Mudd Fund for the support of this work.

C. C. LAURITSEN
H. R. CRANE

Kellogg Radiation Laboratory,
California Institute of Technology,
March 13, 1934.

Errata:—The Mass of the Neutron and the Stability of Heavy Hydrogen

(PHYS. REV. **45**, 224, 1934)

Professor Uhlenbeck has kindly drawn my attention to the fact that there is a mistake in the value given in my former letter for the upper limit of the mass of the neutron when calculated from the production of neutrons by bombarding Li with α-particles. If one assumes the kinetic energy (k.e.) of the neutrons to be zero, the k.e. of the recoil B nucleus comes out as 0.0022_4 (in mass units) and the neutron mass as 1.0067 (instead of 1.0093); if one puts the k.e. of the neutrons equal 0.0005, the k.e. of the recoil B nucleus comes out as 0.0012_6 and the neutron mass as 1.0072, i.e., equal to the proton mass.

RUDOLF LADENBURG

Palmer Physical Laboratory,
Princeton University,
March 10, 1934.

Excitation and Disintegration of Protons and the Neutret

The gamma-rays produced in experiments of Lea[1] by bombarding hydrogen with neutrons, can be explained by a mechanism which has advantages over those suggested by Lea[1] and Auger.[2] It may be supposed[3] that under special conditions a proton may be decomposed into a neutron and a positive electron. Moreover as Auger[2] has remarked there may be excited states of the proton where the positive electron may be thought of as occupying a higher energy level than in the normal state. The excitation process would be peculiar in that a change from Fermi to Bose statistics would be involved. This difficulty embarrasses all theories which do not consider the proton and the neutron to be elementary particles. Tentatively the interaction between neutron and positive electron must be regarded as non-electromagnetic. In such case not only would the transition from an excited to the normal state be forbidden by an almost rigorous selection principle because of conservation of momentum, but also transitions between excited states with emission of photons would also be unlikely because there is no coupling with the electromagnetic field. The present problem is apparently closely related to the difficulty of continuous β-ray spectra. It seems to the writer that even if the difficulty cannot be resolved by quantum mechanics in the present form it is legitimate to make use of the implications of the difficulty in the manner of this note.

A valence electron around such an excited proton could, without violating a selection principle, annihilate the excited positive electron and leave a neutron and a photon. Taking the mass of the neutron to be 1.0062[4] the energy of the photon would be equivalent to 1.5 million volts plus the excitation energy of the proton. Thus the radiation observed by Lea could be explained easily.

A natural step from the preceding argument is the idea of spontaneous disintegration of the excited proton. The normal proton has more energy than a neutron and a positive electron but presumably cannot break up because of the selection principle already mentioned. In the long lived excited state the transition to the normal state is forbidden and therefore the disintegration is not. This may be an interpretation of the long continued emission of positive electrons observed by Curie and Joliot[5] after α-ray bombardment of certain substances. Indeed the mechanism involving intermediate products such as N^{13} is unnecessarily indirect and involves the emission of a neutron from nuclei known to be capable of expelling a proton. A further application of the suggestions of this article is to the production of various γ-rays by transitions between excited proton levels. At this point a serious

[1] D. E. Lea, Nature **133**, 24 (1934).

[2] P. Auger, Comptes Rendus **198**, 365 (1934).

[3] R. M. Langer, Science **76**, 294 (1932); I. Curie and F. Joliot, Comptes Rendus **196**, 1885 (1933).

[4] R. M. Langer, Phys. Rev. **45**, 137 (1934). A smaller mass would permit still more energy.

[5] I. Curie and F. Joliot, Comptes Rendus **198**, 254 (1934).

question arises. Why are not all such γ-rays observed in all processes involving high energy protons? The answer is not clear.

A fairly sound test of the hypothesis is obvious. Photon production should endure in some cases as long as positive electron emission does.

The considerations of this article undergo a slight modification if one chooses to introduce the notion of a light neutron such as that proposed by Pauli several years ago. This particle for which the name "neutret" is proposed (rather than the Italian form neutrino often used) ought to have Fermi statistics and a mass of the order of that of the electron. As mentioned in recent literature these properties would explain away the difficulties in transitions from the proton to the neutron as well as those of continuous β-ray spectra. In fact, it would follow that all β-ray spectra, positive as well as negative, would be continuous.

The excitation of the proton would presumably involve the ejection or annihilation of the neutret. The second alternative might correspond to the production of a negative proton from the neutron. The excited proton would definitely then be a Bose particle and would endure until annihilation or disintegration of the positive electron occurred. The energy available for the photons of the Lea effect or the β^+ emission might be less than that already mentioned by the mass and the binding energy of the neutret. This, however, is not serious.

One of the attractive features of the neutret hypothesis is the possibility of building an energetically stable proton with its help. This would require a mass at least as great as the difference between the proton and the sum of a neutron and a positive electron.

Note added March 15. The best available method for estimating the mass of the neutret is probably from the recent experiments in this laboratory where proton bombardment yielded positive electrons with energies up to at least 1.5×10^6 volts. The mass-equation gives $p-n-\beta^++\Delta E$ for the mass of the neutret where p, n, β^+ stand for the masses of the proton, neutron and positive electron and ΔE is the difference between the threshold energy for the incident protons and the kinetic energy of the products. Numerical values show that the rest mass of the neutret is probably smaller than that of the electron. This is as F. Perrin (Comptes Rendus **197**, 1625 (1933)) has already pointed out in good agreement with the distribution of energy in beta-ray disintegrations.

R. M. LANGER

California Institute of Technology,
February 20, 1934.

The Vibrational Spectrum of Water Vapor

Recently R. Mecke[1] has published a rather complete analysis of seventeen of the vibration rotation bands of water vapor, together with an assignment of the vibrational quantum numbers. This work provides accurate values for the centers of most of the bands, though a few in the visible region of the spectrum seem for several reasons somewhat doubtful. With such complete information available, it seemed desirable to carry out a theoretical investigation of a nonlinear, symmetric triatomic molecule, similar to the treatment used by Adel and Dennison[2] on CO_2, and to apply the results to H_2O. This has been done by using first and second order perturbation theory, and it has been found that the vibrational energies of this type of molecule may be expected, to the degree of approximation involved, to obey a formula of the form

$$W=x_1V_1+x_2V_2+x_3V_3+x_{11}V_1^2+x_{22}V_2^2+x_{33}V_3^2 +x_{12}V_1V_2+x_{13}V_1V_3+x_{23}V_2V_3+x_0,$$

where the V's are the vibrational quantum numbers, and the x's are coefficients which may be determined from the experimentally observed positions of the bands. Nine of the known bands are necessary in determining the constants, and the remainder may be used to check the validity of the equation. The check here is satisfactory for all but two bands, and the discrepancy for these is probably due to uncertainty in the positions of the band centers.

The theoretical treatment gives these x's in terms of the true mechanical frequencies of vibration of the molecule for infinitesimal amplitudes, of the interatomic distances, and of the constants in the assumed potential function. These expressions may be solved at once for the mechanical frequencies, which are necessary for the evaluation of the zeroth order binding constants, giving the results:

$$\omega_1=x_1-x_{11}-\tfrac{1}{2}x_{12}-\tfrac{1}{2}x_{13},$$
$$\omega_2=x_2-x_{22}-\tfrac{1}{2}x_{12}-\tfrac{1}{2}x_{23},$$
$$\omega_3=x_3-x_{33}-\tfrac{1}{2}x_{13}-\tfrac{1}{2}x_{23}.$$

For water the numerical values of the coefficients x_{ij} are as follows:

$x_1=3796.0$ cm^{-1} $\quad x_{11}=-39.5$ cm^{-1} $\quad x_{12}=-106.1$ cm^{-1},
$x_2=3674.8$ cm^{-1} $\quad x_{22}=-70.2$ cm^{-1} $\quad x_{13}=-21.0$ cm^{-1},
$x_3=1615.0$ cm^{-1} $\quad x_{33}=-19.5$ cm^{-1} $\quad x_{23}=-18.9$ cm^{-1}.

Calculating from these the values of the ω's, these results are obtained:

$\omega_1=3899.0$ cm^{-1}, $\quad \omega_2=3807.5$ cm^{-1}, $\quad \omega_3=1654.5$ cm^{-1}.

It is interesting to note that one of these, ω_1, differs by as much as 150 wave numbers from the observed position of the fundamental.

It is hoped before long to publish this treatment in more detail and to give the values of the constants appearing in the potential function used.

LYMAN G. BONNER

California Institute of Technology,
March 13, 1934.

[1] R. Mecke *et al.*, Zeits. f. Physik **81**, 313, 445, 465 (1933).
[2] A. Adel and D. M. Dennison, Phys. Rev. **43**, 716 (1933).

On the Hypothesis of the Instability of the Deuton

Our attention has been called by Dr. C. C. Lauritsen to a possible alternative explanation of the experiments recently reported by us.[1] In these experiments pairs of targets containing respectively light and heavy hydrogen were bombarded by hydrogen molecule ions. Protons having ranges up to 20 cm were observed from both targets but in greater numbers from the targets containing heavy hydrogen and this difference was attributed to the disintegration of the deutons of the targets by the protons of the beam. The fact that both targets yielded these particles was attributed to a small contamination (about 1 part in 30,000) of H^{2+} in the H^{1+}_2 beam.

The point raised by Dr. Lauritsen is that the contamination of H^2 in the apparatus must be largely increased when the beam is playing on the target containing heavy hydrogen and this added contamination might produce just the effect observed by us, since all of the hydrogen in the chamber contributed to the beam.

It had been our intention to employ in this experiment not the H^{1+}_2 beam but the simple H^{1+} beam which could contain no such contamination; however, this experiment was delayed owing to the rather extensive readjustments of the apparatus that would be required. Now owing to the obvious ambiguity of the experiments which we reported, we recognize that for a final settlement of this question experiments with a pure H^{1+} beam are essential.

We now think it altogether possible however that the results of such an experiment will be negative. For recently alternative and reasonable explanations have been found for those phenomena which originally led us to the hypothesis of the instability of the deuton. There is evidence[2, 3] in the important case of carbon under deuton bombardment that two nuclear reactions occur:

$$C^{12}+H^2 \rightarrow C^{13}+H^1+\gamma,$$
$$C^{12}+H^2 \rightarrow N^{13}+n.$$

At least at low voltages, these reactions appear to account for the long range protons and neutrons observed. It appears not unlikely that similar reactions with other nuclei and the possibility of carbon and oxygen contamination[4] of targets will ultimately account completely for our observations.

G. N. Lewis
M. S. Livingston
M. C. Henderson
E. O. Lawrence

Radiation Laboratory,
Department of Physics,
Department of Chemistry,
University of California,
March 15, 1934.

[1] G. N. Lewis, M. S. Livingston, M. C. Henderson and E. O. Lawrence, Phys. Rev. **45**, 242–244 (1934).

[2] C. C. Lauritsen and H. R. Crane, Phys. Rev. **45**, 345–346 (1934). C. C. Lauritsen, H. R. Crane and W. W. Harper, Science **79**, 234 (1934).

[3] M. C. Henderson, M. S. Livingston and E. O. Lawrence, Phys. Rev. **45**, 428 (1934).

[4] We are indebted to Dr. J. D. Cockcroft for communicating to us evidence that the long range protons observed when tungsten is bombarded by deutons are in fact due to a contamination.

Further Experiments with Artificially Produced Radioactive Substances

C and B_2O_3 bombarded with protons

After having observed induced radioactivity in a number of substances bombarded with deutons,[1] it seemed desirable to bombard the same targets with protons. This led to the striking observation that two of the targets, namely carbon and boron oxide, showed an appreciable activity which decayed at the same rate as did the activity produced by deutons. The intensity of the activity produced by protons, as compared to that produced by deutons under similar conditions was, in the case of carbon, about 10 percent, and in the case of the boron oxide, about 20 percent. That the ion beam could contain 10 to 20 percent deutons due to contamination of the tube with H^2 (adsorbed on the walls, etc.) seems highly improbable, since on other occasions we have changed from deutons to protons and have observed no more of the deuton effect than could be accounted for by the normal amount of H^2 in ordinary hydrogen—about one part in 6000. The fact that the decay periods of the active substances produced by protons and by deutons are quite exactly the same suggests strongly that the same radioactive products are formed. In the case of deuton bombardment the radioactive substances are supposedly N^{13} and C^{11}, respectively, and hence for the case of proton bombardment we may suggest the following alternative reactions which would involve the same radioactive products:

$$\begin{aligned} &C^{12}+H^1 \rightarrow N^{13} \rightarrow C^{13}+\epsilon^+ \quad (+6\times10^6 \text{ e.v.}),\\ &B^{10}+H^1 \rightarrow C^{11} \rightarrow B^{11}+\epsilon^+ \quad (+9\times10^6 \text{ e.v.}), \end{aligned} \tag{1}$$

where the excess energy calculated from the change in mass in the overall reaction is given, and

$$\begin{aligned} &C^{13}+H^1 \rightarrow N^{13}+n^1 \rightarrow C^{13}+n^1+\epsilon^+,\\ &B^{11}+H^1 \rightarrow C^{11}+n^1 \rightarrow B^{11}+n^1+\epsilon^+, \end{aligned} \tag{2}$$

where in accordance with the presumable mass of the neutron the excess energy from the change in mass is nearly negligible and might be either positive or negative.

One hesitates to accept the first type of proposed reaction, mainly because the probability of a particle being

[1] Lauritsen, Crane and Harper, Science **79**, 234 (1934); Crane and Lauritsen, Phys. Rev. **45**, 430 (1934).

added to a nucleus without the ejection of some other particle to carry away the excess energy is extremely small. So far no example of it has been established.

The second type of reaction seems more attractive, since any excess energy could easily be carried away by the neutron. If we take the masses of the proton, neutron and positron as 1.0072, 1.0067 and 0.0005, respectively, then the only kinetic energy available for the neutron and the positron is the kinetic energy contributed by the incident proton (in this case 0.9×10^6 e.v.). Nevertheless, we may not be justified in expecting to find the energies of the positrons limited to 0.9×10^6 e.v., since the known phenomena of the continuous β-ray spectrum have already indicated that the strict law of the conservation of energy may not hold in the case of electron emission. It might be reasonable to expect, however, that the energies of the positrons plus those of the neutrons would satisfy the conservation of energy statistically, and therefore have 0.9×10^6 e.v. as a mean energy.

In a preliminary set of cloud-chamber photographs taken by Dr. Carl D. Anderson and Mr. Seth H. Neddermeyer of carbon after proton bombardment, tracks appear having energies distributed up to above 10^6 e.v. It is interesting to note that the positron energy spectrum is continuous, as in the case of the β-rays, and that some of the positrons come off with energy in excess of the 0.9×10^6 e.v. which would be available on the above assumptions as to reaction and mass. More detailed data regarding the energy spectrum will be published by Anderson and Neddermeyer. A more precise knowledge of the mass of the neutron will be necessary for the further study of the energy relations—both elementary and statistical—in these processes.

Radioactive gases from C and B_2O_3

In observing the activity of a B_2O_3 target in a cloud chamber after deuton bombardment, it was noticed after a short time that a large number of tracks appeared which originated in the gas. Although it has been assumed that the radioactive substance in this case is C^{11}, the above observation would indicate that the active material is a gas which rapidly diffuses out of the B_2O_3. As further evidence, we found that warming the active B_2O_3 to about 200°C in air completely drove off the radioactive constituent. It therefore seemed desirable to collect, and if possible, determine the nature of the active gas. To do this we warmed a small amount of the activated B_2O_3 in a flask containing air, and transferred the air into an ionization chamber, through a liquid air trap. As long as the chamber was protected by the liquid air, no activity was recorded. However, upon removing the liquid air and allowing the trap to rise to a temperature considerably above that of liquid air, a large amount of the active material then made its appearance in the chamber. The B_2O_3 which was left in the flask was afterwards tested and found to have no activity. From this we conclude that after the B_2O_3 is bombarded, nearly all the C^{11} exists in the target as CO or CO_2, and very little, if any, as carbon. It should be noted that in measuring the period of decay of this substance, any method in which the gas is not prevented from escaping will lead to an apparent period which is considerably shorter than the real period. In order to make certain that the effect observed from B_2O_3 was due to the boron, and not to the oxygen, a target of SiO_2 was bombarded with deutons and tested for activity. No measurable effect was found, so it can be assumed that the oxygen contributes little, if any, of the effect.

A graphite target after bombardment with deutons, which supposedly contained N^{13}, was also heated in an effort to drive off the active constituent, but after heating to a red heat, about half the activity remained in the target. This result does not necessarily cast doubt upon the belief that the active substance is N^{13}, because we know that nitrogen, as well as other gases, is very strongly adsorbed on carbon.

We wish to acknowledge our gratitude to the Seeley W. Mudd Fund for the support of this work.

H. R. CRANE
C. C. LAURITSEN

Kellogg Radiation Laboratory,
California Institute of Technology,
March 14, 1934.

Energy Spectra of Positrons Ejected by Artificially Stimulated Radioactive Substances

Curie and Joliot[1] have reported that under the bombardment by α-particles from Po, several of the light elements, *viz.*, B, Mg, Al undergo transmutations which result in the production of radioactive isotopes which have half-lives of the order of several minutes and disintegrate by the ejection of positrons. Lauritsen, Crane and Harper[2] have produced such radioactive substances artificially by the bombardment of various light elements with deutons and protons accelerated to 900,000 e-volts energy. They have very kindly supplied us with several samples of C, B, Be and Al freshly subjected to proton or deuton bombardment. By inserting these samples in a cloud chamber operating in a magnetic field of 800 gauss it was shown that in all cases so far tested the disintegration results in the ejection of positrons of varying energies up to about 1.5 million e-volts. No α-particles or protons are observed and no tracks which can with certainty be ascribed to disintegration negatrons. For convenience we refer in the following to the element bombarded rather than to the supposed radioactive product. A discussion of the various nuclear reactions is being given by Dr. C. C. Lauritsen and H. R. Crane.

The samples so far tested are given in Table I.

When the activated B_2O_3 target was inserted in the chamber a large number of tracks were observed which did not originate in the target itself. Stereoscopic photographs taken with the magnetic field adjusted to the high value of

[1] Curie and Joliot, Comptes Rendus **198**, 254 (1934).
[2] Lauritsen, Crane and Harper, Science **79**, 234 (1934).

TABLE I.

Target	Projectile	Type of disintegration	Energy distribution
Be	Deutons	Positron	See Fig. 1
B_2O_3	"	"	" " 2
C	"	"	" " 3
Al	"	"	" " 4
C	Protons	"	" " 5

19,000 gauss showed that a large percentage of the tracks originated in the gas in all parts of the chamber. After the removal of the source the gas remained active and several tracks per expansion were obtained. This showed that the active element was present as a gas and diffused from the target throughout the chamber. Lauritsen and Crane have subsequently found evidence that the gas in this case is CO or CO_2, in which the carbon is the radioactive C^{11}.

Though these targets, because of the short range of the impinging deutons or protons compared with those of the ejected positrons should be in all cases essentially thin targets, the diffusion of the active material deeper into the target may in some instances introduce an absorbing layer for the positrons to penetrate before they emerge into the chamber for energy measurement. The energy distributions obtained by using a thick carbon target and those obtained using a very thin layer of paraffin as target are very much the same and show that in no case can the energy distribution be markedly affected by energy loss of the positrons before observation. See Fig. 3.

From all targets the positrons emerged with a wide distribution in energy similar to the β-particles from natural radioactive substances. It is, however, not possible on the basis of our present data to make an accurate comparison between energy distributions for the two types of disintegrations. As in ordinary β-disintegration there is here no indication that the disintegration probability is different in different parts of the energy spectrum. All the distribution curves show a striking similarity with one another with the possible exception of Al. The Al data suggest a higher energy limit and Al has a shorter half life than the lighter elements, B and C. To find whether a relation exists between the maximum energy of the bombarding projectiles and the maximum disintegration energy the writers plan to study targets activated by higher or lower energy protons or deutons. This together with an investigation of the neutrons emitted during bombardment may throw light on such questions as the difficulties of energy conservation in β-disintegration, and the mass of the neutron.

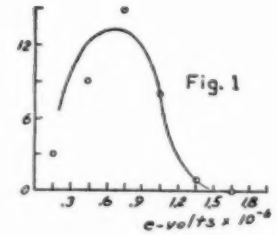

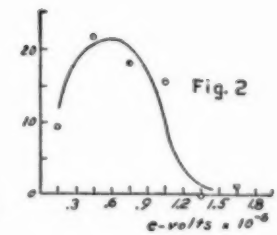

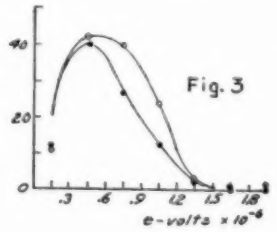

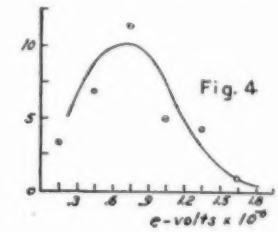

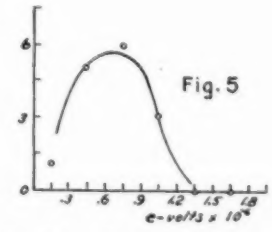

Numbers of positrons in 300,000 volt intervals plotted as a function of energy. The general shape of the smooth curves was obtained by plotting the track counts in overlapping energy intervals but only one set of points is shown.

FIG. 1. Be target bombarded with deutons.
FIG. 2. B target with deutons.
FIG. 3. ●, Very thin paraffin target with deutons; o, C target with deutons.
FIG. 4. Al target with deutons.
Fig. 5. C target with protons.

In the case of Be it is possible that the activity was due to carbon contamination, but this is not likely because of the large activity shown by the Be target.

SETH H. NEDDERMEYER
CARL D. ANDERSON
Norman Bridge Laboratory of Physics,
Pasadena, California,
March 15, 1934.

The Spectrum of Singly Ionized Europium

The main energy levels of Eu II are found to result from the addition of an electron to the common parent term, $4f^7(^8S^\circ)$, of Eu III. The basic levels are $6s\ ^9S_4^\circ$ and $6s\ ^7S_3^\circ$, which result from adding a $6s$ electron to the parent term. The frequency difference of 1669.27 cm^{-1}, which is now shown to be the separation between $^9S_4^\circ$ and $^7S_3^\circ$, was found by Paulson[1] to occur several times among the prominent lines. The metastable $5d$ terms are at about 10,000 cm^{-1}. $^7D^\circ$ was not found probably because most of its combinations with ^9P and ^7P lie beyond the observed region in the red. The height of $5d$ above $6s$ indicates $4f^7 6s^2$ as the normal configuration of Eu I. The locating of the $7s$ levels enables the calculation of an ionization potential of 11.4 volts for Eu II. Three levels

[1] Kayser, Handbuch der Spectroscopie **7**, no. 1.

near 37,000 cm^{-1} of unknown origin combine with the $6s$ and $5d$ levels.

The transition $6p$ to $6s$ accounts for all the very intense Eu II lines in the blue and ultraviolet, while the $6p$ to $5d$ transition explains most of the intense lines in the orange and red.

Table I contains a list of the terms with their energies expressed in wave numbers.

Table II contains the wave-lengths, intensities, temperature class, wave numbers, and combinations. The wave-lengths are from three sources: those without temperature class and intensities without parenthesis are from Eder[1]; those with temperature class from King[2]; and those with intensities in parenthesis are from Exner and Haschek.[3] King's intensity scale is considerably greater than either Eder's or Exner and Haschek's.

WALTER ALBERTSON
George Eastman Research Laboratory of Physics,
Massachusetts Institute of Technology,
March 19, 1934.

TABLE I.

Designation	Level	Designation	Level
$6s\ {}^9S_4°$	0.00	$6p\ {}^9P_5$	26,172.82
${}^7S_3°$	1,669.27	${}^7P_4$	26,838.44
		${}^7P_3$	27,104.15
$5d\ {}^9D_2°$?	9,923.02?	${}^7P_2$	27,256.33
${}^9D_3°$	10,081.68		
${}^9D_4°$	10,312.80	$1_{3,4}$	36,627.9
${}^9D_5°$	10,643.45	2_4	37,010.6
${}^9D_6°$	11,128.49	3_4	37,223.9
$6p\ {}^9P_3$	23,774.27	$7s\ {}^9S_4°$	49,127.87
${}^9P_4$	24,207.82	${}^7S_3°$	49,646.73

[1] King, Astrophys. J. **72**, 1 (1930).

[2] Exner and Haschek, *Wellenlangen Tabellen, Funkenspektren.*

TABLE II.

λ*IA*	Int.	ν(vac)	Designation	λ*IA*	Int.	ν(vac)	Designation
7370.25	−4	13,564.34	${}^9D_5°-{}^9P_4$	4129.734	−500*R* III	24,207.83	${}^9S_4°-{}^9P_4$
7301.16	−5	13,692.69	${}^9D_3°-{}^9P_3$	4011.71	−25*V*	24,920.01	${}^9P_4-{}^9S_4°$
7217.55	−8	13,851.31	${}^9D_2°-{}^9P_3$	3971.989	−400*R* III	25,169.21	${}^7S_3°-{}^7P_4$
7194.80	−8	13,895.10	${}^9D_4°-{}^9P_4$	3943.10	−12*V*	25,353.61	${}^9P_3-{}^9S_4°$
7077.13	−8	14,126.13	${}^9D_3°-{}^9P_4$	3930.504	−300*R* III	25,434.85	${}^7S_3°-{}^7P_3$
6645.19	−20	15,044.33	${}^9D_6°-{}^9P_5$	3929.88	−(2)	25,438.89	${}^9P_4-{}^7S_3°$
6437.64	−15	15,529.36	${}^9D_5°-{}^9P_5$	3907.113	−300*R* III	25,587.12	${}^7S_3°-{}^7P_2$
6303.42	−10	15,860.02	${}^9D_4°-{}^9P_5$	3864.11	−(2)	25,871.87	?${}^9P_3-{}^7S_3°$
6173.03	−10	16,195.03	${}^9D_5°-{}^7P_4$	3819.66	−(50) III	26,172.94	${}^9S_4°-{}^9P_5$
6049.55	−8	16,525.59	${}^9D_4°-{}^7P_4$	3799.02	−(2)	26,315.1	${}^9D_4°-1_{3,4}$
5966.09	−5	16,756.76	${}^9D_3°-{}^7P_4$	3791.53	−(1)	26,367.1	${}^9D_5°-2_4$
5953.90	−2	16,791.07	${}^9D_4°-{}^7P_3$	3765.95	−(2)	26,546.2	${}^9D_3°-1_{3,4}$
5873.02	−5	17,022.31	${}^9D_3°-{}^7P_3$	3761.15	−(3)	26,580.1	${}^9D_5°-3_4$
5820.91	−2	17,174.69	${}^9D_3°-{}^7P_2$	3744.15	−(1)	26,697.9	${}^9D_4°-2_4$
5818.75	−5	17,181.07	${}^9D_2°-{}^7P_3$	3724.95	−(20)	26,838.39	${}^9S_4°-{}^7P_4$
4539.29	−2*V*	22,023.72	${}^7P_3-{}^9S_4°$	3714.90	−(2)	26,911.0	${}^9D_4°-3_4$
4522.602	−200*r* III	22,104.99	${}^7S_3°-{}^9P_3$	3688.42	−(20)	27,104.19	${}^9S_4°-{}^7P_3$
4485.17	−6*V*	22,289.47	${}^7P_4-{}^9S_4°$	3683.26	−(1)	27,142.2	${}^9D_3°-3_4$
4464.94	−10*V*	22,390.45	${}^7P_2-{}^7S_3°$	2859.68	−(2)	34,958.7	${}^7S_3°-1_{3,4}$
4435.602	−400*r* III	22,538.55	${}^7S_3°-{}^9P_4$	2828.70	−(3)	35,341.5	${}^7S_3°-2_4$
4434.81	−8*V*	22,542.57	${}^7P_3-{}^7S_3°$	2811.73	−(2)	35,554.8	${}^7S_3°-3_4$
4383.14	−15*V*	22,808.31	${}^7P_4-{}^7S_3°$	2729.36	−(3)	36,627.8	${}^9S_4°-1_{3,4}$
4355.10	−30*V*	22,955.16	${}^9P_5-{}^9S_4°$	2701.13	−(3)	37,010.6	${}^9S_4°-2_4$
4205.046	−600*R* III	23,774.28	${}^9S_4°-{}^9P_3$	2685.64	−(2)	37,224.0	${}^9S_4°-3_4$

Collision Problems and the Conservation Laws

Recent correspondence in the *Physical Review** suggests that a rapid means of recognizing the implications of the laws of conservation of momentum and energy in collision problems is desirable. Let x_4 be the coordinates of an event in space-time, x_α being the relative spatial coordinates, and $x_4=ict$, where t is the relative time; here (as in what follows) Roman suffixes have the range 1,2,3,4, and Greek suffixes have the range 1,2,3. The momentum-energy 4-vector M_r of any entity has components

$$M_\alpha=\mu_\alpha/c, \quad M_4=iE/c^2,$$

where μ_α are the components of relative momentum and E is the relative energy. In the case of a particle we have

$$M_\alpha=m_0\gamma u_\alpha/c, \quad M_4=im_0\gamma, \quad \gamma=1/(1-u^2/c^2)^{\frac{1}{2}},$$

where m_0 is the proper mass and u_α the relative velocity. For a photon we have

$$M_\alpha=h\nu l_\alpha/c^2, \quad M_4=ih\nu/c^2,$$

where h is Planck's constant, ν the relative frequency, and l_α the relative direction cosines of the direction of propagation.

* Cf. A. L. Hughes and G. E. M. Jauncey, Phys. Rev. **45**, 217 (1934).

The laws of conservation of momentum and energy are most compactly expressed by stating that *the sum of the momentum-energy 4-vectors before collision is equal to the sum of the momentum-energy 4-vectors after collision*. This is the generalization into four dimensions of the law of conservation of momentum in classical mechanics, and we can think in terms of the parallelogram law in four dimensions also. However, since visualization in four dimensions is difficult, we may obtain a picture, valid for many purposes, by depriving space of one dimension, and taking x_1, x_2, ct as rectangular Cartesian coordinates for purposes of representation. The momentum-energy of any entity will appear as an ordinary vector in this three-space with components M_1, M_2, M_4/i. In general, it is not permissible to throw away one dimension of space, but if the vectors with which we have to deal are contained in a flat three-space, we may choose the axis of x_3 (in space-time) perpendicular to this three-space, and the picture proposed will be a completely accurate representation of the three-space $x_3=$const. All processes of composition by addition or subtraction of vectors in a flat three-space lead to vectors in that three-space.

In the three-space in question, there is a null-cone,

$$x_1^2+x_2^2-c^2t^2=0.$$

A time-like vector (such as the momentum-energy of a particle) lies inside this cone: a null-vector (such as the momentum energy of a photon) lies on the null-cone. For we have (with the usual summation convention), since $M_3=0$,

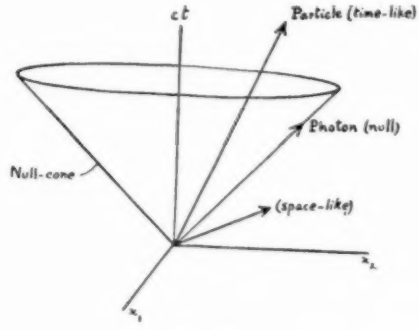

FIG. 1.

$$M_1^2+M_2^2-(M_4/i)^2=M_rM_r\begin{cases}=-m_0^2<0, \text{ for a particle;}\\ =0, \text{ for a photon.}\end{cases}$$

The hypothesis that no entity can have a velocity exceeding c rules out the existence of space-like momentum-energy vectors, which would lie outside the null-cone.

The following facts are then intuitively evident from the diagram, bearing the parallelogram law in mind:

(i) the sum of two time-like vectors is a time-like vector;
(ii) the sum of two null-vectors is a time-like vector, unless the null-vectors are co-directional in space-time;
(iii) the sum of a time-like vector and a null-vector is a time-like vector;
(iv) a time-like vector may be resolved into two null-vectors, with two degrees of arbitrariness.

In regard to the last point, the two null-vectors have 8 components, connected by 4 conditions of equivalence with the given vector and 2 conditions that they shall be null-vectors.

Let us examine the physical implications of the above rules.

(i) If two particles collide and coalesce, they form a particle, not a photon.
(ii) If two photons combine to form a single entity, it is a particle, not a photon, unless the photons are travelling in the same direction in space, in which case a photon is formed.
(iii) If a photon and a particle combine to form a single entity, it is a particle, not a photon.
(iv) A particle may disintegrate into two photons, with two degrees of arbitrariness.

In addition to the above law of conservation, we are to add the law of the conservation of charge. Applying this to (iv), the disintegration is possible only in the case of a single neutral particle, or in the case where two particles of equal and opposite charges collide, their combined momentum-energy vector being the 4-vector which is to be resolved into two null-vectors.

J. L. SYNGE

Department of Applied Mathematics,
University of Toronto,
Toronto, Canada,
March 16, 1934.